Assessment Strategies for Data-Limited Chinook Salmon Stocks of Western Alaska

by

Benjamin Andrew Staton

A thesis submitted to the Graduate Faculty of
Auburn University
in partial fulfillment of the
requirements for the Degree of
Master of Science

Auburn, Alabama
December 12th, 2015

Keywords: Integrated analyses, Bayesian analyses, state-space models, spawner-recruit analysis, Pacific salmon management, data-limitation

Approved by

Matthew J. Catalano, Chair, Assistant Professor of Fisheries, Aquaculture, and Aquatic Sciences
Russell A. Wright, Associate Professor of Fisheries, Aquaculture, and Aquatic Sciences
Conor P. McGowan, Assistant Professor of Forestry and Wildlife Sciences

ABSTRACT

Management strategies for Alaskan Pacific salmon species are conducted in the face of substantial uncertainty, particularly in large drainage systems. In addition to the interacting sources of partial observability and environmental stochasticity, substantial uncertainty exists around the appropriate way to structure an assessment. Assessment approaches vary in their statistical and biological complexity, which inherently leads to trade-offs and questions about the optimal assessment approach. In this thesis, I develop and investigate a range of assessment approaches that address multiple sources of uncertainty by casting them in a Bayesian state-space modeling framework. Chapter 1 presents an introduction to the topics of Pacific salmon management in Alaska, assessment strategies, and uncertainty to provide the necessary background for the following chapters. Chapter 2 investigates trade-offs of estimating abundance and the characteristics of the population dynamics in an integrated analysis as opposed to a sequential analysis. Chapter 3 investigates potential management implications of declining trends in age- and size-at-maturity that have been widely observed but are typically not addressed in assessment models. Chapter 4 revisits a previously developed habitat-based predictive model for stocks that lack adequate assessment data by developing a hierarchical framework and applying a suite of variable selection techniques to decide which habitat variables have predictive credibility. Themes and topics that are addressed continuously in this thesis include spawner-recruit analysis, measurement error, and methods to incorporate multiple sources of uncertainty so that their implications can be more fully addressed.

ACKNOWLEDGEMENTS

I would first like to thank my major professor, Dr. Matthew Catalano for providing me the opportunity to pursue the quantitative research that ultimately lead to this thesis. Early in my time at Auburn, he spent extensive amounts of time teaching me one-on-one about statistics, modeling, and programming primarily with respect to this project, but in a larger context as well. He funded multiple trips to Alaska where I had opportunities to see various assessment projects, learn from other top scientists in the field, and present findings to biologists who are familiar with issues related to my thesis work. These experiences contributed greatly to my ability to complete this project and I am forever grateful for them. I would also like to thank my other committee members, Drs. Rusty Wright and Conor McGowan, for their insight and valuable advice along the way. By not working directly with the models or study system, they were able to bring fresh ideas to the table based on their own extensive experience in the field. I would like to thank Steve Fleischman for his pioneering work on the models that are presented in this thesis. Without his work, this project would likely have never come about. Additionally, Drs. Dan Gwinn and Lew Coggins provided valuable insight on the models presented in this thesis, particularly those in Chapters 3 and 4. Finally, I would like to thank my loving family and girlfriend, Michelle, for their understanding and support while I worked on completing this spectacular opportunity.

TABLE OF CONTENTS

LIST OF FIGURES

Chapter 1 Figures

Chapter 2 Figures

LIST OF TABLES

CHAPTER 1

THESIS INTRODUCTION

Salmon Fisheries in Alaska: Assessment, Management, and Uncertainty

Salmon runs across the state of Alaska support substantial fishery harvests and form an integral component of the ecosystem. Five species of anadromous Pacific salmon, *Oncorhynchus* spp., return to Alaskan streams annually to spawn including chum *O. keta*, pink *O. gorbuscha*, coho *O. kisutch*, sockeye *O. nerka*, and Chinook *O. tshawytscha* and each species constitutes an important fishery resource in various regions throughout the state. Salmon in Alaska provide substantial subsistence, commercial, and recreational resources that support a diversity of cultural lifestyles and user groups. Thus, informed management of these stocks is critical not only to the long-term success and sustainability of the resources, but the cultures that depend on them as well. To this end, this thesis will focus on assessment strategies for Chinook salmon fisheries in western Alaska, particularly in data-limited cases.

Salmon fisheries in Alaska are managed primarily through the use of fixed escapement goal policies: biologists and managers decide, as objectively as possible, the optimal number of salmon that should escape fishing and spawn each year and set that as a management goal. Any amount of salmon in excess of that escapement goal may be harvested. Alaskan regulation policy mandates that escapement goals must not be arbitrary, but rather scientifically defensible and formulated using the best available data (Clark et al. 2009, 5 AAC 39.223). Escapement goals are often given as ranges, which represent the uncertainty in the estimate of optimal escapement. In light of this policy mandate and biological uncertainty, a rigorous, objective method for informing escapement goals is necessary.

Uncertainty is an underlying theme in all ecological assessments, and those involved in the management of Alaskan Pacific salmon are no exception. However, management decisions must be made in the face of uncertainty. In order to make these decisions with the best scientific understanding of the plausible states of the resource, it is important to address as many sources of uncertainty as possible in the assessment, particularly for high-stakes fisheries with multiple user groups. There are several primary causes for the large amount of uncertainty in salmon assessments including: data-limitation, partial observability (measurement error), process variation (environmental stochasticity), parametric uncertainty (surrounding parameter estimates), and structural uncertainty (about biological process) (Williams 1997). This thesis develops and evaluates methods that accommodate these sources of uncertainty in assessments for Chinook salmon across the state of Alaska.

Data-limitation is a type of partial observability in which the available data are not sufficient to be used in traditional assessment techniques (Shotwell and Adkison 2004). Data-limitation can arise from either monetary or logistical constraints to sampling or through some combination of these. In large river systems, like the Kuskokwim or Yukon rivers in western Alaska, it is incredibly difficult to conduct representative sampling programs due to the size and remoteness of the sub-drainages. These constraints result in the necessity to selectively choose where and how to sample, which oftentimes constitutes a very small portion of the total river system. In these data-limited situations, case-specific models must be developed that allow for multiple sources of information to be included in order to maximize the utility of the information content of the individual data sources.

Even if it were possible to sample every area in the river drainage, managers would still have an imperfect perception of the system due to measurement error. Measurement error

propagates through making observations on a system when the measurement device or technique is imperfect. For example, counting fish passage using a weir may seem like an accurate means to enumerate escaping fish to a tributary, however flooding or damages occur that render the weir inoperable which allow fish to pass uncounted. While an estimate exists for escapement to that tributary, it is important to realize that the time series of observations is imprecise at best, and at worst, biased. Assessment scientists are constantly faced with utilizing imperfect data and so the necessity is to develop techniques that cope with these data to extract as much useful information as possible.

Even if this hypothetical example is taken to the extreme, where all areas are sampled perfectly, managers and biologists would not be able to perfectly understand the system dynamics. This is due to natural environmental stochasticity or process variation. Process variation arises when external variables cause fluctuations around the expected system state. This source of uncertainty cannot be reduced with greater sampling effort, but it can be accounted for, explained, and quantified in assessment models.

Salmon assessment, which relies heavily upon spawner-recruit analyses, faces each of these challenges. In a spawner-recruit analysis, reliable estimates of brood year spawner and return counts are used to estimate the biological productivity and carrying capacity of the stock, which can then be used for determining optimal escapement targets. This spawner-recruit input information is difficult to collect in large drainages where much of the spawning escapement goes uncounted and is made up of individuals from four cohorts. For example, the run that occurred in the calendar year 2015 was made up of fish that were spawned in the brood years 2008 (age seven), 2009 (age six), 2010 (age five), and 2011 (age four), (Table 1.01). Thus, the issues of data-limitation and measurement error become readily apparent. Process variation

enters when a spawner-recruit analysis is conducted on the spawner and return counts (or estimates) and the manager sees that large positive or negative residuals can occur at any spawner abundance. This implies that even if the fishery were managed optimally in terms of maximum sustainable yield, there would still be a chance of recruitment failure.

The Ricker (1954) spawner-recruit model is typically used for Pacific salmon assessment primarily because of its ability to deal with overcompensation (reduced recruitment at large stock abundances), which is a phenomenon frequently observed in these species (Fleischman et al. 2013). Furthermore, the Ricker model tends to provide more conservative estimates of population parameters than other models, which decreases the risk of overexploitation (Fleischman et al. 2013). The Ricker spawner-recruit relationship has two primary parameters that determine the productivity and the carrying capacity of the stock of interest. They are α, returns per spawner (R/S) at low spawner density, and β, the rate of decrease in R/S as spawner density increases. Given these two parameters and the residual process error, it is possible to derive the necessary biological reference points used in management. They are (1) equilibrium unfished spawner abundance under constant environmental conditions (S_{eq}), (2) spawner abundance that will produce maximum sustained yield (S_{MSY}), and (3) the spawner abundance that produces the maximum recruitment (S_{MAX}) (Clark et al. 2009; Figure 1.01; see *Chapter 2: Methods* for analytical approximations of these quantities). Each reference point has an associated uncertainty based on the uncertainty in the spawner-recruit parameters, which in part causes escapement goals to be given as ranges rather than single quantities.

Traditional approaches to spawner-recruit analyses have utilized a linear regression method to estimate the parameters of the Ricker (1954) curve as described in Clark et al. (2009). This linear method is commonly used on salmon stocks across Alaska (Clark et al. 2009), but has

distinct statistical shortcomings that can lead to major biases. First, it assumes a stationary spawner-recruit relationship (the parameters α and β do not change over time), which is known to be violated for exploited stocks (Walters and Martell 2004). Secondly, use of the regression model makes the assumption that the independent variable, the spawner abundance, is not influenced by the dependent variable, recruitment. This is clearly not the case since the spawning escapement is the result of past years' recruitment (Fleischman et al. 2013). The combination of these two issues leads to a phenomenon known as time series bias (Walters 1985). Time series bias has been shown to result in overestimated productivity at low stock sizes, leading to higher estimates of α than the stock actually exhibits which causes biases in biological reference points and could lead to overexploitation in the long-term (Walters 1985). Another assumption of the regression approach is that the independent variable is measured without error. Measurement of escapement is largely imperfect which violates this assumption and leads to a statistical situation known as errors-in-variables bias. This problem can cause the spawner-recruit relationship to depict more visual "scatter" than is found in reality and leads to further biases in parameter values (Walters and Ludwig 1981; Walters and Martell 2004). Combined with the data-limited situation of many salmon stocks, these additional biases have the potential to cause traditional spawner-recruit approaches to inadequately estimate biological reference points. Thus, more complex approaches to spawner-recruit analyses must be conducted in order to address these statistical problems (Fleischman et al. 2013).

State-space Models as a Tool for Dealing with Uncertainty in Spawner-Recruit Analyses

Due to the problems inherent to using the traditional linear regression approach to spawner-recruit analysis, more robust methods are necessary to adequately describe the recruitment dynamics of data-limited salmon stocks. One method that has shown promise for Pacific salmon is the state-space modeling approach (Meyer and Millar 2001; Fleischman et al.

2013). This approach has the ability to incorporate data-limited time series in a way that more fully addresses uncertainty by allowing both measurement error and process variation to occur simultaneously with in a single model. The state-space model in the spawner-recruit context functions by treating brood year recruitment as partially observed states defined by a latent state process submodel (i.e., the spawner-recruit relationship), and reconstructs a recruitment time series that is most likely to have given rise to the escapement and harvest observations defined by an observation submodel. It simultaneously uses this reconstructed time series to fit a spawner-recruit model to retrieve parameters and calculate reference points for setting escapement targets (Meyer and Millar 2001; Fleischman et al. 2013).

State-space models often use a Bayesian methodology when fitting the model to the data (Fleischman et al. 2013). Bayesian estimation forms a joint posterior distribution [P(θ|*data*)] for all unknown quantities in the model (both estimated parameters and derived quantities) that represents the support for various values of the unknowns after the likelihood [P(*data*|θ)] and the prior [P(θ)] are combined. The Bayesian framework is used in state-space modeling because it (1) is a formal way to incorporate prior knowledge and constrain the model to explore only the plausible parameter space, (2) allows for simultaneous integration over parameter values and unobserved states, and (3) allows for intuitive incorporation of multiple types of uncertainty via a hierarchical framework (Bolker 2008). The latter two reasons constitute a major part of what identifies a state-space model, making the Bayesian framework ideal for fitting these models.

Overview of the Kuskokwim River Region and its Chinook Salmon Stock Status

The Kuskokwim River is the second largest drainage system in the state of Alaska (>130,000 km^2), with the main stem traveling approximately 1,500 km from its headwaters in the Kuskokwim Mountains to the southwestern coast where it empties into the Kuskokwim Bay of

the Bering Sea (Hamazaki et al. 2012; Figure 1.02). It has historically provided the largest subsistence fishery for Chinook salmon in the state, with three main population hubs: Bethel (population 6,000+), Aniak (population ~570), and McGrath (population ~470) (Linderman and Bergstrom 2009). While the directed commercial fishery for Chinook salmon was closed in 1987, incidental harvest still occurs in the chum and sockeye commercial fisheries (Linderman and Bergstrom 2009).

The status of the Kuskokwim River Chinook salmon fishery has historically been assessed based on spawning abundance trends on several index streams as the size and remoteness of the Kuskokwim River tributaries prevents complete escapement enumeration. Escapement observations are made on a subset of index streams using a variety of projects including aerial peak spawning surveys (14 tributaries), weir counts (6 tributaries), and periodic mark-recapture estimates (Linderman and Bergstrom 2009; Figure 1.02, Table 2.01). There has been a recent movement to synthesize this information using drainage-wide assessment models so that trends of the aggregate stock could be assessed for sustainability. These models are described in detail in *Chapter 2: Methods.*

Starting in 2007 and continuing to the most recently collected data, drainage-wide escapement has declined sharply resulting in failure to meet escapement goals and the first subsistence fishery restrictions since the initiation of the fishery (Schindler et al. 2013). The 2013 escapement projects counted record low escapements and due to a projected low run for the 2014 season, the Chinook salmon fishery was closed during the majority of the run in an attempt to meet the drainage-wide escapement goal. Based on presently unpublished Alaska Department of Fish and Game (ADF&G) data, 2014 escapement was larger than 2013 and the drainage-wide escapement goal was met, although the run was smaller than average. In a river of such

subsistence importance as the Kuskokwim, the short-term cultural effects of low returns can be disastrous. It is important to note that the Kuskokwim River is not the only drainage facing these declines; other major drainage systems in western Alaska, such as the Yukon River and Nushagak River, are also experiencing low returns of Chinook salmon since 2007 (ADF&G Chinook Salmon Research Team).

The combination of incomplete information on escapement and resulting returns over both space and time leads to a data-limited situation in the Kuskokwim River Chinook salmon stock assessment. This paucity results in large uncertainties and potential biases surrounding spawner-recruit parameters, biological reference points, and subsequent escapement goals. However, as previously stated, the stock must still be managed using scientifically informed decisions. The question becomes not how to sample more effectively, as gaining more complete data is impractical, but how to utilize the available data to its maximum potential. Thus, the necessary approach to assess the data-limited Kuskokwim River Chinook salmon stock (and stocks like it) is one that has the ability to synthesize the available data and explicitly address its uncertainty in order to arrive at robust and reliable estimates of stock abundance, productivity, carrying capacity, and biological reference points.

To this end, the purpose of this thesis is to investigate assessment techniques for Alaskan Chinook salmon stocks with regard to their ability to cope with uncertainty, data-limitation, and sensitivity to assumptions. The second chapter investigates potential trade-offs of integrating multiple assessment steps into one model for Kuskokwim River Chinook salmon. The third chapter extends the integrated model framework to include size-selective components of the fishery to investigate implications of the size-at-age and age composition on management of the Kuskokwim River Chinook salmon stock. The fourth chapter takes a step back from the

Kuskokwim River assessment and investigates habitat-based assessment techniques for stocks without adequate data for spawner-recruit analysis using a variety of model selection methods.

REFERENCES

ADF&G Chinook Salmon Research Team. 2013. Chinook salmon stock assessment and research plan, 2013. Alaska Department of Fish and Game, Special Publication No. 13-01, Anchorage, AK.

Clark, R.A., D.R. Bernard, and S.J. Fleischman. 2009. Stock-recruitment analysis for escapement goal development: a case study of Pacific salmon in Alaska. Pages 743-757 *in* C.C. Krueger and C.E. Zimmerman, ed. Pacific salmon: ecology and management of western Alaska's populations. American Fisheries Society, Symposium 70, Bethesda, Maryland.

Fleischman, S.J., M.J. Catalano, R.A. Clark, and D.R. Bernard. 2013. An age-structured state-space stock-recruit model for Pacific salmon (*Oncorhynchus* spp.). Canadian Journal of Fisheries and Aquatic Sciences. 70(3): 401-414.

Hamazaki, T., M.J. Evenson, S.J. Fleischman, and K.L. Schaberg. 2012. Spawner-recruit analysis and escapement goal recommendation for Chinook salmon in the Kuskokwim River Drainage. Alaska Department of Fish and Game, Fishery Manuscript Series No. 12-08, Anchorage.

Linderman, J.C., Jr. and D.J. Bergstrom. 2009. Kuskokwim management area: salmon escapement, harvest, and management. Pages 541-599 *in* C.C. Krueger and C.E. Zimmerman, ed. Pacific salmon: ecology and management of western Alaska's populations. American Fisheries Society, Symposium 70, Bethesda, Maryland.

Ricker, W.E. 1954. Stock and recruitment. Journal of the Fisheries Research Board of Canada. 11(5):559-623.

Schindler, D., C. Krueger, P. Bisson, M. Bradford, B. Clark, J. Conitz, K. Howard, M. Jones, J. Murphy, K. Myers, M. Scheuerell, E. Volk, and J. Winton. Artic-Yukon-Kuskokwim Chinook Salmon Research Action Plan: Evidence of Decline of Chinook Salmon Populations and Recommendations for Future Research. Prepared for the AYK Sustainable Salmon Initiative (Anchorage, AK). 79 pp.

Shotwell, S.K., M.D. Adkison. 2004. Estimating indices of abundance and escapement of Pacific salmon for data-limited situations. Transactions of the American Fisheries Society 133(3):538-558.

Williams, B.K. 1997. Approaches to the management of waterfowl under uncertainty. Wildlife Society Bulletin. 25(3): 714-720.

CHAPTER 1
FIGURES

Figure 1.01 Example Ricker spawner-recruit curve (bold line) with relevant biological reference points shown. The thin line represents 1:1 replacement, where recruitment equals escapement.

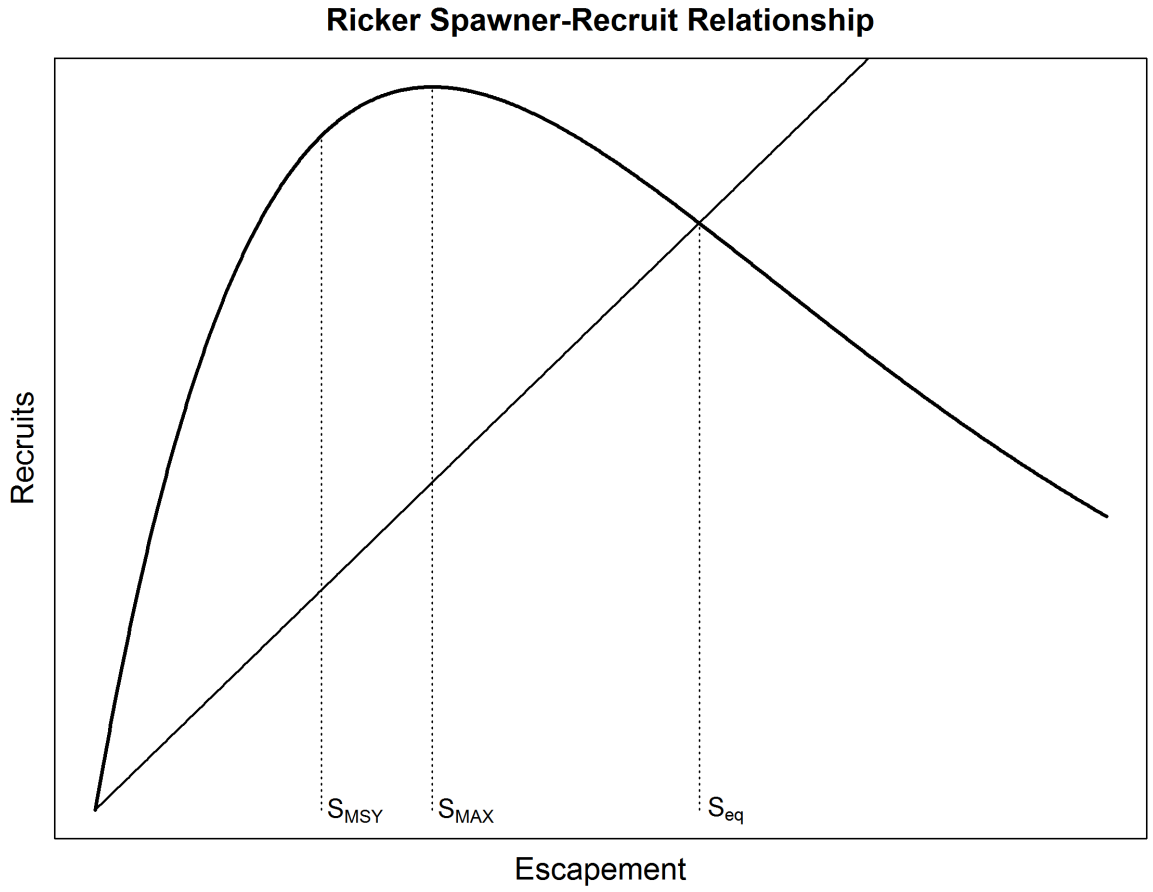

Figure 1.02 The Kuskokwim River drainage with escapement enumeration projects shown. Weir projects are denoted by dots and aerial surveys are denoted by bold lines.

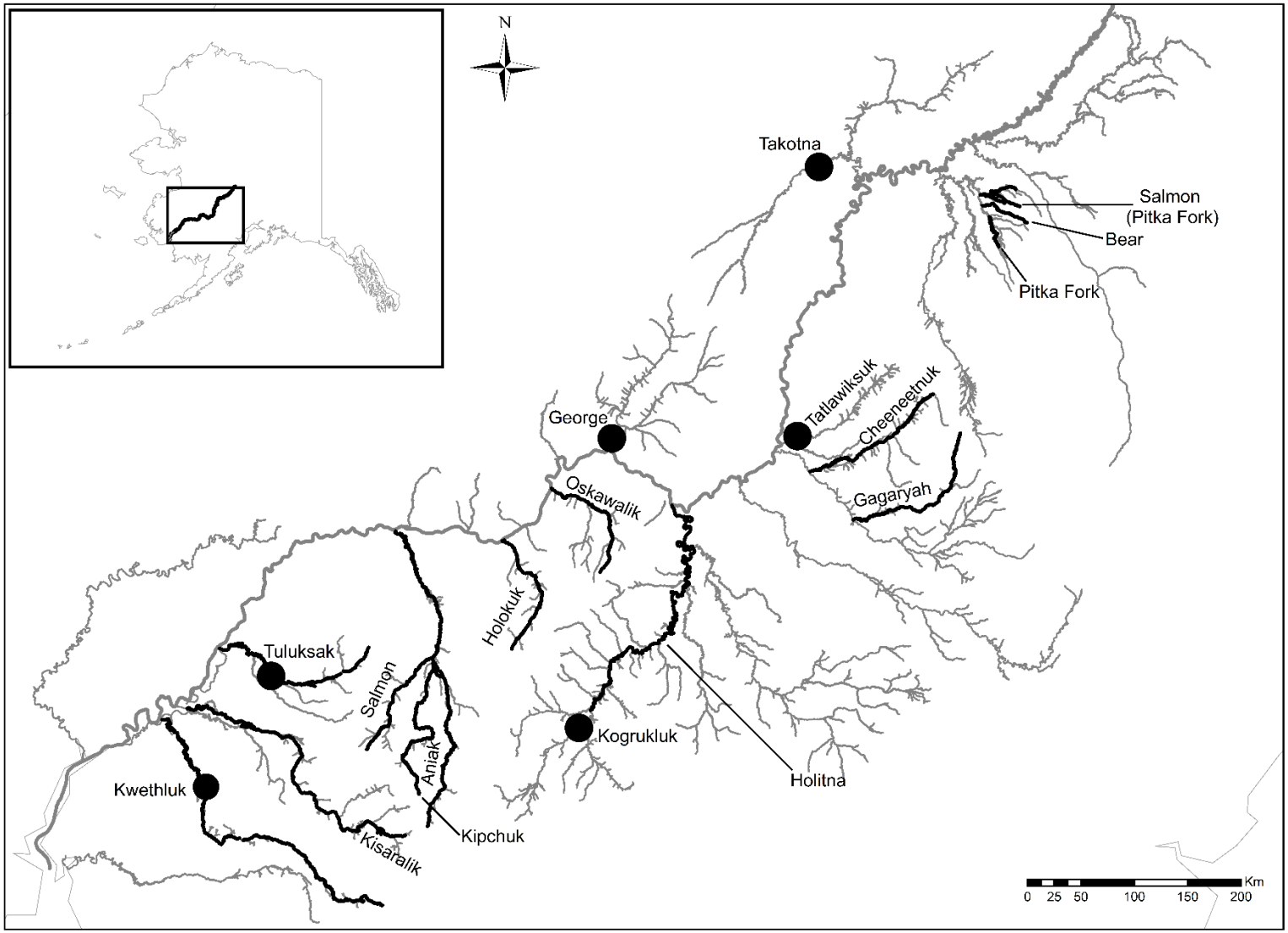

CHAPTER 1
TABLES

Table 1.01 Abundance of adult Chinook salmon by age *a* and year *y* showing the distinction between returns and runs. Bold abundances in the same row ($N_{1,4:7}$) make up the run N_1, whereas the sum of the bold diagonal ($N_{5,4:8,7}$) makes up a cohort from a single brood year which is the return R_1 that the escapement S_1 produced. Adapted from Fleischman et al. (2013).

Year	**Esc.**	**Annual Run: Abundance-at-Age**				**Run**	**Return**
y	S_y	4	5	6	7	$N_y = \sum_{a=4}^{7} N_{y,a}$	$R_y = \sum_{a=4}^{7} N_{y+a,a}$
1	S_1	$\mathbf{N_{1,4}}$	$\mathbf{N_{1,5}}$	$\mathbf{N_{1,6}}$	$\mathbf{N_{1,7}}$	N_1	R_1
2	S_2	$N_{2,4}$	$N_{2,5}$	$N_{2,6}$	$N_{2,7}$	N_2	R_2
3	S_3	$N_{3,4}$	$N_{3,5}$	$N_{3,6}$	$N_{3,7}$	N_3	R_3
4	S_4	$N_{4,4}$	$N_{4,5}$	$N_{4,6}$	$N_{4,7}$	N_4	R_4
5	S_5	$\mathbf{N_{5,4}}$	$N_{5,5}$	$N_{5,6}$	$N_{5,7}$	N_5	R_5
6	S_6	$N_{6,4}$	$\mathbf{N_{6,5}}$	$N_{6,6}$	$N_{6,7}$	N_6	R_6
7	S_6	$N_{7,4}$	$N_{7,5}$	$\mathbf{N_{7,6}}$	$N_{7,7}$	N_7	R_7
8	S_8	$N_{8,4}$	$N_{8,5}$	$N_{8,6}$	$\mathbf{N_{8,7}}$	N_8	R_8
9	S_9	$N_{9,4}$	$N_{9,5}$	$N_{9,6}$	$N_{9,7}$	N_9	R_9
10	S_{10}	$N_{10,4}$	$N_{10,5}$	$N_{10,6}$	$N_{10,7}$	N_{10}	R_{10}

CHAPTER 2

FROM SEQUENTIAL TO INTEGRATED BAYESIAN ANALYSES: EXPLORING THE CONTINUUM WITH A PACIFIC SALMON SPAWNER-RECRUIT MODEL

ABSTRACT

Stock assessment scientists are often faced with decisions regarding how to incorporate information into models. One primary decision revolves around how estimates that are summaries of raw data should be treated (e.g., abundance estimates derived from relative indices of abundance). The choice in this case is to use estimates from a sequence of models as data in the terminal model or to integrate the raw data into the terminal analysis. Each approach has advantages and disadvantages that constitute a suite of trade-offs which are described in further detail. These trade-offs are investigated by comparing a sequential analysis to an integrated analysis for Pacific salmon stock assessment, using the Kuskokwim River Chinook salmon stock, located in western Alaska, as a case study. The major difference between approaches in this case is that abundance and characteristics of the population dynamics are estimated separately in the sequential analysis whereas the integrated approach does so in a single model. Primary findings showed that the two approaches returned very similar estimates of population dynamics parameters and management reference points, both in terms of point estimates and uncertainty, showing that the treatment of measurement error in the sequential analysis was adequate. The primary advantage of the integrated analysis was the added realism of sharing calendar year abundance data between brood years, but came at the cost of slow run times. This exercise showed that while there is a trade-off between sequential and integrated analyses in terms of model complexity and realism, it may not be large enough to warrant an integrated analysis in all cases.

INTRODUCTION

Stock assessment scientists are often faced with decisions regarding how to incorporate information into models. This is particularly true when there are various types of information, some of which are raw data and some are estimates from previous models (e.g., catch-at-age data versus estimates of abundance; Maunder and Punt 2013). Additionally, these cases arise when two processes give rise to the observed dataset, but only one is of interest, such as when data are produced by a population process (i.e., population dynamics) and a measurement process (i.e., sampling), but inference is desired only for the population process. In these cases, the practitioner has the option to either separate the information into a sequence of analyses or integrate the raw information into one analysis. This choice may at first seem arbitrary and inconsequential, but may prove to have substantial ramifications on the results and interpretation of the assessment model (Brooks and Deroba 2015).

Under the sequential analysis approach (often termed "two-step"), raw data are used in one model to produce estimates of interest that are then passed to another model as either data or informative prior distributions (Michielsens et al. 2008). A common example of this practice in stock assessment modeling is the estimation of spawning stock biomass and a recruitment time series from a Virtual Population Analysis-type model that are then passed to a spawner-recruit model to estimate parameters that govern the population dynamics (Maunder and Punt 2013). This sequential approach allows for the inclusion of information in a summarized form into a more simplified terminal model that requires it in that form. However, as noted by Maunder (2001), the sequential approach has some potential disadvantages including loss of information in the raw data that could be exploited by the terminal analysis if not already summarized, inadequate treatment of uncertainty in the observation level-data, and reduced diagnostic ability.

By contrast, an integrated analysis attempts to incorporate the raw data (as fully as appropriate) into a single model (Fournier and Archibald 1982). An integrated analysis is often conducted with the goal of preserving the complete information content of the data and partitioning uncertainty in the analysis due to observation error and process variation. These types of integrated population models are gaining popularity in ecological assessments in both applied and academic settings (Schaub and Abadi 2011; Royale and Dorazio 2008), however, due to the inherent complexity of integrated analyses, they present unique problems, such as how to formulate the joint likelihood, convergence issues, and computational complexities (Maunder and Punt 2013). However, with recent advances in computing power and statistical approaches to fitting complex models, particularly Bayesian estimation using Markov chain Monte Carlo (MCMC) methods, these barriers are becoming less troublesome for the applied stock assessment practitioner.

Even with integrated analyses, however, the investigator is tasked with deciding which data to include in its raw form versus which information should be summarized before inclusion in the model. As such, it is more appropriate to view the contrast between sequential and integrated analyses as a continuum rather than a dichotomy. On the extreme sequential side of the continuum, all raw data are summarized or combined into estimates prior to being included in the final model. On the extreme integrated side of the continuum, every raw data point is included as an observation of the system and is used for inference. There exists intermediate scenarios between these extremes where some data are summarized pre-analysis and some data are included in raw form. As one moves the analysis in either direction along this continuum, the relative advantages and disadvantages of either approach should become apparent in the output of the whole analysis.

Assessment approaches for Pacific salmon typically involve collecting observations of annual spawner abundance and harvest then combining this information into a brood table to obtain brood year recruits based on the year and age at which the fish returned (e.g., Clark et al. 2009; Bue et al. 2012). Note that only the calendar year processes (escapement and harvest) can be observed, which are then used to obtain brood year recruitment that cannot be directly observed. Oftentimes, spawner abundance and harvest are not complete counts and must be estimated (e.g., via run reconstruction; Shotwell and Adkison 2004). These estimates are then passed to a spawner-recruit analysis to estimate productivity, carrying capacity, and variation in recruitment for the derivation of biological reference points used in setting escapement goals (Clark et al. 2009). This approach constitutes a sequential analysis. However, in some cases it is possible to integrate the run reconstruction model directly into the spawner-recruit analysis whereby brood year spawner and recruit abundances are reconstructed from observational-level data and a spawner-recruit relationship is simultaneously fit to these estimates. This approach may have the benefits of more fully addressing uncertainty due to the interaction between the raw data (i.e., observation model) with the spawner-recruit analysis (i.e., process model) and the sharing of information between calendar years due to the intrinsic link between calendar years via the spawner-recruit analysis (Maunder 2001).

In this chapter, I present the application of an analysis that moves a stock assessment further along the continuum from a sequential two-step analysis to a more fully integrated analysis. Potential trade-offs of integrating the analysis will be investigated by independently running both a sequential and an integrated analysis and comparing relevant quantities of interest. The terminal model in both cases is fit using a Bayesian state-space framework to allow for simultaneous incorporation of both measurement error in the input information and process

variation in the spawner-recruit relationship (Fleischman et al. 2013). This analysis is conducted using the Kuskokwim River Chinook salmon stock, located in western Alaska, as a case study. The objectives of this exercise are to (1) confirm that the integrated analysis is computationally feasible in this case given the information content of the data and the model complexity, (2) compare the findings from the integrated model to a sequential assessment to determine if the proposed advantages of integrated analyses are evident in this case and (3) assess the sensitivity of the integrated analysis to parametric uncertainty in terms of assumed variance components and biases in scaling information. The primary *a priori* expectation is that there should be greater posterior uncertainty in quantities from the integrated analysis than the sequential analysis because the measurement error in the raw data is allowed to interact more directly with the spawner-recruit model in the integrated analysis.

METHODS

Study System

The Kuskokwim River is the second largest drainage system in the state of Alaska (~130,000 km^2), with the main stem traveling approximately 1,500 km from its headwaters in the Kuskokwim Mountains to the southwestern coast where it empties into the Kuskokwim Bay of the Bering Sea (Hamazaki et al. 2012, Figure 1.02). Historically, the Kuskokwim River has provided the largest subsistence fishery for Chinook salmon in the state (39 year average ~70,000 fish/year), but has seen low runs in recent years leading to substantial conservation measures including fishery closures for Chinook salmon and other species. While the directed commercial fishery for Chinook salmon was closed in 1987, incidental harvest (28 year average ~14,000 fish/year since closure) of Chinook salmon still occurs in the chum salmon *O. keta* and sockeye salmon *O. nerka* commercial fisheries (Linderman and Bergstrom 2009).

Assessment data for the Kuskokwim River Chinook salmon stock date back to 1976 and consist of escapement counts made at weirs (n = 6), aerial surveys flown at peak spawning (n = 14), total annual harvest estimates from the commercial and subsistence fisheries, historical catch-per-unit-effort data from the commercial fishery, age composition data from various areas in the drainage, and large-scale mark-recapture estimates (Table 2.01; Bue et al. 2012).

Integrated Model Structure

The integrated model combines the estimation of abundance and population dynamics parameters into one Bayesian state-space model (as opposed to separate models, described in *Sequential Analysis Structure* below). This framework moves the assessment further on the continuum towards an integrated analysis and is hereafter referred to as the "integrated model". The integrated model structure has been applied to other salmon assessments across the state of Alaska including the Kenai early and late Chinook runs (McKinley and Fleischman 2013; Fleischman and McKinley 2013) and shows promise in terms of dealing with measurement error and other statistical problems inherent to traditional spawner-recruit analyses (Chapter 1, this Thesis; Fleischman et al. 2013). The general model formulation follows that of Fleischman et al. (2013) who presented an integrated analysis for the Karluk River Chinook salmon population on Kodiak Island, Alaska, which is monitored annually using one weir and harvest sampling. The spawner-recruit analysis served as the unobserved state process submodel which was informed by escapement (weir) and harvest observations in the observation process submodel. The integrated model presented in this chapter extends this formulation to include all of the assessment data from the Kuskokwim River Chinook salmon stock collected over the past 39 years (Table 2.01)

The drainage-wide integrated model was built specifically for the Kuskokwim River drainage Chinook salmon stock. Within the state-space model there are two submodels which are fully described below. The process submodel defines the true unobserved state of the system: the population dynamics of the salmon stock including Ricker spawner-recruit productivity and brood year-specific maturation schedules. Based on these components, the process model produces an expected calendar year run abundance. The observation submodel then links these true states to the observed states by incorporating all of the observations that have been made of the system for the past 39 years (1976-2014). The integrated model is cast in the Bayesian mode of inference and uses MCMC methods to estimate the joint posterior probability distribution for all non-fixed quantities in the model. The process and observation submodels emulated the approaches followed by Fleischman et al. (2013) and Bue et al. (2012), respectively.

Process Submodel

Hereafter, the term "run" refers to the total number of fish coming to the river mouth in a single calendar year which is made of several brood years (cohorts) and the "return" is all of the fish that return in multiple years but were all spawned in the same brood year (R_y; Table 1.01) and can thus be used interchangeably with the term "recruitment" or "recruits". Returns of Chinook salmon to the Kuskokwim River were treated as unobserved states modeled using the linearized Ricker (1954) spawner-recruit model, but adapted for lag-1 auto-regressive [AR(1)] lognormal process error:

$$\ln(R_y) = \ln(S_y) + \ln(\alpha) - \beta S_y + \phi \omega_{y-1} + \varepsilon_y \qquad (2.01)$$

where S_y is the escapement in year y that produced brood year returns R_y. α is the productivity parameter, β is the capacity parameter, and ϕ is the AR(1) coefficient that specifies the strength of serial autocorrelation in the time series of recruitment residuals. AR(1) process errors were

used to account for trends in juvenile survival, wherein positive recruitment residuals in brood year *y*-1 are followed by higher-than-expected residuals in brood year *y*, and vice versa (i.e., autocorrelation). Lognormal errors were used to allow residual variance to increase as the mean increases, a phenomenon commonly observed in spawner-recruit residuals and ecological data in general (Hilborn and Walters 1992). ω_y is the model residual:

$$\omega_y=\omega_{y\text{-}1}+\varepsilon_y \tag{2.02}$$

where ε_y are independent [non-AR(1)] normally-distributed process errors with standard deviation σ_R. The first seven brood year returns, which could not be linked to monitored escapement data through the spawner-recruit relationship, were modeled as random effects drawn from a shared lognormal distribution with parameters $\ln(R_0)$ and σ_{R_0}.

The model was age-structured to account for recruits from a given brood year being able to return at age four, five, six, or seven (Table 1.01). Furthermore, the model allowed for annual variation the proportion of fish mature-at-age ($p_{y,a}$) from a given brood year (maturation dictates the age-at-return). Brood year maturation schedules were modeled as Dirichlet random effects drawn from a common Dirichlet distribution following Fleischman et al. (2013). The Dirichlet is the conjugate distribution for the multinomial distribution, just as the beta distribution is for the binomial (i.e., it models the probability of success for each possible outcome; here the probability of maturing and returning at a given age; McCarthy 2007). The common (i.e., shared) distribution was implemented hierarchically using the distributions that make up the Dirichlet. Formulating the Dirichlet in this fashion allowed for the hyperparameters to be estimated and monitored including the concentration parameter *D*, which controls the variation in maturation-at-age between brood years (smaller values, more variation) and the vector of expected frequencies of maturation-at-age (γ_a). The Dirichlet distribution was constructed by using a

series of independent Gamma distributions. The hyperparameter vector of expected frequencies for maturing at each age (γ) were independent gamma random variables. These can be used to return the central tendencies of the proportion maturing-at-age from any given brood year from the common (i.e., shared) Dirichlet:

$$\pi_a = \frac{\gamma_a}{\sum_a \gamma_a} \tag{2.03}$$

Brood year-specific maturation schedules were then drawn from this common distribution:

$$p_{y,a} = \frac{g_{y,a}}{\sum_a g_{y,a}} \tag{2.04}$$

$$g_{y,a} \sim Gamma(\text{shape} = \gamma_a, \text{ rate}=1.0) \tag{2.05}$$

The number of fish of age a in the run occurring in year y ($N_{y,a}$) was:

$$N_{y,a} = R_{y-a}\, p_{y-a,a} \tag{2.06}$$

And the total run abundance in calendar year y was:

$$N_y = \sum_{a=4}^{7} N_{y,a} \tag{2.07}$$

The relevant biological reference points for the calculation of escapement goals were calculated within the model which allowed for their marginal posterior distributions to be summarized like any other quantity in the model. The three most relevant reference points are (1) S_{eq}, the spawner abundance that produces replacement recruitment to keep the population at equilibrium, (2) S_{MSY}, the spawner abundance that produces maximum sustained yield (MSY), and (3) S_{MAX}, the spawner abundance that produces maximum recruitment (Figure 1.01). Before calculating the reference points, α was corrected for lognormal process error and autocorrelated recruitment residuals (Hilborn 1985)

$$\ln(\alpha_c) = \ln(\alpha) + \frac{\sigma_R^2}{2(1-\phi^2)} \tag{2.08}$$

Where σ_R is the lognormal process error around the expected spawner-recruit curve. The relevant biological reference points were then calculated:

$$S_{MAX}=\frac{1}{\beta} \tag{2.09}$$

$$S_{eq}=\ln(\alpha_c)\, S_{MAX} \tag{2.10}$$

$$S_{MSY}=S_{eq}(0.5\text{-}0.07\ln(\alpha_c)) \tag{2.11}$$

Observation Submodel

The role of the observation submodel is to synthesize all of the data from the past 39 years from Kuskokwim Chinook salmon sampling and to fit it to the true states given by the process submodel. For simplicity of presentation, the observation submodel can be partitioned into five main components representing the primary data sources: (1) weir and aerial survey counts, (2) commercial catch-per-unit-effort (CPUE), (3) annual escapement estimates from mark-recapture studies, (4) age composition data in the form of scale counts, and (5) total annual harvest components for the commercial and subsistence fisheries. These data were supplied by Alaska Department of Fish and Game (ADF&G) biologists.

(1) Weirs and Aerial Surveys – Weir projects (n = 6) were operated by placing a barrier in the stream channel with a narrow passage opened periodically through which fish are counted as they pass (Blain et al. 2014). Aerial surveys (n = 14) were flown during the expected peak of the run to survey a subset of streams that could not be sampled by weirs due to logistical or monetary constraints (Hansen and Blain 2014). Weirs and aerial surveys could not count all escaping fish to a tributary and therefore counts made by each project should be interpreted as indices of escapement rather than censuses. These counts can be proportionally related to total escapement such that the expected number of fish counted in project *j* in year *y* is:

$$I_{jy} = \hat{S}_y / k_j \quad (2.12)$$

where $\hat{S}_y$ is the total annual escapement in the drainage predicted by the model, I_{jy} is the predicted count from weir or aerial survey project j in year y and k_j is a proportionality coefficient that scales the index to the total drainage-wide escapement. The 'hat' over S_y in equation 2.12 denotes that this value is the predicted drainage-wide escapement in a given year, to make the distinction between observed (estimated) escapements from mark-recapture studies. Note that k_j was constant over time (has no y index), which made the assumption that the proportion of total escapement counted at each tributary was constant every year. These proportionality coefficients represented a mean inverse proportion of the total escapement that each project counted each year.

These index counts were assumed to have a negative binomial sampling distribution to account for over-dispersion (Hilborn and Mangel 1997). The negative binomial distribution was formulated to include an over-dispersion parameter (r_j) which represents the amount of extra-Poisson variation present in the dataset. The tributary counts were over-dispersed because they included both process error (annual variation in the proportion of the total escapement going to each tributary) and measurement error associated with annual sampling.

(2) Commercial CPUE – The commercial CPUE component used weekly (w) catch (C_{yw}) and effort (B_{yw}) data from the commercial fishery that occurs in district W1 near the mouth of the mainstem to serve as a relative index of abundance. Effort data were expressed in units of permit hours per week w. Expected catch was calculated using the Baranov catch equation where weekly catch was a function of the instantaneous fishing mortality (effort times catchability) and the number of fish available for harvest. The number of fish reaching district W1 by week was calculated using run timing estimates from a gill net test fishery operated daily in-season in

Bethel, AK. The proportion of the annual run P_{yw} present in week w of year y was calculated using the test fishery CPUE:

$$P_{yw}=\frac{CPUE_{yw}}{\sum CPUE_{yw}} \tag{2.13}$$

and the number of fish in district W1 in week w of year y (W_{yw}) was:

$$W_{yw}=N_y P_{yw} \tag{2.14}$$

where N_y is the expected run size in year y given by the process submodel. The expected catch in week w of year y was:

$$C_{yw}=W_{yw}(1-e^{-qB_{yw}}) \tag{2.15}$$

where q is the estimated catchability of the gear used. Due to historical changes in gill net restrictions and technologies, separate catchabilities must be estimated for different time periods in equation 2.15. During the first few weeks in the early years of data collection there were no mesh size restrictions were in place (q_{unr}). From 1976-1984 a 6-inch stretched mesh size restriction was put into place (q_{res}). In the early 1980s a new gill net material was introduced that increased the efficiency of gill nets (Bue 1986), and it was assumed that this gear was used from 1985 to the present (q_{mono}). C_{yw} was fit to the observed catch in year y and week w using a lognormal likelihood density function.

(3) Mark-Recapture Scaling – In order to calibrate the relative abundance indices to drainage-wide abundances, a large-scale mark-recapture study was conducted from 2002 to 2007 using the Chapman modification to the Lincoln-Petersen estimator (Schaberg et al. 2012). The 2002 estimate violated the assumption of equal probability of recapture, and thus was excluded from this analysis (Schaberg et al. 2012). Tagging occurred in Kalskag, AK and recaptures were made by observing tagged fish as they passed weirs, so the mark-recapture estimates only accounted for in-river abundance upstream of the tagging site (S_u). Downstream abundance (S_d)

was estimated using the Parken et al. (2006) habitat-based model (Schaberg et al. 2012). Total observed (estimated) escapement was calculated:

$$S_y = S_u + S_d - H_u \tag{2.16}$$

where H_u is the harvest that occurred upstream of the tagging site. Uncertainty in S_u, S_d, and H_u were estimated using bootstrapping, predictive error from the Parken et al. (2006) regression model, and survey/estimation variation, respectively. Because the variance of a sum is the sum of the component variances:

$$\text{var}(S_y) = \text{var}(S_u) + \text{var}(S_d) - \text{var}(H_u) \tag{2.17}$$

The expected escapement $\hat{S}_y$ was fit to the observed escapement S_y given in equation 2.16 using a lognormal likelihood.

(4) Age-Composition – Age-composition proportions for the integrated model were the same as those used in the spawner-recruit analysis by Hamazaki et al. (2012), with additional years (2012-2014) obtained directly from ADF&G biologists. Those proportions were calculated by taking a weighted average of all age sampling projects including commercial and subsistence fisheries, Bethel test fishery, and weir projects (Bue et al. 2012). The result of this weighted average are vectors of calendar year proportions-at-age $q_{obs;y}$ that sum to one. These proportions were then used to inform the expected age proportions using a multinomial likelihood by multiplying the $q_{obs;y}$ vector by the effective sample size (n_y) for year y:

$$X_y = q_{obs;y} n_y \tag{2.18}$$

$$X_y \sim multi(q_y, n_y) \tag{2.19}$$

where

$$q_{y,a} = \frac{N_{y,a}}{N_y} \tag{2.20}$$

from the process submodel. In the multinomial distribution, the n_y specifies how closely the modeled expectation must fit to the observed data X_y, similar to the variance component in a normal likelihood (larger n results in stronger information content about age proportions and a closer model fit; Maunder 2011). The values of n_y were chosen by ADF&G such that age-composition data collected early in the data time series were more flexible in the model than more recently collected age composition data when the scale sampling efforts were more intensive and presumably more representative. For the time periods 1976-1999 and 2000-2014, n_y was set at 25 and 100, respectively following Hamazaki et al. (2012).

(5) Harvest Observations (Total Annual) – The original Bue et al. (2012) run reconstruction model assumed harvest was known perfectly. However, in the state-space framework, it is possible to model the harvest and observation processes that gives rise to the observed harvest estimates in order to include measurement error (i.e., uncertainty in harvest estimates). This component was divided into commercial and subsistence harvests, with each having different assumed observation variances. Since commercial harvest reporting is mandatory, there was assumed to be less observation error than for subsistence harvest. These harvests were modeled using a total finite harvest rate U_y which was further divided:

$$U_{com,y} = U_y \, p_{com,y} \tag{2.21}$$

$$U_{sub,y} = U_y \, (1 - p_{com,y}) \tag{2.22}$$

$$H_{com,y} = U_{com,y} N_y \tag{2.23}$$

$$H_{sub,y} = U_{sub,y} N_y \tag{2.24}$$

$$\hat{S}_y = N_y (1 - U_y) \tag{2.25}$$

where $p_{com,y}$ is the annual proportion of the total harvest rate that was made up of commercial harvest. These harvest components were fit using a lognormal likelihood. It was the $\hat{S}_y$ derived in

equation 2.25 that was used throughout the rest of the observation submodel (e.g., equation 2.12).

Sequential Analysis Structure

In contrast to the integrated analysis, the sequential analysis functioned by estimating abundance and the population dynamics (i.e., spawner-recruit) parameters in two separate and sequential models. The first model was a drainage-wide run reconstruction model (hereafter "run reconstruction") which was developed by Bue et al. (2012) following methods first proposed by Shotwell and Adkison (2004). The run reconstruction served to synthesize the escapement and harvest observations into calendar year run abundance estimates and uncertainty, expressed as a coefficient of variation on each run estimate (CV). Equations 2.12-2.17, 2.25 from the integrated model described above were based on the original run reconstruction formulae presented in Bue et al. (2012) and the two components are equivalent in nearly every regard. Primary differences between the observation submodel of the integrated analysis and the run reconstruction from the sequential analysis is that the latter is fit using maximum likelihood methods, it scales by fitting to a drainage-wide total abundance estimate based on mark-recapture rather than escapement, and assumes harvest is known without error.

In order to estimate the population dynamics parameters, the terminal model in the sequential analysis was a post-hoc Bayesian state-space spawner-recruit model (hereafter "post-hoc model"). This model was originally developed by Hamazaki et al. (2012) and was based on the aforementioned Fleischman et al. (2013) age-structured Bayesian state-space spawner-recruit model. The post-hoc model treated the run abundance estimates from the run reconstruction model as independently observed data with fixed uncertainty captured in the CVs on each run estimate. The post-hoc model was made up of equations 2.01-2.11 and 2.18-2.25 from the

integrated analysis. Note that measurement error and process variation in fish abundance were estimated in separate models under the sequential assessment.

Comparisons between the Integrated and Sequential Kuskokwim Assessments

In order to investigate the trade-offs of integrating the analysis, the most relevant model output from the sequential assessment (run reconstruction then post-hoc spawner-recruit analysis) was compared to the corresponding output of the integrated analysis. Important quantities for comparison to the integrated model included: (1) total run abundance from the run reconstruction and the expected run abundance from the post-hoc model, (2) key spawner-recruit parameters from the post-hoc model, (3) scaling and over-dispersion parameters in the run reconstruction components, and (4) biological reference points. In addition to point estimates (posterior means), uncertainty was expressed in terms of 95% Wald confidence intervals derived from the Hessian matrix (inverse variance-covariance matrix) for the run reconstruction and Bayesian 95% credible intervals for the integrated and post-hoc models. It is important to note that the equations for all model predictions and likelihoods were the same between the integrated model and the sequential analysis. The key difference between the two approaches was the component in the sequential analysis that linked the post-hoc model to the run reconstructed estimates via a likelihood. In the integrated model, the run abundance estimates were simply a required derived quantity, not information that the model was fit to.

To investigate potential biases, the spawner-recruit parameters of interest were further compared to a traditional ordinary least-squares linear regression technique that is more commonly applied to spawner-recruit analyses (e.g, Clark et al. 2009). To conduct this traditional analysis, the run abundance estimates (ignoring their uncertainty) were split into calendar year abundance-at-age according to age-composition information from scale counts and

the appropriate years and ages were summed to arrive at brood year returns (Table 1.01). To obtain brood year escapement, calendar year harvest estimates were subtracted from total calendar year abundance estimates. These brood year escapement and returns were then used in a linear regression:

$$\ln\left(\frac{R_y}{S_y}\right)=\ln(\alpha)-\beta S_y+\varepsilon_y \sim N(0,\sigma) \quad (2.26)$$

to obtain estimates of α, β, and σ. Note that this method ignores measurement uncertainty in the quantities R_y and S_y and assumes that the recruitment residuals are independent and identically distributed through time, which ignores any time series patterns. These assumptions make the traditional spawner-recruit analysis susceptible to both time series and error-in-variables biases (Walters 1985; Walters and Ludwig 1981). Uncertainty in the parameter estimates and derived reference points was estimated using parametric bootstrapping: randomization of the regression residuals, summation with the predicted values from the original fit, and re-estimation of the model parameters (Hamazaki et al. 2012). α, β, and σ were saved and biological reference points were calculated for each bootstrapped sample using equations 2.05-2.08.

Sensitivity Analysis

There are cases where a single dataset includes both measurement and process error and the model is required to separate these sources of variation under the state-space framework. Oftentimes, the model cannot parse out what variation is due to the underlying biological or fishery process and what variation is due to measurement. In these cases, one of the sources of variation must be assumed known. One example is the harvest model presented in equations 2.21-2.25. The variation in the observed harvest arises from two processes: (1) annual variation in the true U_y where fishers harvest fish from the annual run and (2) in the measured (estimated) perception of the total harvest. When provided with an annual data point to inform this

component, it is impossible for the model to partition which variation should lead to uncertainty in the harvest process and which should be assigned to measurement error. It is therefore necessary to provide an assumed variance, and for this case an assumed known observation error was provided and the model was allowed to handle process variation. This was conducted by assuming an observation CV. The CVs on harvest were combinations of output from harvest estimation models used by ADF&G and assumptions based on expert judgement (Hamazaki et al. 2012). The components of the model that included these fixed observation CVs were (1) commercial harvest, (2) subsistence harvest, and (3) the mark-recapture estimates of escapement. Model sensitivity to these assumptions was investigated by altering the assumed CV within reasonable ranges and comparing the resulting changes to the original model. All assumed variances were altered by 50% and 200% to assess the impact of being more or less certain about the corresponding estimates, respectively. Each sensitivity scenario was conducted in isolation of other scenarios so that any changes in model output could attributed to a single source.

Considering that the model was reliant on the mark-recapture estimates of escapement for scaling information, I thought it prudent to investigate the model sensitivity to biases in these estimates. The mark-recapture estimates were altered by ± 5%, 10%, and 20% and the model was fitted to the altered estimates. The relative uncertainty in these estimates was not altered (i.e., the assumed CV remained the same as the base model). Because these estimates constitute the principle scaling information, one would expect to see a proportional increase/decrease in the model expected escapement in not only the years with mark-recapture estimates, but in the whole escapement time series as well.

Computation

The integrated model was fit using Bayesian integration with MCMC methods to sample from the joint posterior probability distribution. MCMC sampling was conducted using parallel computing with the JAGS software ("Just Another Gibbs Sampler", Plummer 2013) implemented through R (R Core Development Team 2014) using the R package "R2jags" (Su and Yajima 2015). Prior distributions on all unknown parameters were uninformative and their structures were based on recommendations from Fleischman et al. (2013) and Bolker (2008) with necessary truncations to prevent the sampler from drawing implausible parameter values (e.g., log(α) had a diffuse normal prior truncated at zero). MCMC sampling was conducted using two chains with different initial values to verify convergence and to detect potential multiple solutions. Convergence of the chains was assessed with visual inspection of the posterior distribution sampled by each chain, trace plots, and the Gelman-Rubin statistic (Gelman et al. 2004). MCMC sampling of all Bayesian models (i.e., integrated model scenarios and post-hoc model) involved a burn-in period of 500,000 iterations, 1,000,000 post-burn-in iterations, and a thinning interval of 200 iterations, using two chains to ensure convergence. This resulted in a total of 10,000 posterior samples retained for analysis. The model converged under these specifications, as evidenced by Gelman-Rubin statistics of <1.05 for every estimated parameter. Point estimates (posterior mean) and Bayesian 95% credible intervals (2.5 and 97.5 percentiles of posterior distribution) for quantities of interest were calculated from their respective marginal posterior distributions.

RESULTS

Comparisons to the Sequential Kuskokwim Assessment

Run Abundance and Uncertainty

The integrated model performed similarly with regards to trends in total run abundance point estimates from both the run reconstruction and post-hoc model (Figure 2.01, upper panel). The integrated model exhibited a mean 2% decrease in run abundance from the run reconstruction, and a mean 3% decrease from post-hoc model. Both the integrated model and the post-hoc model exhibited some shrinkage in run abundance, which is a statistical characteristic of hierarchical models in which quantities at intermediate levels are pulled to the values suggested by higher-level distributions (i.e., hyperdistributions) since all sources of information are simultaneously considered by the model. In this case, the spawner-recruit component treated the extreme high and low run abundances as unlikely to have occurred and tended to pull them toward the mean spawner-recruit curve. This was possible because the run estimates used by the models were not fixed, but had uncertainty and flexibility and could thus be adjusted to satisfy the spawner-recruit likelihood. Run abundance shrank the most when the corresponding CV was large, (e.g., 1981 and 1986; Figure 2.01, lower panel). This was because the more uncertain the information, the less the model is required to fit to it, and the more ability the model has to shrink towards the population mean (i.e., the spawner-recruit prediction curve; Zhou et al. 2012). Both the post-hoc model and the integrated model shrank by approximately the same amount and in the same years.

All three models exhibited a slightly decreasing temporal trend in run abundance CV (Figure 2.01, lower panel), due to the addition of more escapement monitoring projects through time (Table 2.01). The run reconstruction CVs were the most variable between years, while the integrated and post-hoc models resulted in CVs that fluctuated less from year to year (Figure

2.02). This finding resulted from total abundance being estimated nearly independently each year in the run reconstruction (tributary proportionality scalars were shared by all years, which links them) whereas years were linked explicitly in the integrated and post-hoc models via the spawner-recruit relationship. For example, if escapement in one year was uncertain due to very few monitoring projects, it could be informed by later years based on how many recruits it produced. The CVs were relatively similar between the post-hoc model and the integrated model, although the integrated model did consistently show slightly more uncertainty in run abundance (mean 1.2 CV percentage points greater than post-hoc model).

Spawner-Recruit Parameters and Biological Reference Points

Overall, the spawner-recruit point estimates between the integrated and post-hoc models were similar (Table 2.02). The integrated model indicated that the maximum productivity of the stock (α) was between 2.45 and 12.36 recruits per spawner with 0.95 probability whereas the post-hoc model indicated it was between 2.39 and 11.74. Although the credible bounds on α were slightly wider for the integrated model, the post-hoc model estimated slightly wider credible intervals for most other spawner-recruit parameters of interest (Table 2.02). It is clear that overall, both the integrated and post-hoc models treated the spawner-recruit components of the assessment similarly (Figure 2.02). When the traditional linear regression technique was implemented on the run reconstruction estimates, the estimate of α was much higher (7.29; 95% CI 5.62-9.34) than both the integrated and post-hoc models. The linear regression technique showed approximately the same amount of residual variation in the spawner-recruit relationship (σ_R = 0.29; 0.20-0.36) as the integrated (σ_R = 0.23; 0.15-0.34) and post-hoc (σ_R = 0.24; 0.16-0.35) models. In all model runs, the γ parameters (those governing the expected frequencies of fish maturing at age from all brood years) were the slowest mixing (i.e., showed the most MCMC autocorrelation), along with all parameters that were derived from them. The mean

probability of maturing-at-age across brood years (π_a) were essentially the same between the integrated and post-hoc models (Table 2.02).

The amount of serial autocorrelation in the recruitment time series (ϕ), had very similar posterior distributions between both models (Table 2.02). Based on the posterior mean of ϕ under both models, there was a large amount of serial autocorrelation in the recruitment residuals, indicating the potential for time series bias if not accounted for.

With regards to biological reference points, the post-hoc and integrated models resulted in relatively similar point estimates, yet the later estimated wider credible bounds for all three quantities (Table 2.02). The traditional regression approach did not return reference points that were systematically higher or lower than the two Bayesian models, however the confidence bounds were much narrower.

Index Scalars and Over-dispersion Parameters

The proportionality coefficients that controlled the scaling of weir and aerial survey counts to the drainage-wide mark-recapture estimates were very similar between the run reconstruction and the integrated model (integrated scalars mean 3.7% larger than run reconstruction; Figure 2.03). This finding showed that the two models used the escapement index information similarly: on average, each tributary count made up the same proportion of the total escapement in both the run reconstruction and the integrated model. It is clear that both models dealt with over-dispersion similarly as well, with the integrated model estimating slightly more over-dispersion in nearly all projects (Figure 2.04).

Sensitivity Analysis

Assumed Observation CV on Harvest Estimates

When the assumed variances on commercial and subsistence annual harvests were halved or doubled, the model responded by fitting more closely or loosely, respectively (Figure 2.05).

Doubling the CV down-weights those data and loosens the extent to which the model must fit to them (Francis 2011). Both commercial and subsistence harvest exhibited this behavior, although when the subsistence harvest CV was doubled, it lead to much more variation in the expected harvest than did commercial harvest. This discrepancy was due to the greater assumed baseline CV on subsistence harvest estimates (CV varied annually between 1%-10%) than commercial harvest (2% CV in all years).

Assumed Observation CV on Mark-Recapture Estimates of Escapement

Altering the precision of the 2003-2007 drainage-wide escapement estimates had a very small effect on the model point estimates of escapement in those years (Figure 2.06). When the CV was doubled, the point estimates of escapement decreased by 5% on average from the base model estimates. When the assumed CV was halved, the escapement uncertainty in the corresponding years was reduced by 33% on average when compared to the base model. Similarly, when the assumed CV was doubled, the escapement uncertainty in those years increased by 49% on average. Not only did these changes in assumed variances affect uncertainty in the years with mark-recapture estimates, but the uncertainty the whole escapement time series was reduced or increased depending on the scenario.

Sensitivity to Changing the Drainage-Wide Mark-Recapture Estimate

When the sensitivity of the model to biases in the scaling information (i.e., drainage-wide mark-recapture estimates) was investigated, the model responded by scaling with the altered estimates (Figure 2.07). Changing the mark-recapture estimate by ±5%, 10%, and 20% resulted in average changes of ±4%, 9%, and 18%, respectively. These percent changes were consistent for years with mark-recapture estimates and the whole time series (Figure 2.08).

DISCUSSION

With the analyses presented in this chapter, it is clear that the integrated model is a feasible model formulation for the Kuskokwim River Chinook salmon fishery assessment. The model converged well, did not show any major MCMC or residual problems, and provided very similar estimates to the two-step assessment approach (which is currently used by ADF&G). Similar point estimates were expected, as both assessment approaches used the same data and the same equation structures (e.g. same tributary count model, same spawner-recruit function, etc.). The key difference in the two analyses is that under the sequential analysis, the run reconstruction was fit with maximum likelihood estimation that provided run estimates and uncertainty to the post-hoc model, whereas this happened simultaneously under the integrated model in a single Bayesian framework. The overall consistency in estimates between the two approaches suggested that integrating the analysis did not change the inference regarding stock abundance, productivity, carrying capacity, or management recommendations.

Somewhat contrary to the *a priori* expectations, however, was the similarity in the posterior uncertainty in quantities of interest between the integrated and post-hoc models. It was expected that the integrated model would lead to substantially greater posterior uncertainty in quantities like run abundance, spawner-recruit parameters, and biological reference points due to the direct interaction between the observation-level data (e.g., weir and aerial survey counts) and the process (i.e., spawner-recruit) submodel. As these analyses have shown, the extent of the increase in uncertainty was not as large as expected. Posterior uncertainty in run abundance under the integrated model was slightly higher than the post-hoc model, suggesting it accounted for measurement error more fully. This difference is likely due to the assumption of statistical independence of the run abundance estimates under the post-hoc model. After investigating the correlations in estimated run abundances from the run reconstruction, it was found that the run

estimates were indeed correlated in the run reconstruction model (0.30 mean correlation, 0.57 maximum correlation). The post-hoc model did not carry these correlations forward by treating them as independent observations, which ignored that there was information about other estimates contained in any one estimate and thus resulted in underestimation of the posterior uncertainty in run abundance. One advantage of the integrated model is that it was able to internally address these correlations by estimating the abundances within the same model, as stated by Maunder and Punt (2013). The integrated model estimated slightly more uncertainty in α and D, but all other spawner-recruit parameters had slightly more uncertainty under the post-hoc model. The integrated model did result in more uncertainty in the biological reference points, but likely not enough to alter the management recommendations. This modeling exercise gave credence to the two-step assessment in terms of its ability to deal with measurement uncertainty by capturing it with the CV on the run estimates from the run reconstruction model.

The integrated model proved to be robust to parametric uncertainty, particularly with regards to the assumed fixed CV on the mark-recapture scaling information. The expectation was that when the CVs were increased on the mark-recapture estimates, posterior uncertainty in escapement in that year would increase and vise-versa. Additionally, since the mark-recapture estimates of escapement were the only scaling information provided to the model, changing their uncertainty should not substantially alter the point estimates of escapement in those years. The results of this exercise confirmed these expectations. Even when the CVs on the estimates were doubled, the model showed only minor deviations from the base model point estimates. These deviations were all negative, which showed that doubling the CV on the scaling information may give the model more flexibility to shrink towards the abundance suggested by the spawner-recruit curve and maturation schedule. The model was still robust to parametric uncertainty,

however this finding illustrated that weaker scaling information can facilitate shrinkage (Zhou et al. 2012). The major consequence of doubling the CV, however, was that the posterior uncertainty of abundance quantities was increased, which is what would be expected when weaker scaling information is provided to the model.

As previously mentioned, the only scaling information provided to the model were the drainage-wide estimates of escapement from mark-recapture (and lower river habitat expansion). Thus, altering these point estimates should result in a proportional change in the expected escapement. The results of this exercise confirmed this expectation, not only for escapement in the years with mark-recapture estimates but for the entire escapement time series. This issue is related more to the accuracy of the mark-recapture estimate than the performance of the model. The mark-recapture estimates represent the best-available scientific understanding of drainage-wide escapement, and so sensitivity to these estimates is necessary.

This being said, there are several areas in which the integrated model performed sub-optimally. One case is the slow mixing of the maturation schedule component. This is one of the most complex portions of the model and it came as no surprise that it mixed slowly. In the early years of the data time series, the scale count frequencies were weakly informative and there were some years with missing scale counts. In these cases, the model could satisfy the data in many different ways so the parameters in this component mixed slowly and MCMC samples were highly correlated. The inclusion of the Dirichlet random effects aided this problem, as the model could use the more informative years to inform the central tendency of the proportions mature-at-age (π_a). However, this formulation assumes that the central tendency does not change over time (all brood year proportions are drawn from the same multivariate distribution) which may not be

realistic given size-selective fishing pressure and potentially biased age sampling. These topics will be dealt with in more detail in Chapter 3.

The slow mixing behavior of the maturation schedule required a large number of posterior samples to be drawn with a wide thinning interval to achieve convergence. This resulted in long run times for the integrated model, nearly 24 hours. The post-hoc model only required approximately eight hours to complete the same number of posterior samples and burn-in period. This extended time period is cumbersome when running a large amount of sensitivity analyses, like those presented in this chapter, but is relatively irrelevant when the model has been finalized and needs only to be run once every year. This disadvantage was expected and is consistent with the literature (e.g., Maunder and Punt 2013) as the integrated analysis was a more complex model involving more priors, data, and likelihoods than the post-hoc model in the sequential analysis.

I presented this analysis as moving further down the continuum towards fully integrated analyses because there are still estimates that are passed to the model as "data" (in the sense that they are fit to in the joint likelihood). One key example is the mark-recapture estimates which represent a summary of a large number of tagged and recaptured fish observations. It would be possible to incorporate the mark-recapture estimation model within this assessment to make it more fully integrated, however, these analyses have shown that this is likely not necessary. It seems that fitting to their estimates and including their uncertainty in the form of a CV is an adequate expression of the information content of these data.

Integrated analyses, particularly Bayesian state-space models, are gaining popularity throughout the state of Alaska and in the stock assessment and ecological literature as a whole (Maunder and Punt 2013; Schaub and Abadi 2011). The overall theme of using a Bayesian state-

space framework for addressing the problems in the traditional spawner-recruit analysis is apparent in the present analysis. The traditional spawner-recruit analysis yielded a higher α value which is potentially positively biased due to the time series problems inherent to the linear regression approach, as noted by Walters (1985) and Walters and Ludwig (1981). However, this did not lead to systematically higher or lower estimates of biological reference points, as one might expect. Outside of the similar reference point estimates under the traditional approach, it was clear that the Bayesian state-space approaches increased the uncertainty in these quantities, likely due to the incorporation of measurement error into the spawner-recruit analysis. This alone is a meritorious reason to favor the state-space spawner-recruit approach. If one is to manage a stock based on biological reference points, it is critical that the uncertainty in those quantities be fully addressed and taken into account in management objectives and actions.

Other investigators have shown promise for the Bayesian state-space approaches to spawner-recruit analyses for Pacific salmon including Meyer and Millar (2001) using pink salmon data from the Fraser River in British Columbia, the aforementioned Fleischman et al. (2013) analysis on the Karluk River Chinook salmon stock, Fleischman and Borba (2009) with Yukon fall chum salmon, the work with Kenai Chinook salmon stocks by McKinley and Fleischman (2013) and Fleischman and McKinley (2013), and a meta-analysis of Alaskan Chinook stocks by Catalano (2012). All of these analyses used the Bayesian state-space spawner-recruit analysis framework presented here (although some were two-step analyses) and found reasons to suggest that this approach is superior to the traditional linear regression technique in terms of dealing with statistical problems and accounting for measurement error. Clearly, this approach is general enough for application to many different stocks and flexible enough to deal

with multiple different species of anadromous Pacific salmon with various life histories and population parameters.

Although the integrated model and the two-step analysis provided very similar overall estimates, there are still advantages to the integrated analysis. The most obvious reason is that the whole process is contained in a single model, which makes for straightforward implementation by biologists and a seamless framework for sensitivity analysis. All of the sensitivity scenarios presented in this chapter were conducted by changing several lines of code and re-running the model. Under the two-step approach, one would need to alter the run reconstruction, make note of the changes, and then pass the altered estimates through to the post-hoc model. In the integrated analysis, this process was seamless, and any changes in the model were reflected in a single joint posterior probability distribution. Another advantage to the integrated analysis is the fact that the sequential analysis forced the run reconstruction model to estimate each year's abundance in isolation of all other data (with the exception of the common tributary scalars across all years within a single project). There is no intrinsic link between years under the run reconstruction, however, there is in reality. In the real system, counts made in four consecutive years are all counting some proportion of fish that were all from the same brood year produced by the same number of spawners, creating a link between years. Integrating the analysis allowed the run estimates to be informed by the spawner-recruit analysis (and vice-versa) which accounts for this very real time linkage which ultimately leads to a more realistic model, regardless of how similar the estimates are to the two-step approach. This sort of information sharing is one of the primary advantages to an integrated analysis (Maunder 2011; Maunder and Punt 2013). One could argue that integrated models like the one presented in this chapter are advantageous purely because of this added realism.

REFERENCES

Blain, B.J., T.R. Hansen, J.N. Clark, L.M. Robbins, and K.L. Schaberg. 2014. Salmon escapement monitoring on the Kuskokwim River, 2012. Alaska Department of Fish and Game, Fishery Data Series No. 14-34, Anchorage, AK.

Bolker, B.M. 2008. Ecological models and data in R. Princeton University Press, New Jersey.

Brooks E.N and J.J. Deroba. 2015. When "data" are not data: the pitfalls of post hoc analyses that use stock assessment model output. Canadian Journal of Fisheries and Aquatic Sciences. 72(4): 634-641.

Bue, B.G. 1986. Effects of gill net selectivity on sockeye salmon in the Egegik and Naknek-Kvichak Districts, Bristol Bay, Alaska. University of Alaska, Fairbanks.

Bue, B.G., K.L. Schaberg, Z.W. Liller, and D.B. Molyneaux. 2012. Estimates of the historic run and escapement for the Chinook salmon stock returning to the Kuskokwim River, 1976-2011. Alaska Department of Fish and Game, Report to the Board of Fisheries, Anchorage.

Clark, R.A., D.R. Bernard, and S.J. Fleischman. 2009. Stock-recruitment analysis for escapement goal development: a case study of Pacific salmon in Alaska. Pages 743-757 *in* C.C. Krueger and C.E. Zimmerman, ed. Pacific salmon: ecology and management of western Alaska's populations. American Fisheries Society, Symposium 70, Bethesda, Maryland.

Fleischman, S.J. and B.M. Borba. 2009. Escapement estimation, spawner-recruit analysis, and escapement goal recommendation for fall chum salmon in the Yukon River drainage. Alaska Department of Fish and Game, Fishery Manuscript Series No. 09-08, Anchorage.

Fleischman, S.J., M.J. Catalano, R.A. Clark, and D.R. Bernard. 2013. An age-structured state-space stock-recruit model for Pacific salmon (*Oncorhynchus* spp.). Canadian Journal of Fisheries and Aquatic Sciences. 70(3): 401-414.

Fleischman S.J., and T.R. McKinley. 2013. Run reconstruction, spawner-recruit analysis, and escapement goal recommendation for late-run Chinook salmon in the Kenai River. Alaska Department of Fish and Game, Fishery Manuscript Series No. 13-02, Anchorage.

Fournier, D. and C.P. Archibald. 1982. A general theory for analyzing catch at age data. Canadian Journal of Fisheries and Aquatic Sciences. 39(8): 1195-1207

Francis, R.I.C. C., 2011. Data weighting in statistical fisheries stock assessment models. Canadian Journal of Fisheries and Aquatic Sciences. 68(6): 1124-1138.

Gelman, A., J.B. Carlin, H.S. Stern, and D.B. Rubin. 2004. Bayesian data analysis. Second ed. CRC/Chapman & Hall, Boca Raton, Florida.

Hamazaki, T., M.J. Evenson, S.J. Fleischman, and K.L. Schaberg. 2012. Spawner-recruit analysis and escapement goal recommendation for Chinook salmon in the Kuskokwim River Drainage. Alaska Department of Fish and Game, Fishery Manuscript Series No. 12-08, Anchorage.

Hansen, T.R. and B.J. Blain. 2014. Salmon escapement monitoring in the Kuskokwim River, 2013. Alaska Department of Fish and Game, Fishery Data Series No. 14-54, Anchorage, AK.

Hilborn, R. 1985. Simplified calculation of optimum spawning stock size from Ricker's stock recruitment curve. Canadian Journal of Fisheries and Aquatic Sciences. 42(11): 1833-1834.

Hilborn, R., and C.J. Walters. 1992. Quantitative fisheries stock assessment: choice, dynamics, and uncertainty. Dluwer Academic Publishers, Boston, Massachusetts.

Hilborn, R., and M. Mangel. 1997. The ecological detective: confronting models with data. Princeton University Press, New Jersey.

Irwin, B.J., M.J. Wilberg, M.L. Jones, and J.R. Bence. 2011. Applying structured decision making to recreational fisheries management. Fisheries 36(3): 113-122.

Linderman, J.C., Jr. and D.J. Bergstrom. 2009. Kuskokwim management area: salmon escapement, harvest, and management. Pages 541-599 *in* C.C. Krueger and C.E. Zimmerman, ed. Pacific salmon: ecology and management of western Alaska's populations. American Fisheries Society, Symposium 70, Bethesda, Maryland.

Maunder, M.N. 2001. Integrated tagging and catch-at-age analysis (ITCAAN). Pages 123-146 *in* G.H. Kruse, N. Bez, A. Booth, M.W. Dorn, S. Hills, R.N. Lipcius, D. Pelletier, C. Roy, S.J. Smith, and D. Witherell, ed. Spatial processes and management of fish populations. Alaska Sea Grant College Program Report No. AK-SG-01-02, University of Alaska, Fairbanks.

Maunder, M.N. 2011. Review and evaluation of likelihood functions for composition data in stock-assessment models: estimating the effective sample size. Fisheries Research. 109(2): 311-319.

Maunder, M.N. and A.E. Punt. 2013. A review of integrated analysis in fisheries stock assessment. Fisheries Research. 142:61-74.

McCarthy, M.A. 2007. Bayesian methods for ecology. Cambridge University Press, New York.

McKinley, T.R., and S.J. Fleischman. 2013. Run reconstruction, spawner-recruit analysis, and escapement goal recommendation for early-run Chinook salmon in the Kenai River. Alaska Department of Fish and Game, Fishery Manuscript Series No. 13-03, Anchorage.

Meyer, R. and R.B. Millar. 2001. Bayesian dynamic modeling of stock-recruitment relationships. Technical Report STAT 0004. Department of Statistics, University of Auckland, Auckland, New Zealand.

Michielsens, C.G.J., M.K. McAllister, S. Kuikka, S. Mantyniemi, A. Romakkaniemi, T. Pakarinen, L. Karlsson, and L. Uusitalo. 2008. Combining multiple Bayesian data analyses in a sequential framework for quantitative fisheries stock assessment. Canadian Journal of Fisheries and Aquatic Sciences. 65(5): 962-974.

Parken, C.K., R.E. McNicol, and J.R. Irvine. 2006. Habitat-based methods to estimate escapement goals for data limited Chinook salmon stocks in British Columbia, 2004. Department of Fisheries and Oceans, Canadian Scientific Advisory Secretariat Research Document 2006/083.

Plummer, M. 2013. JAGS Version 3.4.0 user manual.

R Development Core Team. 2014. R: A Language and Environment for Statistical Computing. R Foundation for Statistical Computing. Version 3.1.0. Vienna, Austria. http://www.R-project.org.

Ricker, W.E. 1954. Critical statistics from two reproduction curves. Journal of the Fisheries Research Board of Canada. 11(5):559-623.

Royale, J.A. and R.M. Dorazio. 2008. Hierarchical modeling and inference in ecology: the analysis of data from populations, metapopulations, and communities. Academic Press, San Diego, CA. 444 pp.

Schaberg, K.L., Z.W. Liller, D.B. Molyneaux, B.G. Bue, and L. Stuby. 2012. Kuskokwim River Chinook salmon run estimates, 2002-2007. Alaska Department of Fish and Game, Fishery Data Series No. 12-36, Anchorage, AK.

Schaub, M. and F. Abadi. 2011. Integrated population models: a novel analysis framework for deeper insights into population dynamics. Journal of Ornithology 152 (Suppl 1): S227-S237.

Schindler, D., C. Krueger, P. Bisson, M. Bradford, B. Clark, J. Conitz, K. Howard, M. Jones, J. Murphy, K. Myers, M. Scheuerell, E. Volk, and J. Winton. Artic-Yukon-Kuskokwim Chinook Salmon Research Action Plan: Evidence of Decline of Chinook Salmon Populations and Recommendations for Future Research. Prepared for the AYK Sustainable Salmon Initiative (Anchorage, AK). v+70 pp.

Shotwell, S.K., M.D. Adkison. 2004. Estimating indices of abundance and escapement of Pacific salmon for data-limited situations. Transactions of the American Fisheries Society 133(3):538-558.

Su, Y. and M. Yajima. 2015. R2jags: Using R to run "JAGS". R package version 0.5.6. http://CRAN.R-project.org/package =R2jags.

Walters, C.J. 1985. Bias in the estimation of functional relationships from time-series data. Canadian Journal of Fisheries and Aquatic Sciences. 44(1): 147-149.

Walters, C.J., and D. Ludwig. 1981. Effects of measurement errors on the assessment of stock-recruitment relationships. Canadian Journal of Fisheries and Aquatic Sciences. 38(6): 704-710.

Walters, C.J. and S.J.D. Martell. 2004. Problems in the assessment of stock-recruitment relationships. Ch. 7. Pages 151-178 *in* Fisheries ecology and management. Princeton University Press, New Jersey.

Zhou, S., S. Yin, J.T. Thorson, A.D.M Smith, and M. Fuller. 2012. Linking fishing mortality reference points to life history traits: an empirical study. Canadian Journal of Fisheries and Aquatic Sciences. 69(8): 1292-1301.

CHAPTER 2
FIGURES

Figure 2.01 Estimated total run abundance (upper) and corresponding CVs (lower) from three models: the Bue et al. (2012) run reconstruction (MLE RR), the Hamazaki et al. (2012) post-hoc spawner-recruit analysis (Post-Hoc SR), and the integrated model.

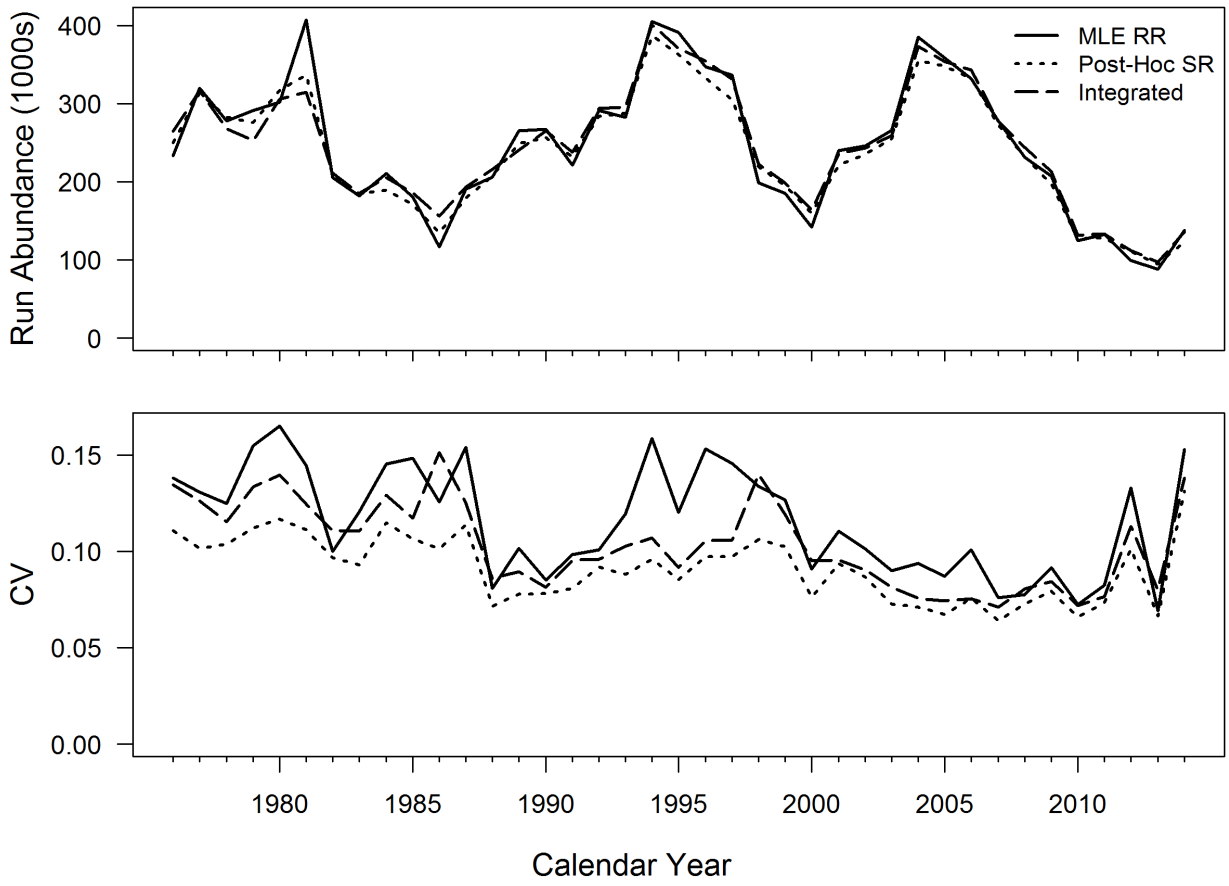

Figure 2.02 Spawner-recruit relationships from the integrated (upper) and post-hoc (lower) models. Error bars on points represent the 95% Bayesian credibility intervals on escapement-recruitment pairs and gray curves are 95% Bayesian credibility intervals for predicted recruitment given stock size. The dashed line represents 1:1 replacement.

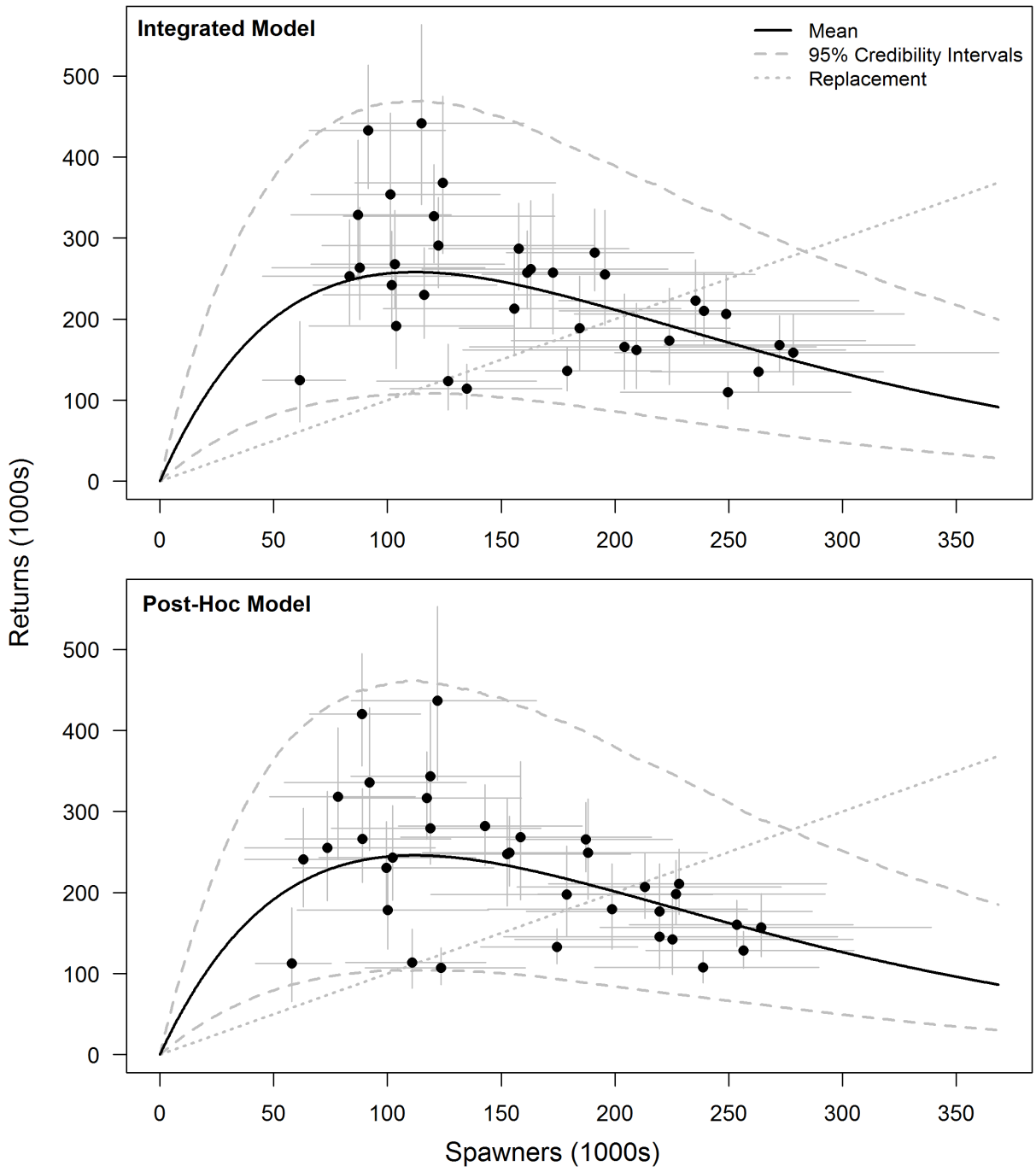

Figure 2.03 Proportionality coefficient estimates from the integrated model (gray bars) and the Bue et al. (2012) run reconstruction. (W) denotes a weir project and (A) denotes an aerial survey. Error bars are 95% Bayesian credibility intervals and 95% confidence intervals for the integrated and Bue et al. (2012) models, respectively.

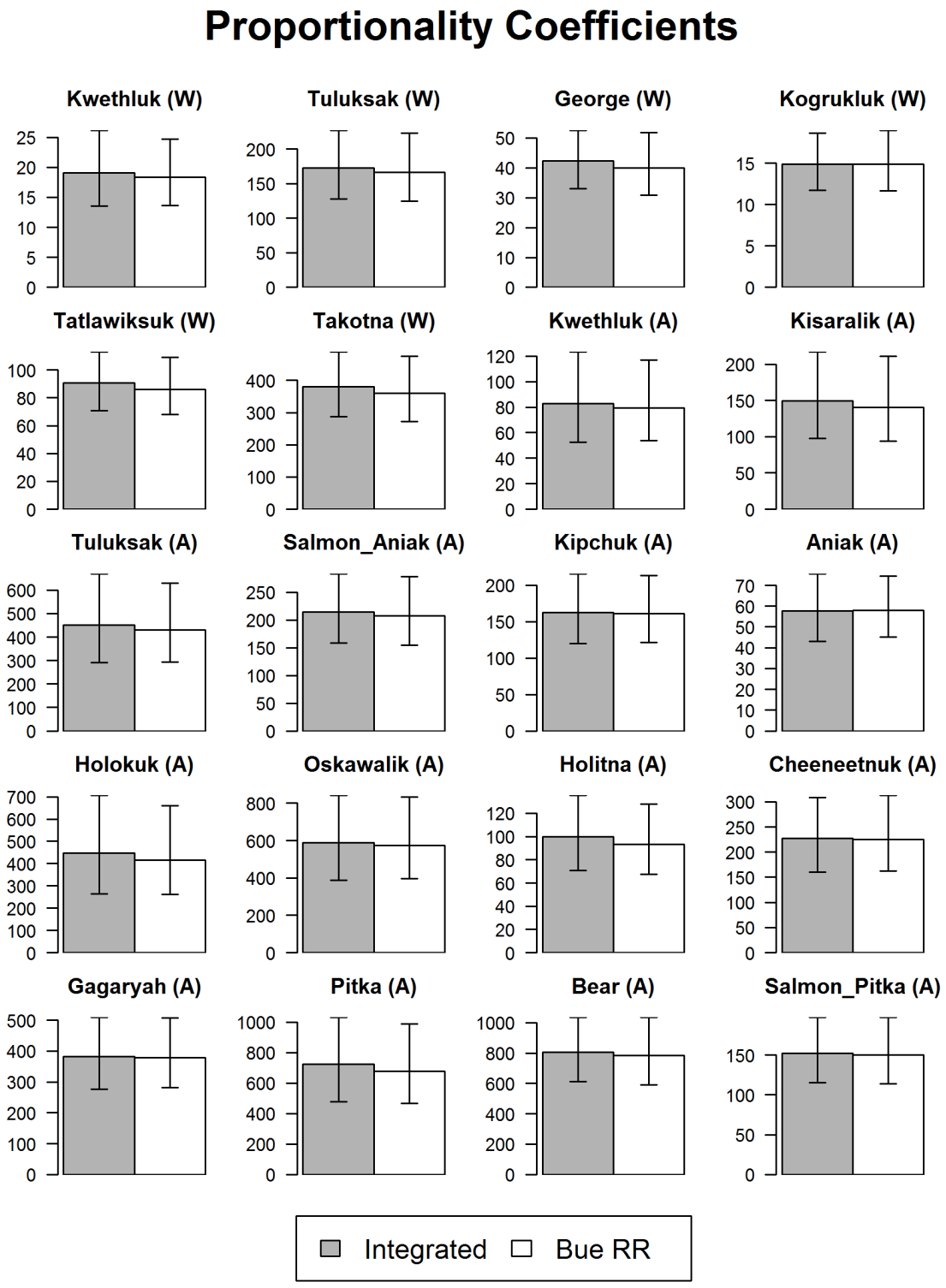

Figure 2.04 Over-dispersion parameter estimates from the integrated model (gray bars) and the Bue et al. (2012) run reconstruction (white bars). Error bars are 95% Bayesian credibility intervals and 95% confidence intervals for the integrated and Bue et al. (2012) models, respectively.

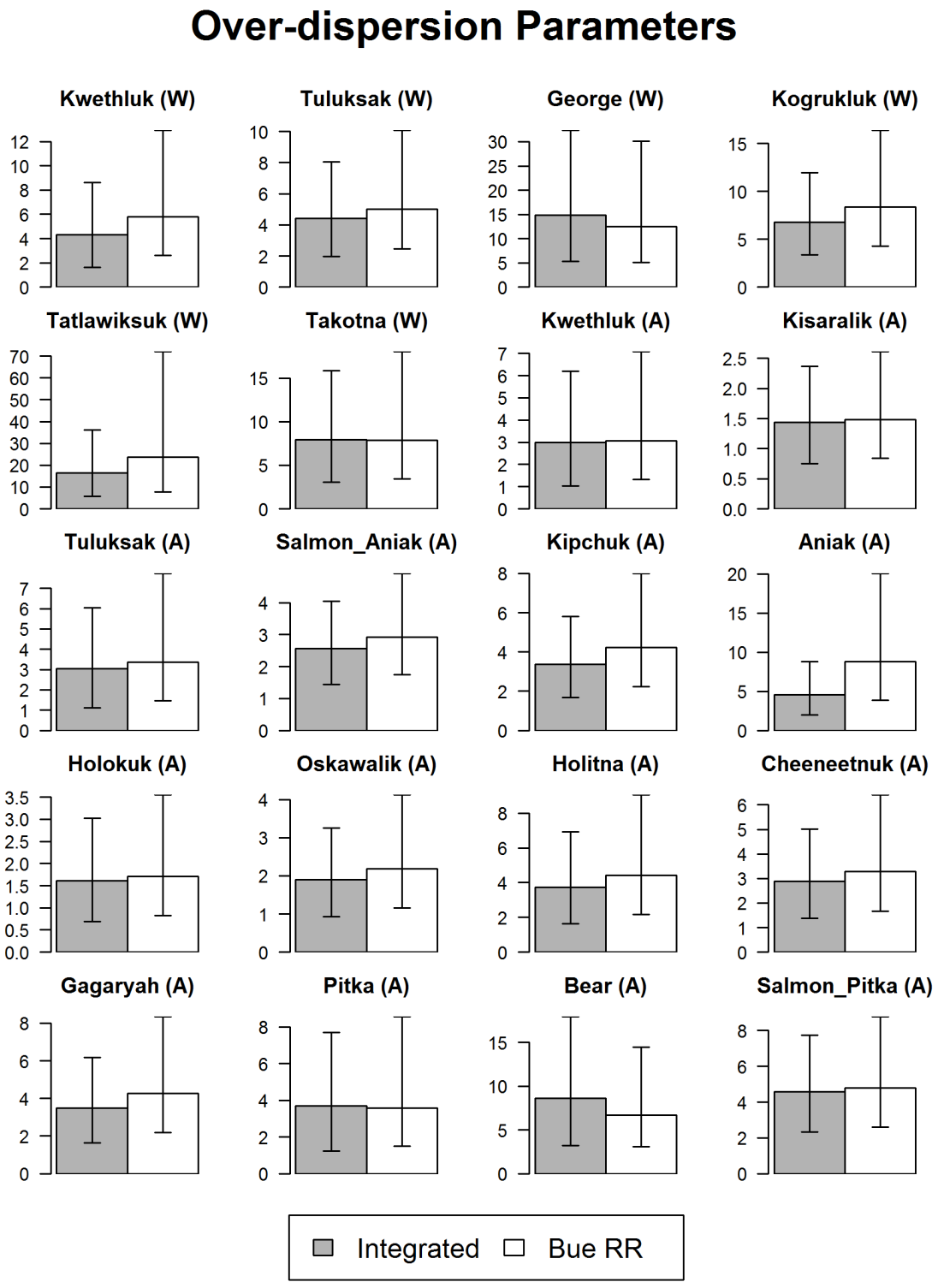

Figure 2.05 Harvest residuals from the integrated model under three observation CV sensitivity scenarios. Each scenario was conducted in isolation of the others.

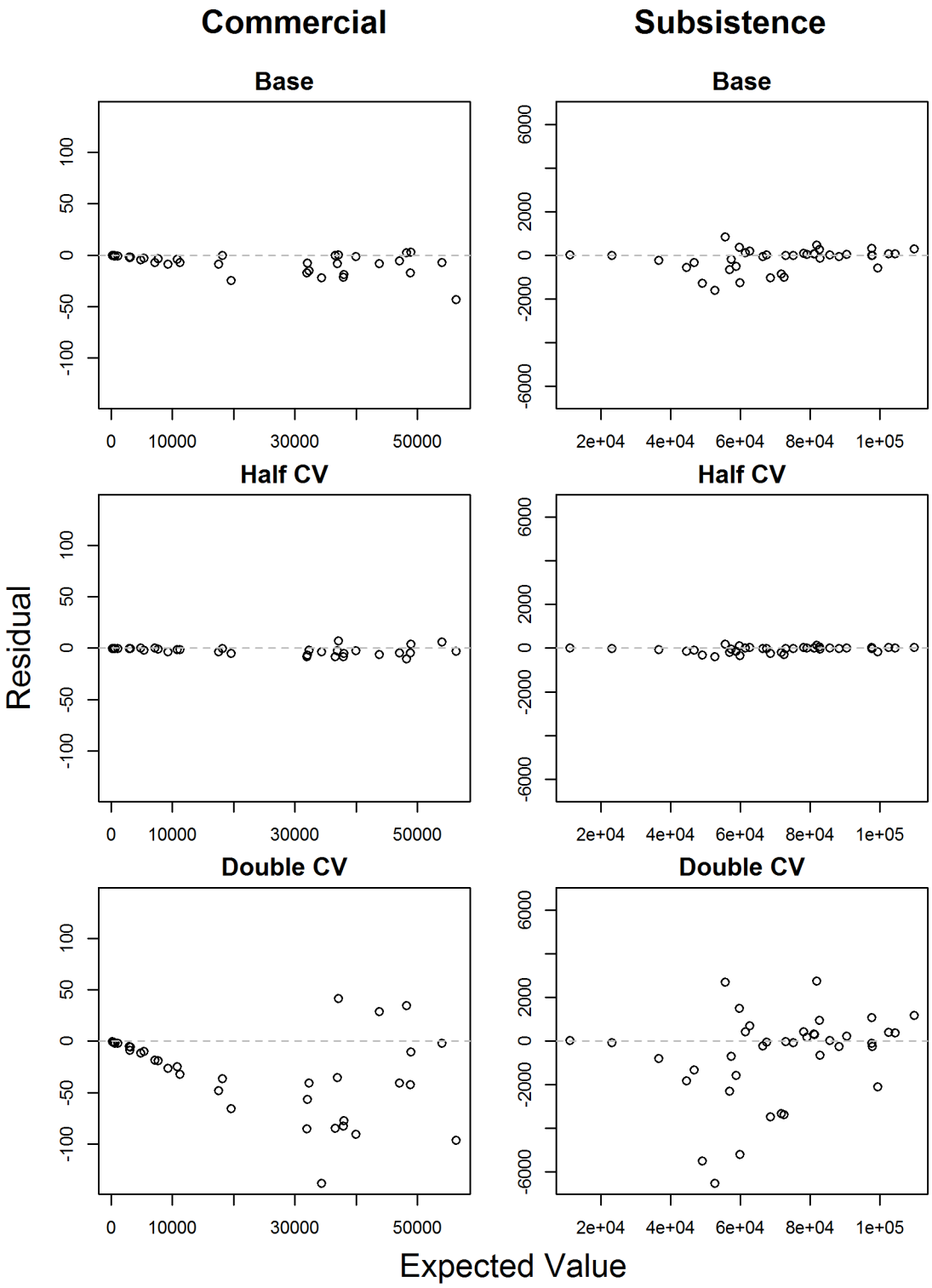

Figure 2.06 The effect of changing the observation variance on the mark-recapture estimates reported by Schaberg et al. (2012). Uncertainty on Schaberg et al. (2012) estimates are shown as ±1SD; the Bayesian models are 95% credibility intervals. Only years with mark-recapture estimates are shown.

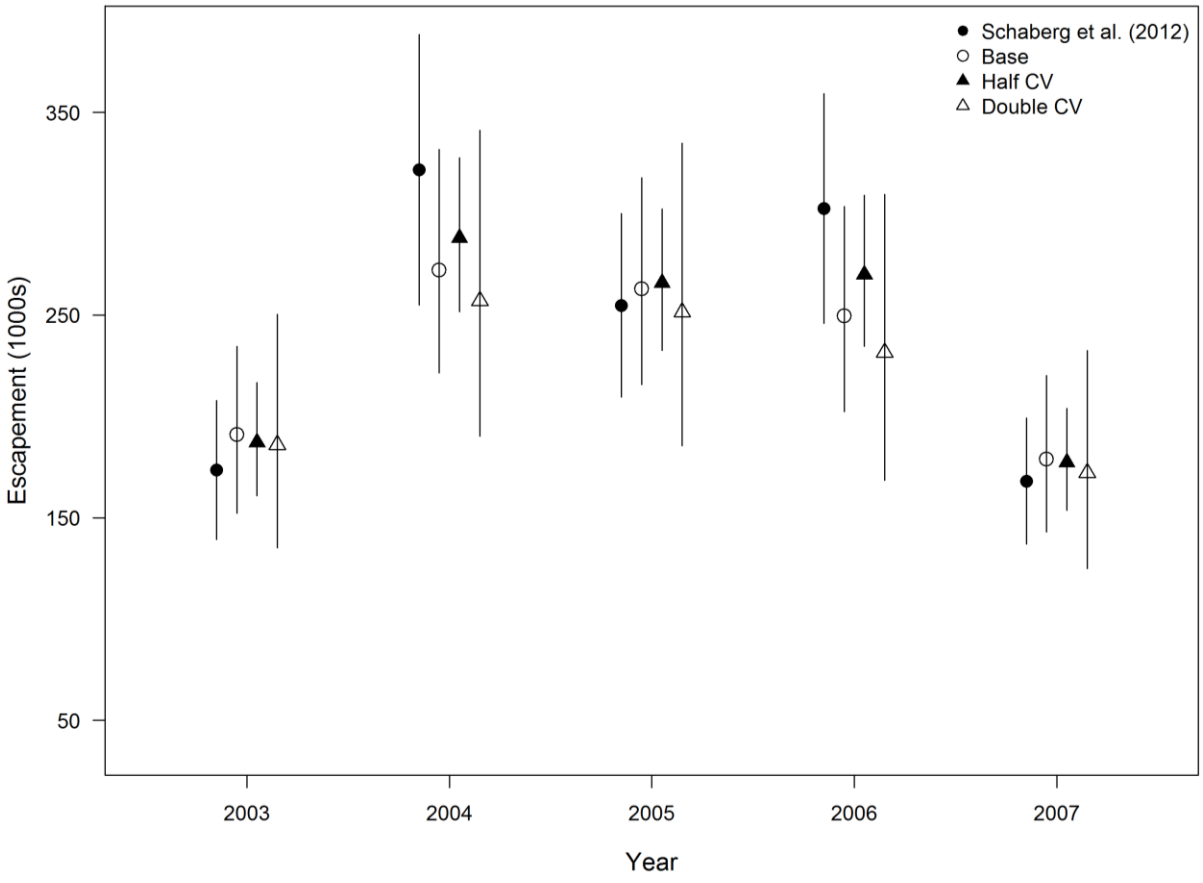

Figure 2.07 The effect of changing the mark-recapture estimate of drainage-wide escapement by ± 5%, 10%, and 20% on the expected escapement in those years.

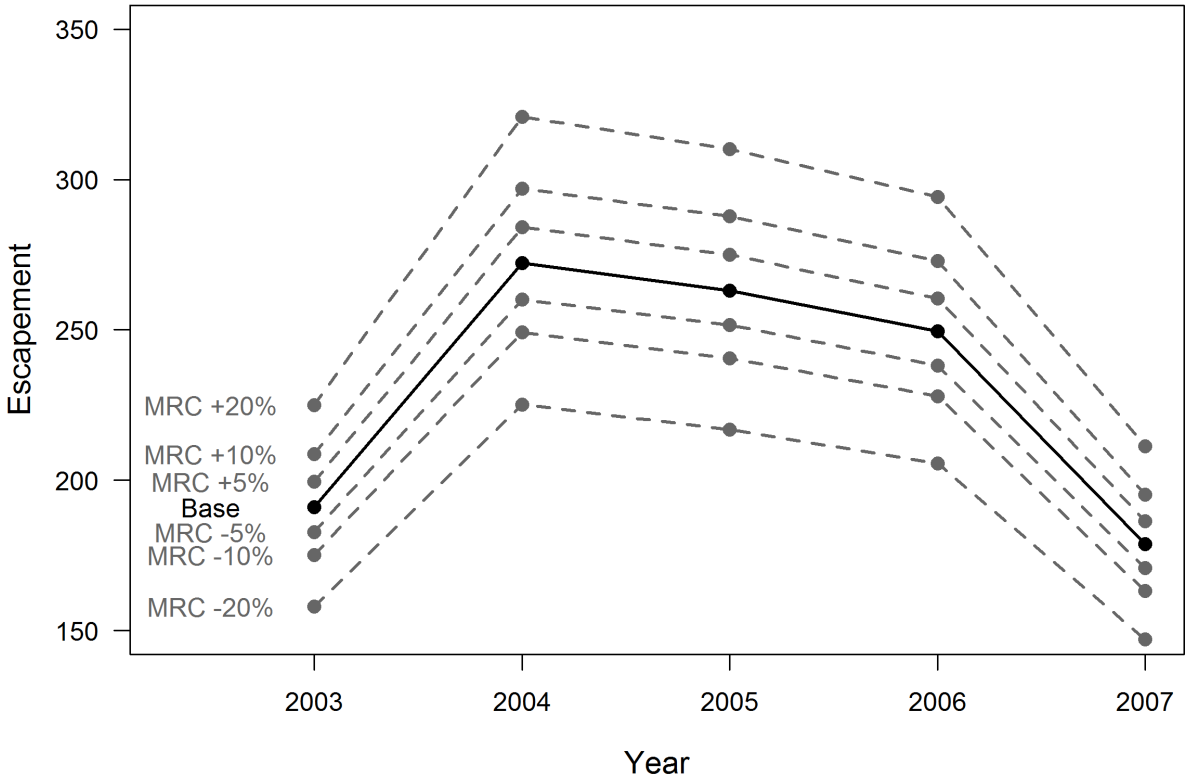

Figure 2.08. The effect of changing the mark-recapture estimate of drainage-wide escapement by ± 5%, 10%, and 20% on the expected escapement in all years.

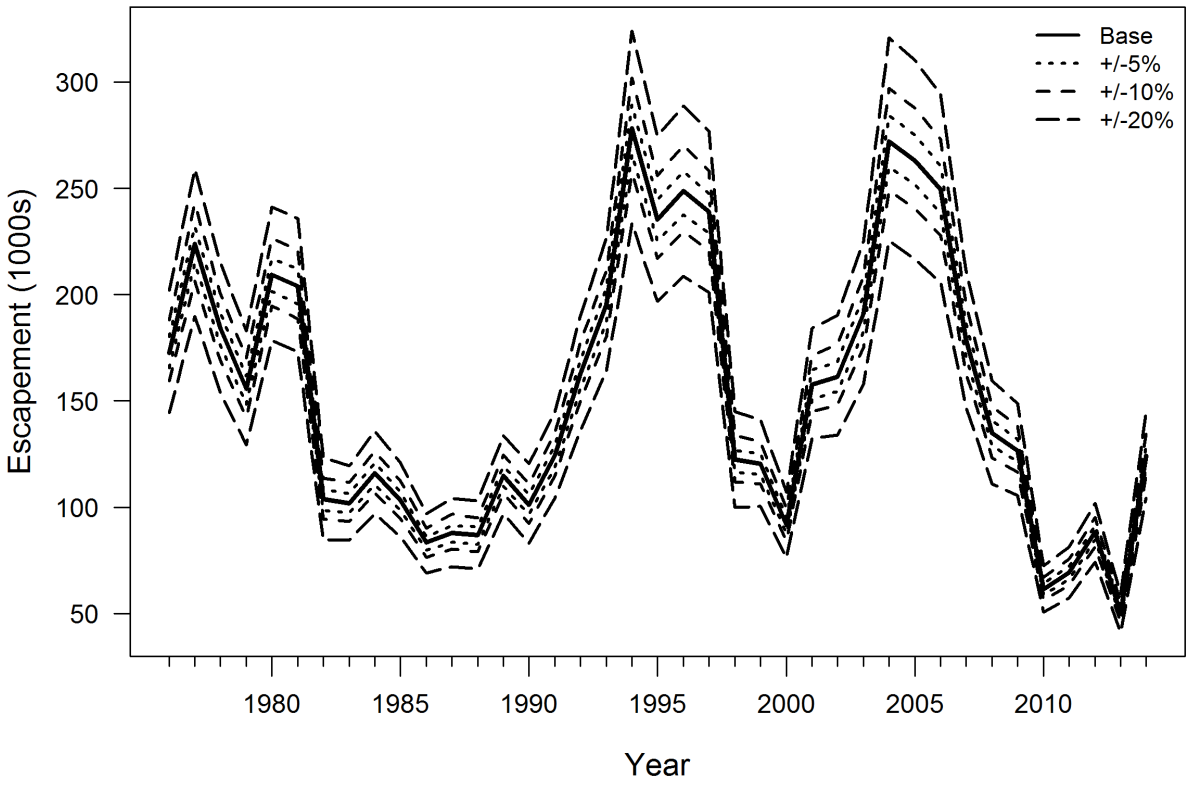

Figure 2.09 Model residuals from every dataset used by the model.

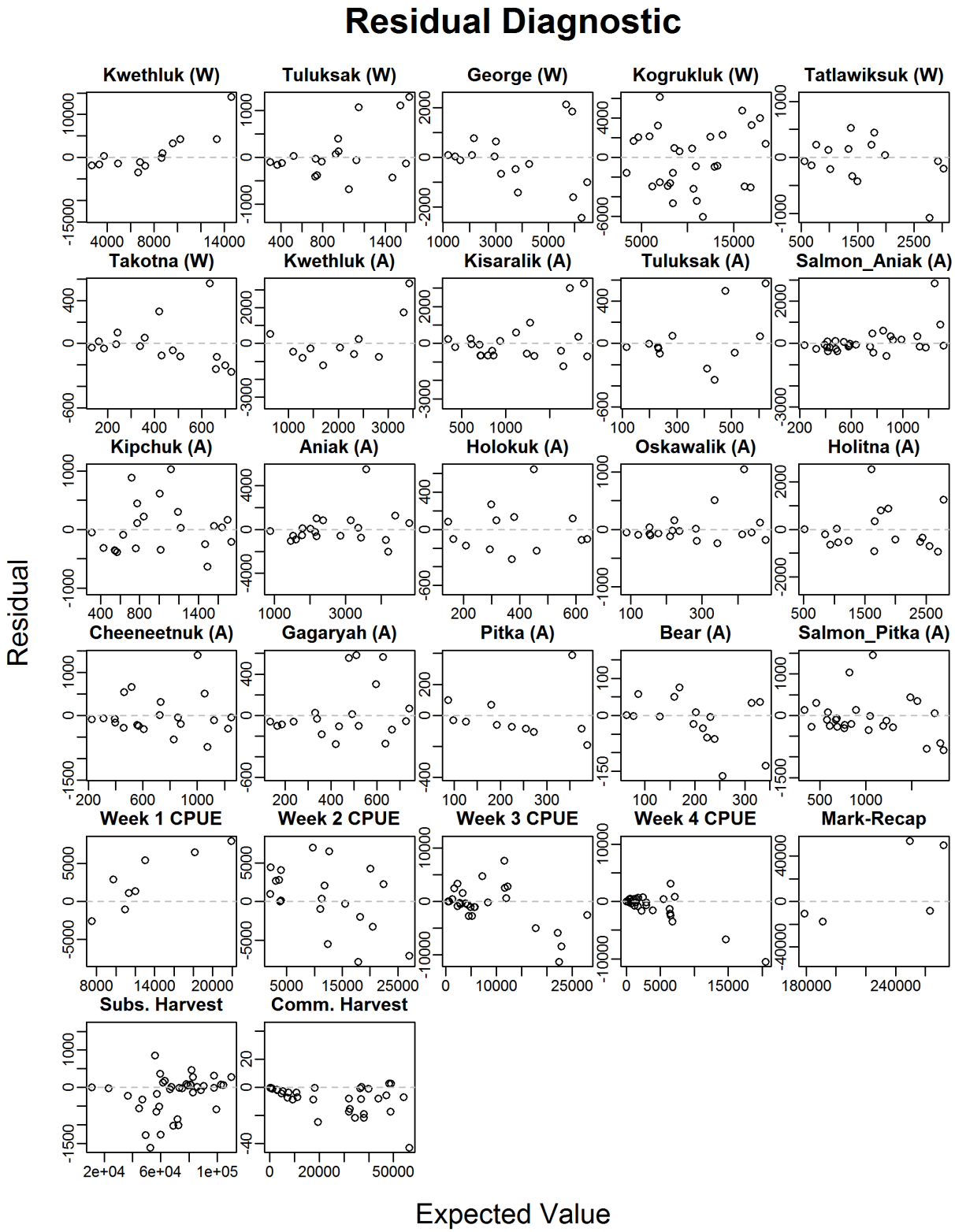

CHAPTER 2
TABLES

Table 2.01 Escapement indices on the tributaries of the Kuskokwim River used by Bue et al.'s (2012) run reconstruction and the integrated model. Years operational are not necessarily consecutive.

Project Type	Tributary	Years in Data	First Year in Data
Weirs	Kwethluk	13	1992
	Tuluksak	18	1991
	George	16	1996
	Kogrukluk	29	1976
	Tatlawiksuk	15	1999
	Takotna	16	1996
Aerial Surveys	Kwethluk	11	1977
	Kisaralik	21	1978
	Tuluksak	12	1977
	Salmon (Aniak)	29	1978
	Kipchuk	22	1987
	Aniak	20	1981
	Holokuk	13	1993
	Oskawalik	19	1987
	Holitna	17	1976
	Cheeneetnuk	21	1977
	Gagaryah	19	1977
	Pitka	11	2001
	Bear	16	1976
	Salmon (Pitka)	26	1977

Table 2.02 Spawner-recruit parameters and biological reference points from three models. Traditional refers to a basic ordinary least squares linear regression model that does not allow for autocorrelated recruitment residuals. Values in parentheses are 95% credible intervals for the two Bayesian models (Post-Hoc and Integrated) and 95% bootstrapped confidence intervals for the traditional model, obtained by randomizing the regression residuals, adding them to the predicted values, and refitting the model as per Hamazaki et al. (2012).

Value	Traditional SR	Post-Hoc Model	Integrated Model
α	7.29 (5.62-9.34)	6.03 (2.39-11.74)	6.33 (2.45-12.36)
β	9.07E-6 (7.70E-6-1.04E-5)	8.88E-6 (6.39E-6-1.14E-5)	8.91E-6 (6.33E-6-1.17E-5)
σ_R	0.29 (0.20-0.36)	0.24 (0.16-0.35)	0.23 (0.15-0.34)
ϕ	—	0.81 (0.49-0.98)	0.81 (0.50-0.98)
D	—	78.59 (42.50-139.80)	75.28 (42.25-134.23)
π_1	—	0.19 (0.17-0.22)	0.19 (0.17-0.22)
π_2	—	0.39 (0.36-0.42)	0.39 (0.36-0.42)
π_3	—	0.39 (0.36-0.42)	0.39 (0.35-0.42)
π_4	—	0.03 (0.02-0.04)	0.03 (0.02-0.05)
S_{MSY}	80,041 (73,829-87,551)	76,985 (56,506-102,696)	77,944 (56,232-104,722)
S_{MAX}	110,458 (96,546-129,888)	115,167 (87,483-156,464)	115,069 (85,419-157,951)
S_{eq}	223,593 (210,329-237,917)	211,188 (139,156-324,362)	215,338 (139,760-332,249)

APPENDIX I
INTEGRATED MODEL CODE

```
#############################################################################################
################################ INTEGRATED MODEL CODE #####################################
#############################################################################################

### Priors for SR portion
  lnalpha ~ dnorm(0,1.0E-2) %_%I (0,6)
  beta ~ dunif(0,10)
  phi ~ dunif(-1,0.99)
  tau.white ~ dgamma(0.01,0.01)
  log.resid.0 ~ dnorm(0,tau.red)
  tau.red <- tau.white * (1-phi*phi)
  sigma.white <- 1 / sqrt(tau.white)
  sigma.red <- 1 / sqrt(tau.red)
  alpha <- exp(lnalpha)

  ### Ricker spawner-recruit with autocorrelated lag-1 residuals: for years with
spawner/recruit link
  for (y in (A+a.min):(Y+A-1)) {
    log.R[y] ~ dnorm(log.R.mean2.a[y], tau.white)
    R[y] <- exp(log.R[y])
    log.R.mean1.a[y] <- lnalpha + log(S[y-a.max]) - beta * S[y-a.max]
    log.resid.a[y] <- log(R[y]) - log.R.mean1.a[y]
    ### RPS: Return per spawner
    RPS.a[y] <- R[y]/S[y-a.max]
  }

  log.R.mean2.a[A+a.min] <- log.R.mean1.a[A+a.min] + phi * log.resid.0
  for (y in (A+a.min+1):(Y+A-1)) {
    log.R.mean2.a[y] <- log.R.mean1.a[y] + phi * log.resid.a[y-1]
  }

  ### Brood year returns without SR link; drawn from a common lognormal dist
  mean.log.R0 ~ dnorm(0, 1.0E-4)
  tau.R0 ~ dgamma(0.1, 0.1)
  R.0 <- exp(mean.log.R0)
  sigma.R0 <- 1 / sqrt(tau.R0)
  for (y in 1:a.max) {
    log.R[y] ~ dnorm(mean.log.R0,tau.R0)
    R[y] <- exp(log.R[y])
  }

  ### monitoring quanities that don't start at y = 1 (JAGS quirk)
  log.resid <- log.resid.a[(A+a.min):(Y+A-1)]
  RPS <- RPS.a[(A+a.min):(Y+A-1)]
  log.R.mean1 <- log.R.mean1.a[(A+a.min):(Y+A-1)]
  log.R.mean2 <- log.R.mean2.a[(A+a.min):(Y+A-1)]

  ### Biological Reference Points
  lnalpha.c <- lnalpha + (sigma.white * sigma.white / 2 / (1 - phi * phi))
  S.max <- 1 / beta
  S.eq <- lnalpha.c * S.max
  S.msy <- S.eq * (0.5 - 0.07 * lnalpha.c)
```

```
  ### Generate Y+A-1=42 maturity schedules, one per brood year
  ### Proportion mature (returning to spawn) at age modeled as drawn from a common
dirichlet distribution across brood years
  D.scale ~ dunif(0,1)
  D.sum <- 1 / (D.scale * D.scale)
  prob[1] ~ dbeta(1,1)
  prob[2] ~ dbeta(1,1)
  prob[3] ~ dbeta(1,1)
  pi[1]<- prob[1]
  pi[2] <- prob[2] * (1 - pi[1])
  pi[3] <- prob[3] * (1 - pi[1] - pi[2])
  pi[4] <- 1 - pi[1] - pi[2] - pi[3]

  for (a in 1:A) {
    gamma[a] <- D.sum * pi[a]
    for (y in 1:(Y+A-1)) {
      g[y,a] ~ dgamma(gamma[a],1.0)
      p[y,a] <- g[y,a]/sum(g[y,])
    }
  }

  ### Calculate the numbers at age matrix as brood year recruits at age*proportion
that matured that year
  for (t in 1:Y) {
    for(a in 1:A){
      N.ta[t,a] <- R[t+A-a] * p[t+A-a,a]
    }
  }

  ### Calculate escapement as N-Harvest, after modeling harvest in both commercial and
subsistence fisheries
  for (t in 1:Y) {
    N[t] <- sum(N.ta[t,1:A])
    S[t] <- N[t] * (1 - U[t])
    log.S[t] <- log(S[t])

    #taus for harvest as known data
    sigma.H.com[t] <- sqrt(log(pow(cv.H.com[t],2)+1))
    tau.log.H.com[t] <- 1/pow(sigma.H.com[t],2)
    sigma.H.sub[t] <- sqrt(log(pow(cv.H.sub[t],2)+1))
    tau.log.H.sub[t] <- 1/pow(sigma.H.sub[t],2)

    U[t] ~ dunif(0.0001, 0.9999) # allow it to get very close to zero, never exactly
zero
    p.com[t] ~ dunif(0.0001, 0.9999)

    u.com[t] <- U[t] * p.com[t]
    u.sub[t] <- U[t] * (1-p.com[t])

    pred.com.catch[t] <- u.com[t] * N[t]
    pred.sub.catch[t] <- u.sub[t] * N[t]

    log.pred.com.catch[t] <- log(pred.com.catch[t])
    log.pred.sub.catch[t] <- log(pred.sub.catch[t])
```

```
    com.cat[t] ~ dlnorm(log.pred.com.catch[t], tau.log.H.com[t])
    sub.cat[t] ~ dlnorm(log.pred.sub.catch[t], tau.log.H.sub[t])

    ### Multinomial scale sampling on total annual return N
    for(a in 1:A){
      q[t,a] <- N.ta[t,a] / N[t]
    }
    x[t,1:A] ~ dmulti(q[t,],n[t])
  }

  ### ASSESSMENT(i.e., run reconstruction) SUBMODEL ###

  # Escapement Indices
  for (j in 1:20) {
    # overdispersion parameters
    r[j] ~ dgamma(0.001, 0.001)
    # proportionality scalars
    k[j] ~ dnorm(10, 1E-8)
  }

  ### Negative binomial likelihood on weirs and aerial surveys
  for (i in 1:num.index) {
    est.esc[i] <- S[esc.year[i]] / k[trib[i]]
    p.esc[i] <- r[trib[i]] / (est.esc[i] + r[trib[i]])
    index[i] ~ dnegbin(p.esc[i], r[trib[i]])
  }

  ### Weekly commericial CPUE
  tau.cat ~ dgamma(0.001, 0.001)
  for (q in 1:3) {
    ln.Q[q] ~ dnorm(0, 1E-10)
    Q[q] <- exp(ln.Q[q])
  }
  q.unr <- Q[1]
  q.res <- Q[2]
  q.mono <- Q[3]

  ### estimated commercial catch and fitting it to obs
  for (i in 1:num.com) {
    est.c.catch[i] <- log(pp[i] * N[c.year[i]] * (1 - exp(-Q[gear[i]] * effort[i])))
    catch[i] ~ dlnorm(est.c.catch[i], tau.cat)
  }

  ### in river likelihood. using total estimated escapement (mark recap + lower river
expansion). Harvest is flexible, so it doesn't make sense to use a fixed N to fit to
  for(i in 1:n.mrc.yrs){
    inr.s[mrc.yrs[i]] ~ dlnorm(log.S[mrc.yrs[i]], tau.inr.s[mrc.yrs[i]])
  }
}

### END MODEL CODE ###
```

CHAPTER 3

DECLINING ESCAPEMENT AGE AND SIZE STRUCTURE INFLUENCES MANAGEMENT REFERENCE POINTS FOR A CHINOOK SALMON STOCK

ABSTRACT

Over the past several decades, declining trends in age- and length-at-maturity of many Pacific salmon, *Oncorhynchus* spp., stocks have been observed across the western coast of North America, which have led to concerns about their genetic diversity, productivity, and overall sustainability. However, most salmon assessment models are focused on the abundance of returns and escapement, and as a result these issues are not typically addressed in the assessment or management of Pacific salmon fisheries. Here I present an age- and sex-structured assessment that incorporates fishery selection and declining age- and- size-at-maturity for the Kuskokwim River Chinook salmon stock, located in western Alaska. The model tracks the age and sex composition of various components of the population including commercial and subsistence harvest and escapement in order to allow for spawners of different sizes and sexes to contribute differentially to the spawning output of the population in terms of age- and year-specific fecundity. Primary findings from the model showed there is evidence for substantial fishery selection in the age composition data, but that exploitation is not intense enough to substantially alter the age composition of the escapement from of the unfished run. Furthermore, investigation of mean fecundity showed that the average spawner in recent years is contributing approximately 10% less to the annual egg production than one did 40 years ago. The combination of fishery selective forces and these changes in egg production indicate that the optimal number of escaping fish to achieve maximum sustained yield is greater when these fishery and demographic characteristics are included compared to when they are ignored.

INTRODUCTION

Over the past several decades, declining trends in age- and length-at-maturity of many Pacific salmon, *Oncorhynchus* spp., stocks have been observed across the western coast of North America (Bigler et al. 1996). These wide-spread declines have led to concerns of long-term changes in genetic composition and productivity of these stocks, due to the heritability of traits like age-at-maturity (Hankin et al. 1993) and the differential reproductive success of spawners of varying sizes (Ricker 1981; Bigler et al. 1996). Examples of declines in age-at-maturity and length-at-age in Pacific salmon are pervasive in the literature. Ricker (1981) performed a meta-analysis of stocks in British Columbia and found declines dating back to the 1920s of varying degrees in size-at-age in all five species of anadromous Pacific salmon. A similar meta-analysis was conducted by Bigler et al. (1996), which found matching decreasing trends in size-at-age and age-at-maturation. Lewis et al. (2015) investigated these life history trends in only Chinook salmon (*O. tshawytscha*) stocks across the state of Alaska and found that both average size and the proportion of older fish (3 and 4 ocean age fish) has declined in the returning spawners.

While the trends are widespread, their causes are under some debate. Bigler et al. (1996) stated that two primary hypotheses are driving the discussion of the causes of changes in these life history characteristics: density dependent growth during the ocean phase of the life cycle and fisheries-induced evolutionary changes due to the disproportionate harvest of larger, older fish in size-selective fisheries. Ricker (1981) suggested that stocks harvested by troll fisheries were particularly vulnerable to the size-selective hypothesis because fish that mature older are exposed to exploitation for longer periods of time. There is also some speculation that size-at-maturity is influenced by environmental drivers like sea-surface temperature, evidenced by correlation (Morita and Fukuwaka 2007). Regardless of the cause, long-term changes in size- and age-at-maturity in these stocks may negatively affect their productivity and sustainability, particularly

those stocks that are exploited by fisheries. Underscoring the importance of this issue, a recent expert panel consisting of 13 leading salmon scientists listed declines in size- and age-at-maturity as one of seven leading hypotheses that could explain the widespread declines of Chinook salmon across the Arctic-Yukon-Kuskokwim (AYK) region in western Alaska (Schindler et al. 2013). One recommendation from the panel was to incorporate these demographic changes into assessment models, particularly spawner-recruit analyses, to investigate their potential impact on management recommendations.

Assessment models for Pacific salmon are typically age-structured, but consider only the number of adults returning to spawn over time. This return abundance is then linked to spawner abundance via a spawner-recruit relationship, which is then used to derive management reference points (e.g., Clark et al. 2009). Because of their abundance-centered nature, these models do not explicitly account for these declining trends in life history characteristics. These trends should be investigated because they may have impacts on the productivity of these populations as older and larger fish contribute more to the spawning output in terms of total fecundity and egg quality (Quinn 2005). Considering that these stocks, particularly in Alaska, are managed with fixed escapement goal policies derived from spawner-recruit analyses, ignoring the presence of these declines may have negative consequences for the sustainability of these fisheries. Since larger, older fish are those that contribute most per spawner to the population fecundity (Quinn 2005), their increasing rarity may have implications for the way these populations are managed. For example, the greater prevalence of smaller, younger fish in recent years may result in a greater number of escaping fish required to sustain the population. A related issue is that the incorporation of changes in size- and age-at-maturity may affect how spawner-recruit analyses are interpreted. For example, if a low abundance of spawners was comprised mostly of small

individuals, then per capita reproductive rates may be underestimated and vice versa. These issues are not addressed in typical salmon assessment models and thus management based on them may lead to overexploitation.

In the Chinook salmon fisheries of the Kuskokwim River, Alaska, which are the focus of this chapter, fish are harvested almost exclusively with gill nets within the river channel when they return as mature adults to spawn (Liller et al. 2013). Older and larger fish may experience greater exploitation in these fisheries due to the size-selective large mesh gear used in the subsistence fishery (Bromaghin 2005). Preferential harvest of older/larger fish has the potential to reduce the average age/size of fish reaching the spawning grounds in relation to that of the run. Furthermore, because females are typically larger, they may be more heavily exploited by these size-selective fisheries, which may further lead to the potential to reduce the population fitness. Since larger females are more fecund (Quinn 2005) with larger eggs which may exhibit higher egg survival (Quinn et al. 2011; Beacham and Murray 1987), their presence in the escapement is critical to the spawning output of the population and their disproportionate removal may have serious consequences for the sustainability of the stock. Trends in declining age- and size-at-maturation have been observed in several Kuskokwim River substocks (e.g., the Kogrukluk River which has the longest time series of age, sex, and length data; Figures 3.01, 3.02). These issues have been discussed by Kuskokwim area stakeholders, biologists, and managers, however there has been little attempt or progress at incorporating these issues into assessment and management strategies (Hamazaki et al. 2012).

It is possible to incorporate these considerations into an assessment model by including the age composition of various components of the population including fishery harvests and escapement and the declining trends in size-at-age. Developing a model with this structure

(hereafter "spawner quality model") is the focus of this chapter. The purpose of developing the spawner quality model is to incorporate changes in life history characteristics, regardless of their cause, to determine if their inclusion alters the way the stock would be optimally managed. Based on the propositions already stated, one would expect *a priori* that the required number of fish escaping each year will increase when these life history and fishery selectivity considerations are included into the assessment. The objectives of this study are to (1) develop a model that accounts for size-selective harvest and differential spawning contribution of fish of different sizes, (2) investigate the behavior of the spawner-recruit relationship after incorporating these components, and (3) compare the management reference points derived from this model to one that ignores the age composition of the escapement (hereafter "base model"; Chapter 2, this Thesis). The spawner quality model is developed for the Kuskokwim River Chinook salmon stock, for which data on these components of the population have been collected for the past 39 years.

METHODS

Spawner Quality Model Structure

The spawner quality model was cast in an age- and sex-structured Bayesian state-space assessment framework similar to that of Fleischman et al. (2013) and Chapter 2 (this Thesis) to determine if incorporating trends in life history characteristics influences management reference points. The model structure deviated from that of Fleischman et al. (2013) in two primary ways. First, the observation submodel consisted of a more complex run reconstruction model that estimated annual run abundance using multiple indices of escapement, harvest estimates, and mark-recapture estimates of drainage-wide escapement abundance (Chapter 2, this Thesis). This represented a more fully integrated modeling approach. Secondly, the spawner quality model

tracks harvest and escapement on an age- and- sex-specific basis to facilitate incorporation of fishery selectivity and changes in size-at-age. The output of the spawner quality model was compared to a model that ignored fishery selectivity and size-at-age (base model, same as the base integrated model in Chapter 2, this Thesis).

Spawner-Recruit Submodel

In order to allow for older/larger fish to contribute more to the annual spawning potential, the spawner-recruit model was reformulated to specify that recruits were produced from eggs, rather than raw numbers of spawners as in (Chapter 2, this Thesis)

$$\ln(R_y) = \ln(S_y) + \ln(\alpha) - \beta F_y + \phi \omega_{y-1} + \varepsilon_y \quad (3.01)$$

Note that the meanings of the productivity parameter α and the capacity parameter β are now in terms of returns per egg rather than returns per spawner. Total annual egg production was calculated as:

$$F_y = \sum_a \hat{S}_{y,a,females} E_{y,a} \quad (3.02)$$

where $\hat{S}_{y,a,females}$ is the number of model predicted female spawners-at-age a in calendar year y (derived later in the text) and $E_{y,a}$ is the fecundity of a female at age a in year y. Note that only females contributed to the annual egg production.

In order to incorporate this change, information on individual age-specific fecundity through time was required. This information was taken from the Yukon River (Jasper and Evenson 2006), as Kuskokwim River-specific information was not collected. To arrive at $E_{y,a}$, a weight-to-eggs predictive linear relationship was formed using data from Jasper and Evenson (2006). Then, a length-to-weight predictive relationship was formed using data in Jasper and Evenson (2006) using an exponential growth function. Length-at-age information for escaping females counted at weirs (n = 6) in the Kuskokwim drainage was obtained from the AYK

Database Management System (DBMS) and mean length-at-age by year was calculated. This mean length-at-age was then used to predict weight and then eggs-at-age and year ($E_{y,a}$) using the aforementioned sequence of predictive relationships.

In order to allow comparison between the productivity parameter α from the spawner quality model to the base model, a quantity known as $\hat{\alpha}$ was calculated for the base model. This quantity represents the expected maximum lifetime recruits produced per spawner (Myers 1999; note that this definition is the same as the productivity parameter given by the base model; Chapter 2, this Thesis) and was calculated as:

$$\hat{\alpha}=\alpha \sum_s \sum_a \pi_{a,s} E_{a,s} \tag{3.03}$$

where $\pi_{a,s}$ is the mean probability of returning at age a and sex s (see *Maturation Schedule* below) and $E_{a,s}$ is the mean eggs per spawner at age a and sex s over the last 39 years (males have zero eggs).

Maturation Schedule

Since female Chinook salmon have a tendency to spawn at older ages than males (Healey 1991), it is important to model their maturation separately (e.g., the probability of maturing at age ($\pi_{a,s}$) for a female was allowed to be different than that for a male of the same age). This was modeled by altering the Dirichlet process described in (Chapter 2, this Thesis) to include eight outcomes (rather than four) for any given recruit from any given brood year. A recruit can either return to the river to spawn as a four, five, six, or seven year-old male, or a female at one of these ages. Since these events are mutually exclusive (e.g., if a recruit returns as a four year old male, it cannot return as any other age or sex) and collectively exhaustive (all possible age/sex combinations are described here), they can be modeled in this fashion. The new maturation

schedule was included to account for numbers of fish returning-at-age as either sex by modifying equation 2.06 (Chapter 2, this Thesis) to include sex:

$$N_{y,a,s} = R_{y\text{-}a}\, p_{y\text{-}a,a,s} \tag{3.04}$$

where $R_{y\text{-}a}$ is the unobserved true recruitment state from the population process model (i.e., spawner-recruit analysis) and $p_{y\text{-}a,a,s}$ is the probability of a fish from brood year $y\text{-}a$ maturing at age a with sex s.

Harvest Submodel

In the Kuskokwim River, gill net fishery selectivity operates as a filter that results in the age composition of the escapement being different from that of the annual unfished run (Liller et al. 2013). This process was modeled by estimating fishery selectivity parameters within the model informed by catch- and escapement-at-age information. Selectivity is defined here as the proportion of the total annual finite harvest rate that is experienced by each age class in the fishery. Each age and sex combination was assigned a selectivity parameter ($v_{a,s}$), given an independent and uninformative beta prior (*beta*[1,1]), that represented this quantity. An assumption was made that rendered one age/sex combination fully selected by the gear (i.e., selectivity fixed at one) and all other age/sex combinations were freely estimated in relation to it for a given gear type (see Myers et al. 2014). Prior to the official 1987 closure of the directed Chinook salmon commercial fishery, in 1985 the commercial fishery was restricted to using ≤ 6 inch mesh gill nets to target chum (*O. keta*) and sockeye (*O. nerka*) salmon while reducing the harvest of Chinook salmon (Liller et al. 2013). This represented a substantial shift in the way that the commercial gear selected for Chinook salmon and therefore must be modeled with different selectivity parameters (unrestricted: v_{unr}, restricted: v_{res}). In the subsistence fishery, the gear was never restricted, until the most recent years where fishing for Chinook salmon has been closed.

For the unrestricted selectivity with larger mesh, female age seven fish were assumed to be fully selected and female age four fish were assumed fully selected under the restricted selectivity.

The annual intensity of the fishing exploitation was modeled using a finite total annual harvest rate that represented the proportion of the fully-vulnerable fish that were harvested. These parameters varied over time and both the commercial (U_{com}) and subsistence (U_{sub}) fisheries were assigned unique parameter vectors. These harvest rates were assigned independent uniform priors ranging from 0.01 to 0.99 to prevent the possibilities of either none or all fish from being harvested in a given year. It was assumed that rather than operating at the same time on the same fish, the subsistence fishery harvested fish first, and the remaining population was available for harvest by the commercial fishery, which reflects the way the stock is managed, though not precisely implemented (Liller et al. 2013). The model-predicted harvest-at-age-and-sex in year *y* in the subsistence fishery was:

$$H_{sub,y,a,s} = N_{y,a,s} U_{sub,y} v_{unr,a,s} \tag{3.05}$$

and the remaining fish left to be harvested by the commercial fishery was:

$$N'_{y,a,s} = N_{y,a,s} - H_{sub,y,a,s} \tag{3.06}$$

For the years 1976-1984, the number of fish harvested in the commercial fishery was:

$$H_{com,y,a,s} = N'_{y,a,s} U_{com,y} v_{unr,a,s} \tag{3.07}$$

and

$$H_{com,y,a,s} = N'_{y,a,s} U_{com,y} v_{res,a,s} \tag{3.08}$$

for the years 1985-2014 to account for the difference in fishery selectivity between the different gear (mesh) types between these periods. The model-predicted escapement-at-age-and-sex in year *y* was then

$$\hat{S}_{y,a,s} = N'_{y,a,s} - H_{com,y,a,s} \tag{3.09}$$

To inform the age and sex components of harvest and escapement, multinomial likelihoods were used. The year-specific probability parameter vectors of the multinomial distribution were calculated from the model-predicted counts

$$q_{i,y,a,s} = \frac{Q_{i,y,a,s}}{\sum_s \sum_a Q_{i,y,a,s}} \tag{3.10}$$

where $Q_{i,y,a,s}$ was the model-predicted count of fish in observation component i [escapement ($\hat{S}_{y,a,s}$), commercial harvest ($H_{com,y,a,s}$), or subsistence harvest ($H_{sub,y,a,s}$)] at year y, age a, and sex s. These proportions were then fit to age composition information collected from these components of the population

$$x_{i,y,a,s} \sim multi(q_{i,y,a,s}, n_{i,y}) \tag{3.11}$$

The harvest age/sex composition effective sample sizes (ESS; n_{sub} and n_{com}) were chosen following Hamazaki et al. (2012) where harvest age/sex composition data collected prior to 2000 were assigned an ESS of 25 and after 2000 were assigned an ESS of 100. The age/sex composition of the escapement was calculated as a weighted average of all the age/sex samples collected at weirs operating each year. The annual ESS of the weir age/sex composition data was chosen such that the number of weirs that contributed to its age composition information was reflected. In years where all six weirs collected age composition information, the ESS was set to 100. When only one weir collected age composition information, the ESS was 100 * 1/6, and so on. This forced the model to fit more closely to the information when there were more weirs collecting data (which made the resulting information presumably more representative of the whole drainage; Maunder 2011). These age/sex composition data for harvest and escapement were obtained from the AYK DBMS which contains individual records of fish samples collected by year, age, and sex from a wide variety of projects. These data were summarized into annual

age/sex composition information into the form required by the model (annual proportion by age and sex for each population component).

The total numbers of harvest were fit to harvest estimates from the two fisheries with a lognormal density function. To obtain the model-predicted harvest in a year, $H_{sub,t,a,s}$ and $H_{com,t,a,s}$ had to be summed within a year. The total escapement numbers were informed by the run reconstruction observation submodel the same as in (Chapter 2, this Thesis):

$$\hat{S}_{total,y}=N_{total,y}-H_{total,y} \quad (3.12)$$

where $\hat{S}_{total,y}$ is the total escapement (regardless of age or sex) informed by weir and aerial survey counts by the same proportional assumption made in (Chapter 2, this Thesis), and $N_{total,y}$ and $H_{total,y}$ are the calendar year total run abundance and total harvest, respectively.

The spawner quality model was fit using Bayesian integration with MCMC methods to sample from the joint posterior probability distribution. MCMC sampling was conducted using parallel computing with the JAGS software ("Just Another Gibbs Sampler", Plummer 2013) implemented through R (R Core Development Team 2014) using the R package "R2jags" (Su and Yajima 2015). Prior distributions on all unknown parameters were uninformative and their structures were based on recommendations from Fleischman et al. (2013) and Bolker (2008) with necessary truncations to prevent the sampler from drawing implausible parameter values (e.g., log(α) had a diffuse normal prior truncated at zero). MCMC sampling was conducted using two chains with different initial values to verify convergence and to detect potential multiple solutions. Convergence of the chains was assessed with visual inspection of the posterior distribution sampled by each chain, trace plots, and the Gelman-Rubin statistic (Gelman et al. 2004). The MCMC sampling of the base and spawner quality models involved a burn-in period of 500,000 iterations, 1,000,000 post-burn-in iterations, and a thinning interval of 200 iterations,

using two chains to ensure convergence. These specifications resulted in 5,000 posterior samples retained for analysis from each chain. Point estimates (posterior mean) and Bayesian 95% credible intervals (2.5 and 97.5 percentiles of posterior distribution) for quantities of interest were calculated from their respective marginal posterior distributions.

Biological Reference Points: Equilibrium Spawner-Recruit Models

The management implications from the spawner quality model were compared to a model that ignores age, sex, and size composition of the escapement (base model) by evaluating differences in estimates of the biological reference point S_{MSY}, the equilibrium escapement that produces maximum sustained yield (MSY). MSY was obtained via iterative numerical search by finding the finite harvest rate that maximized equilibrium harvest using an equilibrium version of the age/sex structured spawner-recruit model. The equilibrium equations follow those proposed by Myers (1999) and Walters and Martell (2004). Equilibrium recruitment was calculated as

$$R_{eq} = \frac{\ln(\alpha_c EPR)}{\beta EPR} \tag{3.13}$$

where α_c is the productivity parameter corrected for lognormal process error and serial autocorrelation (Hilborn 1985) and EPR is the lifetime expected equilibrium eggs per recruit, which was calculated by incorporating harvest rate, fecundity, and maturation of individual age and sex combinations

$$\text{EPR} = \sum_s \sum_a \bar{E}_{y,a} \bar{\pi}_{a,s} (1 - U_{max} v_{a,s}) \tag{3.14}$$

where $\bar{E}_{y,a}$ is the mean eggs per female-at-age for the last decade and $\bar{\pi}_{a,s}$ is the vector of maturation probabilities-at-age-and-sex ($p_{y,a,s}$) averaged across the last decade, and U_{max} is the candidate harvest rate on fully selected age classes that is iteratively varied. Male fecundity was zero for all ages. Equilibrium recruitment was partitioned into numbers at age and sex according to the maturation schedule

$$N_{eq,a,s} = R_{eq}\bar{\pi}_{a,s} \quad (3.15)$$

The age and sex specific harvest rate was applied to obtain equilibrium escapement

$$S_{eq} = \sum_s \sum_a N_{eq,a,s}(1-U_{max}v_{a,s}) \quad (3.16)$$

and total harvest

$$H_{eq} = \sum_s \sum_a N_{eq,a,s} U_{max} v_{a,s} \quad (3.17)$$

Total harvest (H_{eq}) was maximized by iteratively changing the harvest rate U_{max}. When a maximum was found, convergence was verified and S_{eq} was accepted as S_{MSY}. This model was fit individually for all posterior samples so that posterior uncertainty in the input quantities from the spawner-recruit model (e.g., α, β, and $\bar{\pi}_{a,s}$) could be propagated into S_{MSY}. The model was ran under the different selectivity periods (v_{unr} and v_{res}) separately to allow for derivation of S_{MSY} under the current selectivity for each the commercial fishery and the subsistence fishery.

After preliminary runs of this equilibrium model for the spawner quality estimates, it was found that it was possible to maximize yield by harvesting all of the male fish. This was possible because the model was formulated such that males did not contribute to the spawning potential and thus there was no benefit to letting them escape fishing. The equilibrium model obviously did not reflect reality in this sense as males are required for egg fertilization. Thus, a penalty was introduced to specify that some number of males was required. This was implemented by specifying a threshold sex ratio that if the model resulted in sex ratios beyond, the objective function would be penalized heavily. Since it was unclear what a realistic sex ratio cap should be, a range of penalty sex ratios (female:male) was chosen from a range of 1 to 4 by increments of 0.25.

For more consistent comparisons between the base and spawner quality models, a similar equilibrium model was developed for the base model estimates that did not use age/sex composition or fishery selectivity. In this model, the equilibrium recruits was

$$R_{eq} = \frac{\log(\alpha_c(1-U))}{\beta(1-U)} \tag{3.18}$$

where the parameters α_c and β were posterior samples from the base model and U was the parameter that was iteratively searched for to maximize harvest. All other equations were the same as the spawner quality equilibrium model however there was no age/sex structure.

Iterative derivation of S_{MSY} using posterior samples was implemented using original R code with numerical optimization conducted using the "optim" function in the base "stats" package (R Core Development Team 2014) using the "BFGS" search algorithm. Summaries of S_{MSY} were calculated just like any other posterior distribution, with the mean of all samples representing the point estimate and the 2.5th and 97.5th percentiles representing the range of uncertainty in the estimates.

RESULTS

Spawner-Recruit Submodel

Since the spawner-recruit portion of the spawner quality model was altered to include eggs rather than aggregate spawners (as in Chapter 2, this Thesis), its productivity parameter α and capacity parameter β were expressed in terms of returns per egg rather than per spawner, making its estimates difficult to compare to the base model in this regard. The spawner quality model indicated that the maximum returns per egg was 0.002 (0.0009-0.003) (Table 3.01). This quantity, when transformed into $\hat{\alpha}$ which represents the number of returns per spawner, was 4.84 (2.33-8.23). When compared to the base model (6.33, 2.45-12.36), the spawner quality value was

substantially lower and more precise, showing that the maximum reproductive potential was less under the spawner quality model.

While it is difficult to compare the spawner-recruit parameters between the spawner quality and base models directly, the resulting spawner-recruit relationships can be compared graphically (Figure 3.03). When using eggs to predict returns, the relationship itself appeared less uncertain (95% credible lines closer to the mean prediction line) than the base model (Figure 3.03). However, when comparing the distribution of points around the prediction line, the spawner quality model showed more variation than the base model (Figure 3.03). This point is further evidenced by comparing the recruitment process variation σ_R between the two models (spawner quality = 0.34 [0.23-0.48], base = 0.23 [0.15-0.34]; Table 3.01). The parameter that governed the amount of serial autocorrelation in the recruitment time series ϕ was smaller under the spawner quality model (0.62; 0.21-0.95) than under the base model (0.81; 0.50-0.98), which is visually evident when comparing the recruitment time series between the two models (Figure 3.04, upper panel). While both models predicted similar recruitment time series, the spawner quality model had more extreme "peaks and valleys" from year to year which is consistent with the lower autocorrelation coefficient ϕ. Despite the large alterations to the process submodel component of the spawner quality model relative to the base model, the two models treated the brood year returns and calendar year run and escapement very similarly (Figure 3.04). High return abundance brood years were produced in years with low spawner abundances and vice versa. This result shows that the Ricker density dependent compensatory mechanisms were behaving similarly in both models (Figures 3.03, 3.04).

The inclusion of size-at-age information for females into the annual age-specific fecundity showed that per capita fecundity has changed over time. Mean eggs per spawner was

calculated by dividing the total annual egg production (E_y) by the total number of females, regardless of age ($\sum_a \hat{S}_{y,a,female}$). In 1976 the mean eggs per spawner was 7,383 (7,061-7,637) versus 6,494 (6,329-6,628) in 2014. Assuming a linear relationship with time, mean eggs per spawner declined significantly through time; 25 eggs/year ($p < 0.0001$; Figure 3.05).

The sex-structured maturation schedule indicated that there were substantial differences between the probabilities of maturing-at-age between the sexes (Table 3.01). Overall, the probability of returning as a male of any age was much higher (0.65 [0.62-0.67]) than that for females (0.35 [0.32-0.37]). Additionally, males had a substantially higher probability of returning younger at ages four and five than did females which for the most part returned at age six (Table 3.01). Individuals were approximately twice as likely to return as an age seven female than an age seven male. When the probabilities of returning at age were summed by sex, the probabilities were very similar to those estimated by the base model, which ignored sex composition (Table 3.01).

Harvest Submodel

The inclusion of age/sex composition information from harvest and escapement revealed substantial fishery size-selection (Figure 3.06). Age four males had lower selectivity than age seven males under the unrestricted gear (early commercial years; all subsistence years), whereas females were more uniformly selected across ages (Figure 3.06). Females at age seven were assumed to be fully selected, since they are the largest individuals on average in the population and this gear had the largest mesh. For the restricted gear, females were again chosen as the most selected, but at age four since this gear was smaller. While the unrestricted gear showed an increasing trend of selectivity with age for both sexes, the restricted gear generally showed a decreasing trend where older fish were less selected. It was clear that the model did not have

very informative data on these quantities, as the selectivity parameters for some age/sex combinations showed substantial posterior uncertainty.

This size selective behavior of the fishery was evident when the age composition output from various population components through time was investigated. The subsistence fishery harvested substantially fewer age four males and substantially more age six males than what was present in the escapement (Figure 3.07), which was consistent with the unrestricted gear selectivity parameters for males. Conversely, the subsistence fishery harvested females relatively in proportion to their abundance in the escapement, which reflects the more uniform shape of the unrestricted selectivity curve for females. The one exception was age seven, for which there was a clear separation between the subsistence and escapement female age compositions (Figure 3.07).

The mesh restriction on the commercial fishery in the mid-1980s resulted in substantial changes in the way the commercial fishery selected for the various age/sex combinations. Prior the mesh restriction, the commercial fishery behaved very similarly to the subsistence fishery because they were using the same size gear (Figure 3.08, Liller et al. 2013). However, after the 6 inch mesh restriction was imposed, the selection of the commercial fishery switched towards selecting for more young fish and fewer older fish (Figure 3.08).

As substantial as the fishery selection was, it did not seem to have a large impact on changing the age composition of the escapement relative to the unfished run. The age composition of the run (pre-harvest) and escapement (post-harvest) showed only slight differences through time (Figure 3.09) for females (mean change in composition of <1% for all ages). Male age composition changed more between the run and escapement, particularly for

ages four (mean decrease in composition of 4.8%) and six (mean increase in composition of 2.5%).

Biological Reference Points

The spawner abundance that produced MSY (S_{MSY}) was 64,600 (45,078-95,068) fish under the base model. This model ignored differential spawning contribution of individuals of different ages, age/sex composition, and fishery selectivity. These issues were addressed in the spawner quality model and their inclusion yielded largely different results. Under the unrestricted gear selectivity scenario, S_{MSY} was 119,500 (79,255-178,808). This quantity did not change across the range of penalty sex ratios (Figure 3.10). S_{MSY} under the restricted gear did change with the penalty, however. When the sex ratio was 1:1 (female:male), S_{MSY} was similar to that of the unrestricted gear (111,534 [58,980-187,102]), but decreased asymptotically with increasing penalty sex ratio to an S_{MSY} of 54,918 (35,031-91,115) at a sex ratio of 4:1 (Figure 3.10). This sensitivity to the penalty was due to the loosening of the constraint as the sex ratio increased, which allowed the model to maximize harvest by taking a large proportion of the males and shows that its inclusion was necessary for this model to be biologically realistic (i.e., males are needed for reproduction).

DISCUSSION

The altered model structure under the spawner quality model did have substantial ramifications on the optimal number of escaping fish to sustain the population under maximum sustained yield. This finding was caused by the interactions between fishery selectivity and reductions in age-specific fecundity. These management recommendations were largely dependent on the direction of selectivity (i.e., toward older/larger or younger/smaller fish) and the sex ratio constraint. As there is no longer a directed commercial fishery for Chinook salmon

in the Kuskokwim River, the unrestricted gear selectivity may be the more realistic scenario to base management decisions on, particularly as it is the more conservative of the two scenarios and it is insensitive to the assumed sex ratio of the escapement. The optimal escapement nearly doubled under the unrestricted gear when compared to the base model that ignored fishery selectivity and differential spawning contribution of different age/sex classes. However, since there is some incidental harvest of Chinook salmon in the commercial fishery for chum and sockeye salmon and subsistence gear may be restricted in low abundance years, both scenarios should be considered.

If the spawner quality model were to be used as the basis for management, it is highly likely that the escapement goal would be raised substantially from the current 65,000-120,000 range (Hamazaki et al. 2012) to one that places the point estimate of ~120,000 fish derived from this analysis in the center of the target range. Adopting this change would require extensive sensitivity analyses of this model by state biometricians, review by the Board of Fisheries, and substantial shifts in the management paradigm to one that places more emphasis on the quality of the spawning escapement and recognizes that the size-selective behavior of the fishery can affect the way it is managed.

When comparing the maximum reproductive potential of the population between the spawner quality and base models, it was determined that the spawner quality model suggested that the population was less productive. While this is useful in explaining the larger number of escaping fish required to produce MSY, it is somewhat counterintuitive as well. One may expect that if the larger, more fecund spawners were less prevalent, then each individual spawner would need to be more productive to result in the same recruitment time series (which did not change substantially between the spawner quality and base models). However, this was not the case, as

suggested by the value of $\hat{\alpha}$ under the spawner quality model. It was clear that the number of recruits and spawners did not change substantially over time between the two models (Figure 3.04), so the realized population productivity (recruits per spawner) was very similar.

It is important to note that the management recommendations of the spawner quality model were contingent on the assumed sex ratio of the escapement for the restricted gear. Caveats like this reduce the utility of these types of models in management as it is unclear what the escapement sex ratio should be. When the sex ratio penalty was set at 0.55 (the approximate mean ratio between males and females for the past 39 years), the model estimated an unrealistic optimal escapement of approximately 280,000 fish. This is higher than the 39 year average run abundance prior to harvest, and is clearly an unrealistic escapement target. Although sex ratio is clearly important, perhaps management based on escapement quality should focus more on age composition through the use of mesh restrictions than on sex ratios.

Another caveat is that models of this sort require a large amount of additional data. While age, sex, and length sampling programs have been operating throughout the drainage for nearly 40 years, the data for the Kuskokwim Chinook stock may not even be sufficient for this analysis. All parameters were estimable, though not precisely so, and in some cases with weakly informative data. In particular, the escapement and subsistence age/sex composition time series were lacking in extensive temporal coverage. Prior to the early 1990s, the only project collecting information on escapement age/sex composition was the Kogrukluk River weir (dating back to 1976) located in the middle area of the drainage. Clearly, making drainage-wide inferences based on a single weir project has its limitations. This weakness was addressed by loosening the extent to which the model was required to fit to these data through a weakly informative ESS, but this would not correct any biases introduced by relying on the signal indicated by this one project.

Similarly, subsistence harvest age/sex composition information was only available for the years 2001-2013, which were all ESS years with high data weight. Thus, the model was required to use these years to extrapolate the discrepancy in age/sex composition between subsistence and escapement for the years 1985-2000 to estimate the unrestricted gear selectivity parameters (1976-1984 commercial was also unrestricted). This placed a large demand on these data, which clearly showed in the large credible intervals in the selectivity parameters. For these reasons, it is important to recognize these limitations and uncertainties when addressing management concerns. Some may argue that this is one area that informative priors in the Bayesian context are useful, and they certainly could be introduced to aid the model in estimating these parameters. In this exercise, however, I wished to be as objective as possible as analyses of this sort are rare.

While it is widely recognized that demographic qualities of many anadromous Pacific salmon stocks, like age- and size-at-maturity, have been changing over the past several decades, the possible changes in population spawning potential and sustainability are not typically addressed in assessment models. One potential reason for this disparity is that developing assessment models of this nature likely takes less priority than first developing more statistically rigorous approaches to spawner-recruit analyses and escapement goal development, which is an area where Alaska Department of Fish and Game (ADF&G) has made substantial progress in the past decade. ADF&G has a formidable task in assessing run abundance and developing escapement goals for stocks across the state, without even considering these demographic issues. While ADF&G does have an obligation to conservation, their guiding principles in management are based around sustainable yield principles, which do not inherently include considerations of the life history characteristics of the population. Thus, somewhat of a precedent to place an

emphasis on strict numbers of fish escaping may be present and breaking away from such a paradigm would likely require a large perturbation.

Furthermore, there is no rigorously developed and evaluated strategy for escapement goals or in-season management based on the demographic qualities of escapement. Although managers can allow for preferential harvest of certain age/sex classes with gill nets, as revealed by this study and others (e.g., Bromaghin 2005), there is no practical method of harvest that allows for the different age/sex classes to be harvested in proportion to their abundance in the run (i.e., there is always some selectivity). However, as elucidated in this study, even with substantial fishery selectivity and moderate annual harvest rates the potential for in-river fisheries to alter the age composition of escapement relative to the run was limited. This finding shows that the in-season concerns of in-river gill net fishery selectivity may not be as serious as they were perceived *a priori*. This analysis was developed specifically for the Kuskokwim River, so extending this generalization to other stocks may be irresponsible as they may have different maturation schedules and selectivity parameters that could change age composition pre- and post-harvest beyond what has been experienced in the Kuskokwim stock.

Finally, substantially more data must be obtained and passed to the model in order to estimate fishery selectivity. Not all stocks have as rich age/sex composition information for commercial harvest, subsistence harvest, and escapement as the Kuskokwim Chinook salmon stock, which would make models like the spawner quality model presented here impossible for many stocks. Additionally, the lack of Kuskokwim-specific information on weight or fecundity necessitated the borrowing of this information from the Yukon River. Chinook salmon are known to differ substantially between populations in life history strategies (Healey 1991), but if data must be borrowed from another system, the Yukon stock is perhaps the best candidate for

the Kuskokwim due to the similarities in latitude, drainage size, and life-history type (i.e., both stream-type as opposed to ocean-type; Healey 1991). This borrowing of information from other stocks was necessary in this case, but may limit the utility of these methods.

REFERENCES

Beacham, T.D. and C.B. Murray. 1987. Adaptive variation in body size, age, morphology, egg size, and developmental biology of chum salmon (*Oncorhynchus keta*) in British Columbia. Canadian Journal of Fisheries and Aquatic Sciences. 44(2): 244-261.

Bigler, B.S., D.W. Welch, and J.H. Helle. 1996. A review of size trends among North Pacific salmon (*Oncorhynchus* spp.). Canadian Journal of Fisheries and Aquatic Sciences. 53(2): 455-465.

Clark, R.A., D.R. Bernard, and S.J. Fleischman. 2009. Stock-recruitment analysis for escapement goal development: a case study of Pacific salmon in Alaska. Pages 743-757 *in* C.C. Krueger and C.E. Zimmerman, ed. Pacific salmon: ecology and management of western Alaska's populations. American Fisheries Society, Symposium 70, Bethesda, Maryland.

Hankin, D.G, J.W. Nicholas, and T.W. Downey. 1993. Evidence for inheritance of age of maturity in Chinook salmon (*Oncorhynchus tshawytscha*). Canadian Journal of Fisheries and Aquatic Sciences. 50(2): 347-358.

Healey, M.C. 1991. Life history of Chinook salmon (*Oncorhynchus tshawytscha*). Pages 311-394 *in* C. Groot and L. Margolis ed. Pacific salmon life histories. University of British Columbia Press, Vancouver, British Columbia.

Hilborn, R. 1985. Simplified calculation of optimum spawning stock size from Ricker's stock recruitment curve. Canadian Journal of Fisheries and Aquatic Sciences. 42(11): 1833-1834.

Lewis, B., W.S. Grant, R.E. Brenner, and T. Hamazaki. 2015. Changes in size and age of Chinook salmon (*Oncorhynchus tshawytscha*) returning to Alaska. PLoS ONE. 10(6): e0130184.

Liller, Z.W., A.R. Brodersen, T.R. Hansen, D.B. Molyneaux, and E. Patton. 2013. Age, sex, and length composistion of Chinook salmon harvested in the 2008-2011 Lower Kuskokwim River subsistence fishery. Alaska Department of Fish and Game, Fishery Data Series No. 13-10, Anchorage, AK.

Maunder, M.N. 2011. Review and evaluation of likelihood functions for composition data in stock-assessment models: estimating the effective sample size. Fisheries Research. 109(2): 311-319.

Morita, K. and M. Fukuwaka. 2007. Why age and size at maturity have changed in Pacific salmon. Marine Ecology Progress Series. 335: 289-294.

Myers, R.A, M.W. Smith, J.M. Hoenig, N. Kmiecik, M.A. Luehring, M.T. Drake, P.J. Schmalz, and G.G. Sass. 2014. Size- and sex-specific capture and harvest selectivity of walleyes from tagging studies. Transactions of the American Fisheries Society. 143(2): 438:450.

Ricker, W.E. 1981. Changes in the average size and average age of Pacific salmon. Canadian Journal of Fisheries and Aquatic Sciences. 38(12): 1636-1656.

Schindler, D., C. Krueger, P. Bisson, M. Bradford, B. Clark, J. Conitz, K. Howard, M. Jones, J. Murphy, K. Myers, M. Scheuerell, E. Volk, and J. Winton. 2013. Arctic-Yukon-Kuskokwim Chinook Salmon Research Action Plan: Evidence of Decline of Chinook Salmon Populations and Recommendations for Future Research. Prepared for the AYK Sustainable Salmon Initiative (Anchorage, AK), 79 pp.

Su, Y. and M. Yajima. 2015. R2jags: Using R to run "JAGS". R package version 0.5.6. http://CRAN.R-project.org/package =R2jags.

Quinn, T.P. 2005. The behavior and ecology of Pacific salmon and trout. Seattle, WA: University of Washington Press.

Quinn, T.P., T.R. Seamons, L.A. Vollestad, and E. Duffy. 2011. Effects of growth and reproductive history on the egg size-fecundity trade-off in steelhead. Transactions of the American Fisheries Society. 140: 45-61.

CHAPTER 3
FIGURES

Figure 3.01 Trends in mean length-at-age for males and females observed at the Kogrukluk River weir. This project was chosen because it has the longest time series of observations. Trend curves were obtained with general additive models fit using LOESS smoothing.

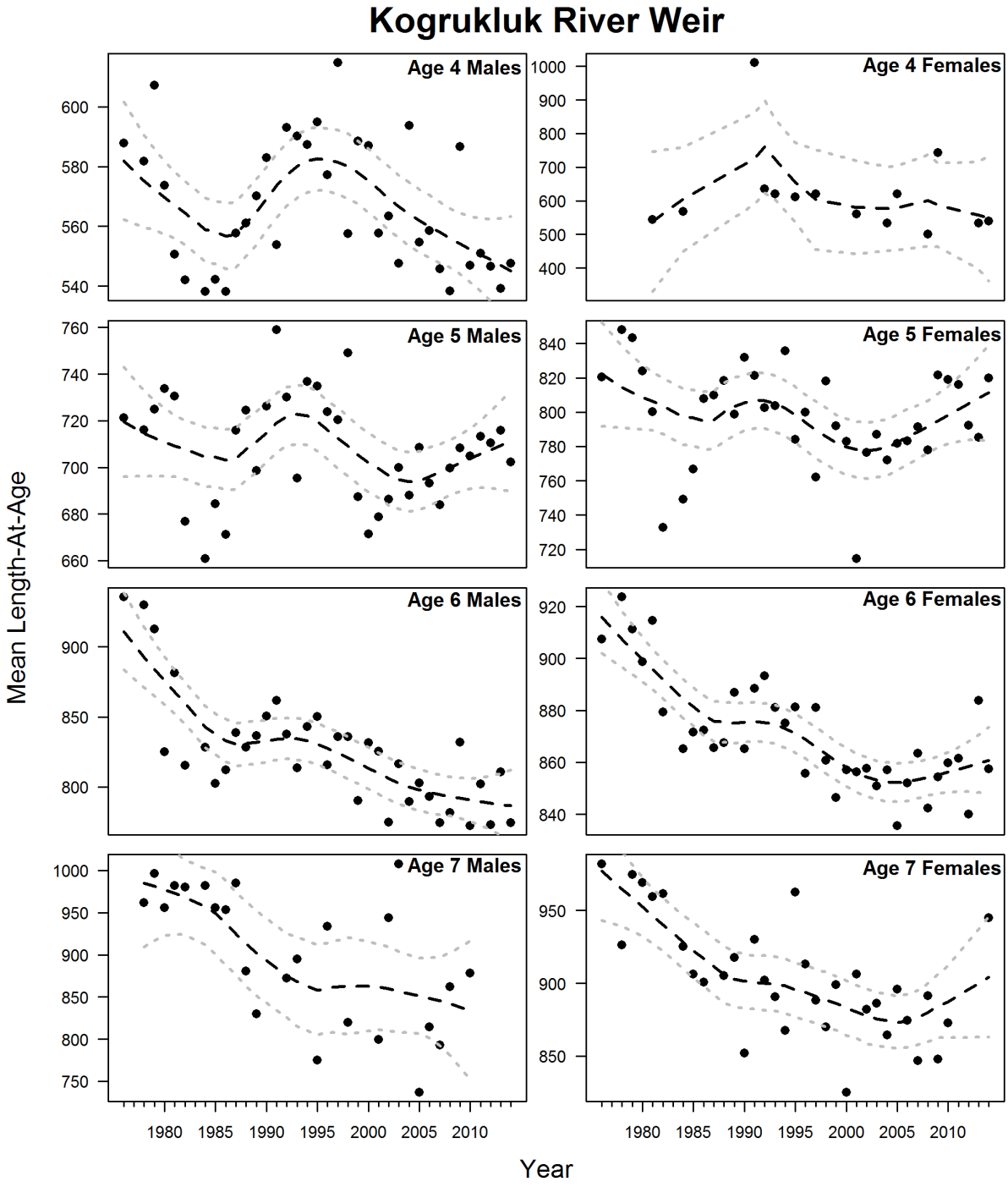

Figure 3.02 Trends in age/sex composition observed at the Kogrukluk River weir. Trend curves were obtained with general additive models fit using LOESS smoothing.

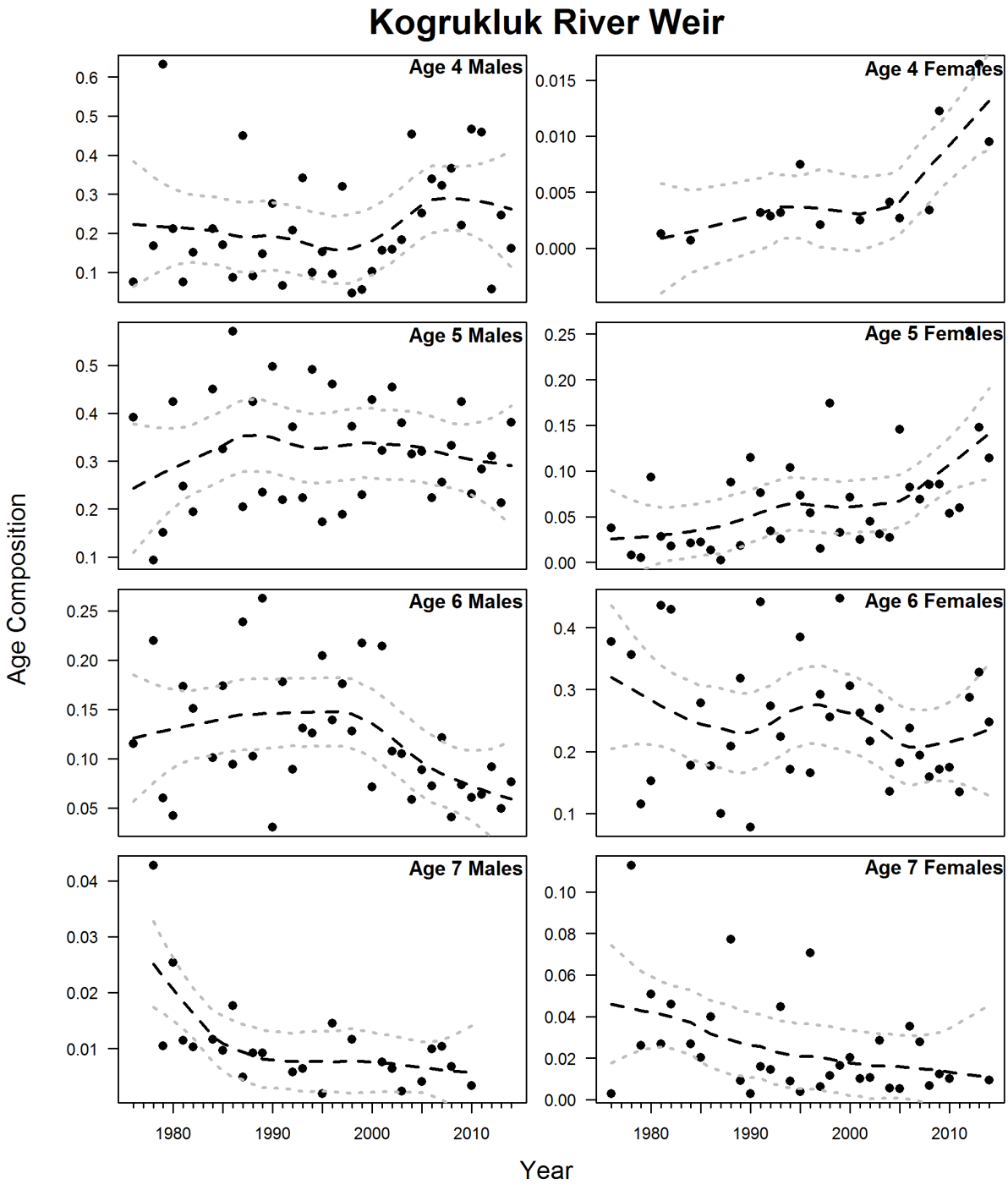

Figure 3.03 Spawner-recruit relationships for the spawner quality model (top panel) and base model (bottom panel). Black points and lines represent posterior means and grey lines represent 95% credible intervals. Note the difference in x-axes between the two panels.

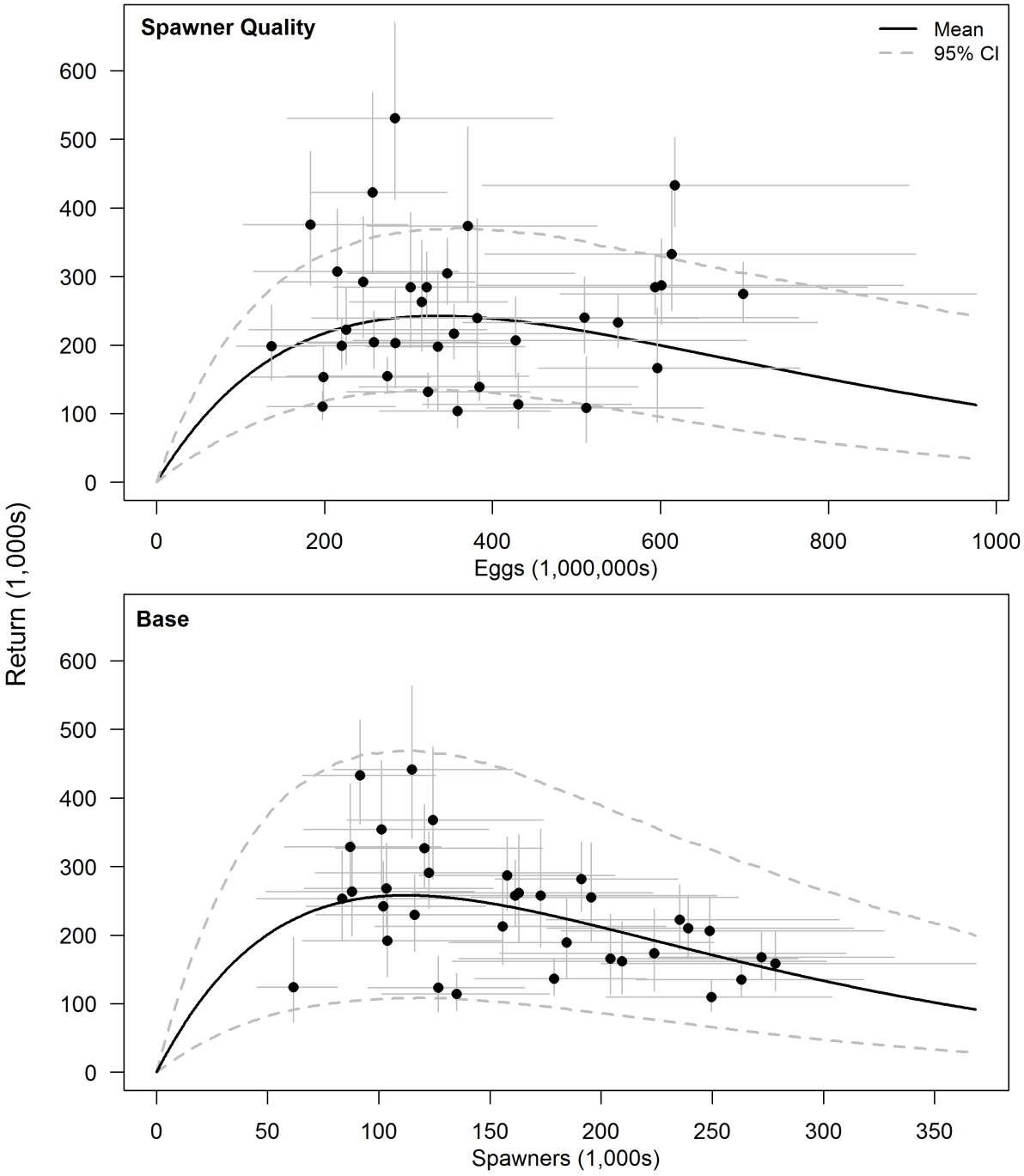

Figure 3.04 Time series comparisons of return, spawner, and run abundances (from top to bottom panels) from the spawner quality and base models. Lines represent posterior means of these quantities. The note the time axis of the recruitment plot corresponds to brood year recruits that were spawned by the matching calendar year escapement abundance.

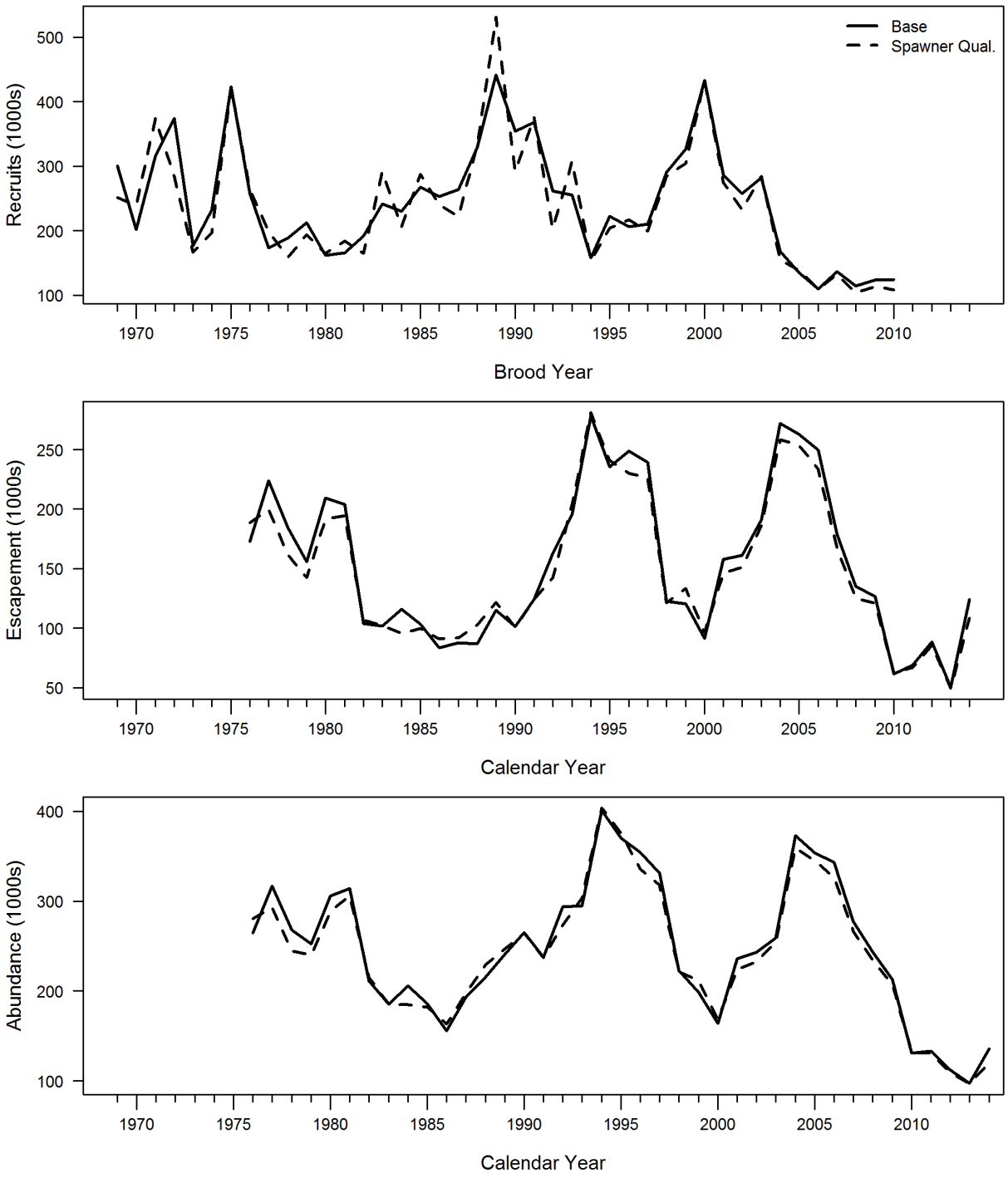

Figure 3.05 Posterior mean eggs per spawner through time. Model fit with a simple linear model assuming independence of residuals.

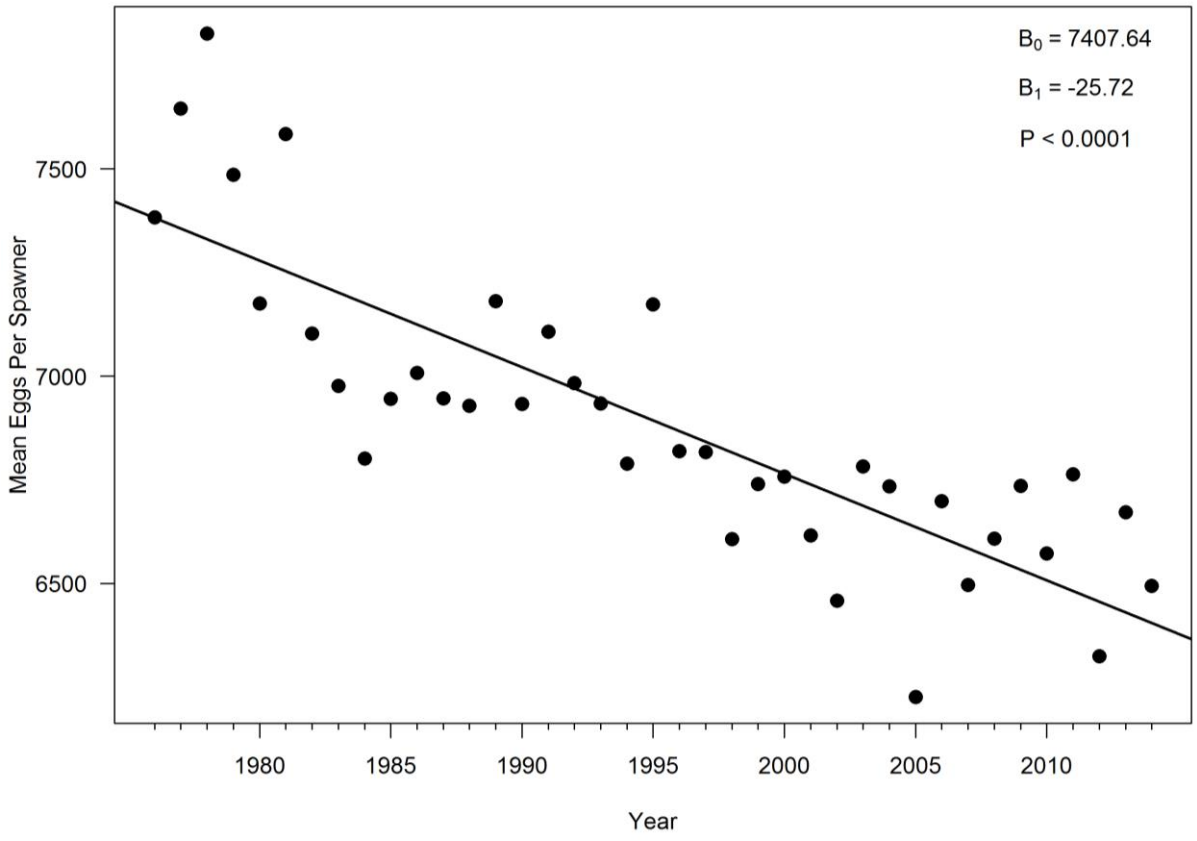

Figure 3.06 Fishery selectivity for males- and females-at-age under two gear types. Selectivity for females was assumed to be one for age seven and age four for the unrestricted and restricted periods, respectively. Points are posterior means and bars are 95% credible intervals.

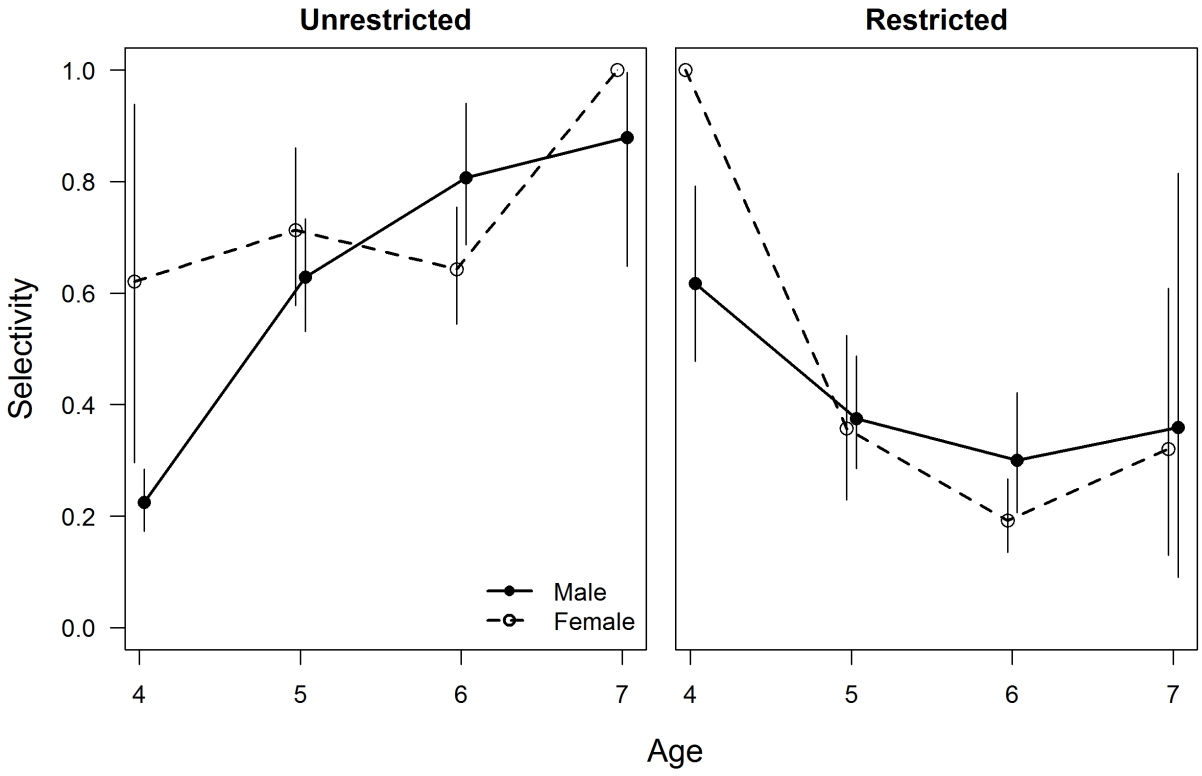

Figure 3.07 Posterior mean age/sex composition of escapement (solid circles and lines) compared to subsistence harvest (open circles and dashed lines).

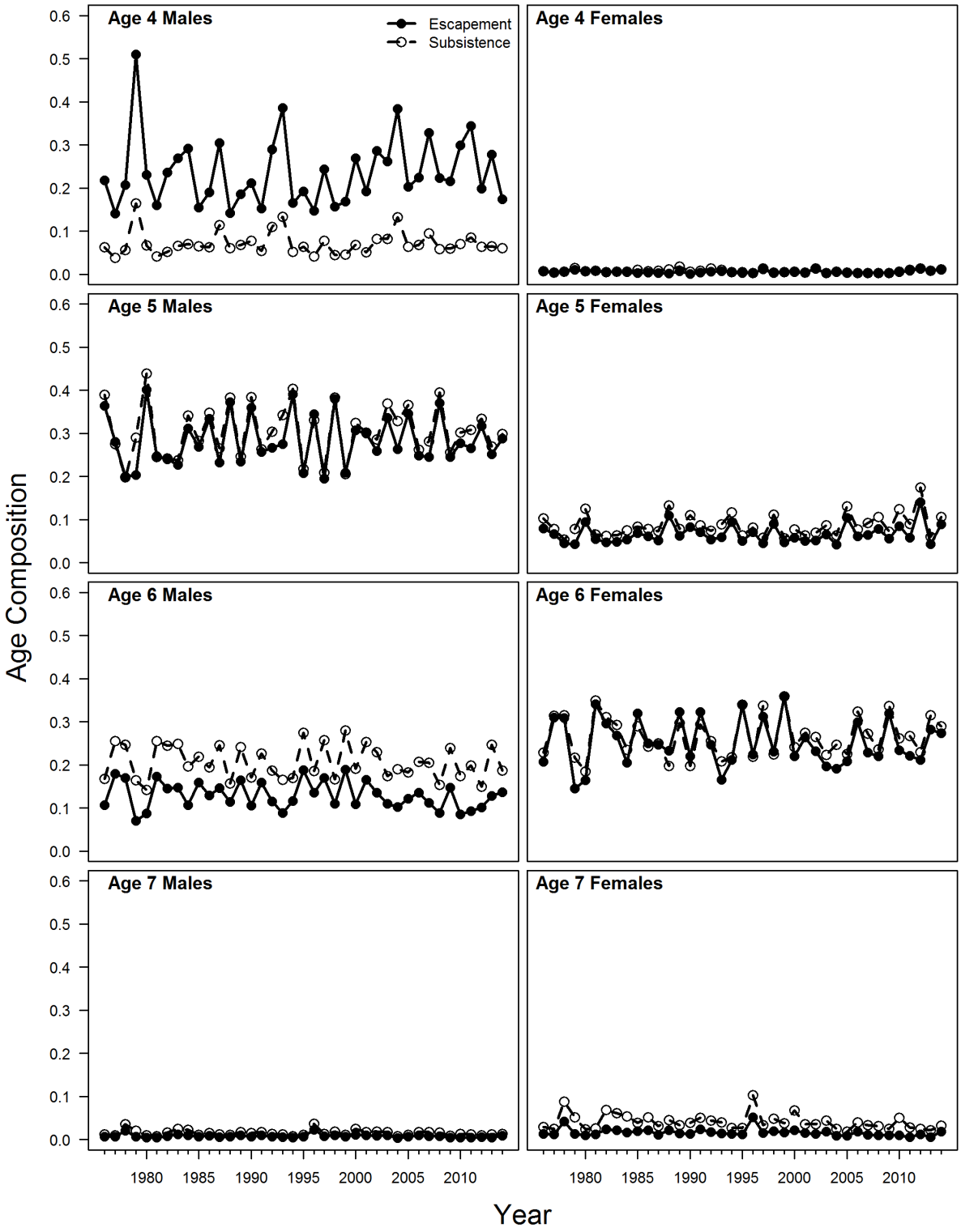

Figure 3.08 Posterior mean age/sex composition of escapement (solid circles and lines) compared to commercial harvest (open circles and dashed lines).

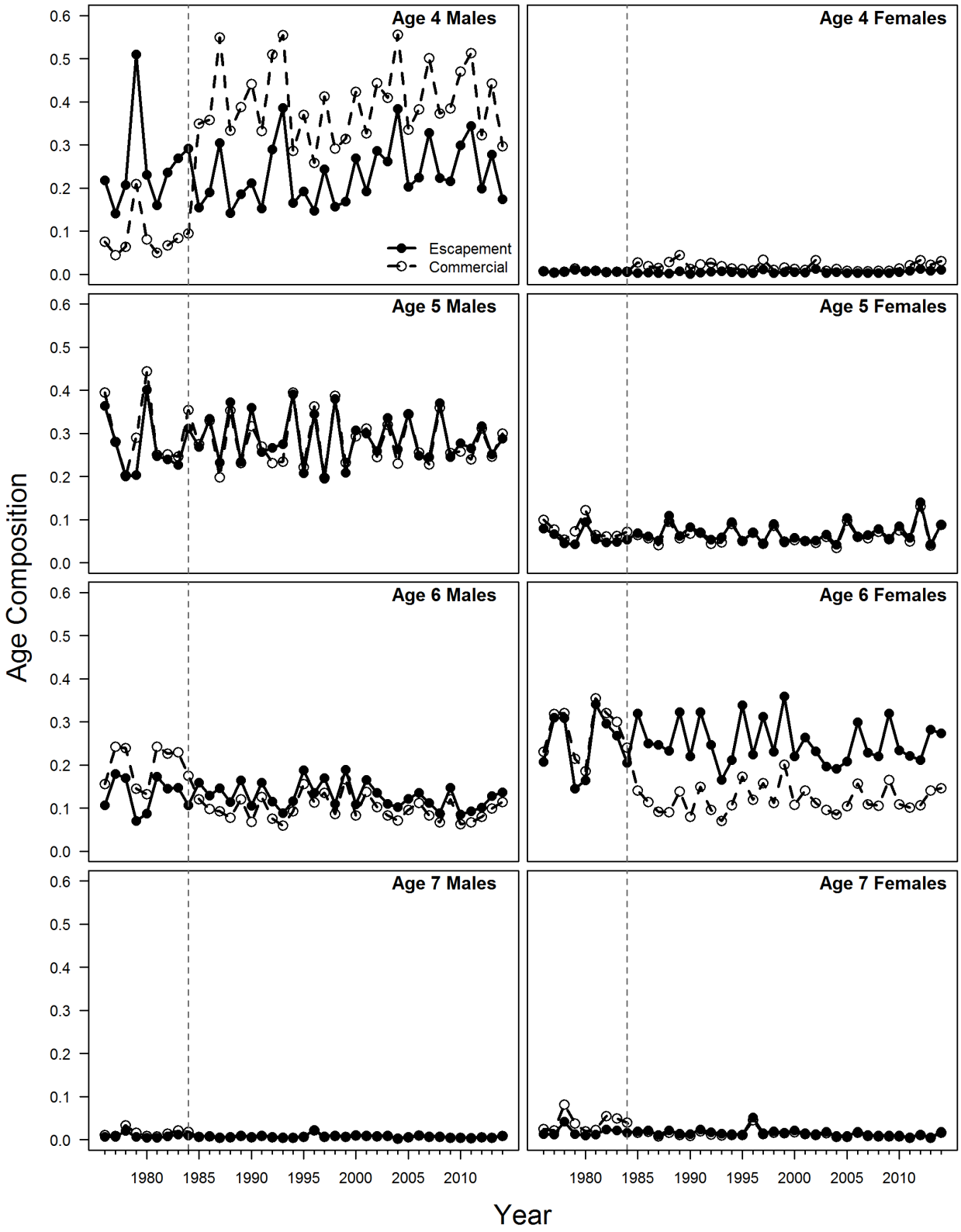

Figure 3.09 Posterior mean age/sex composition of escapement (solid circles and lines) compared to the unfished run (open circles and dashed lines).

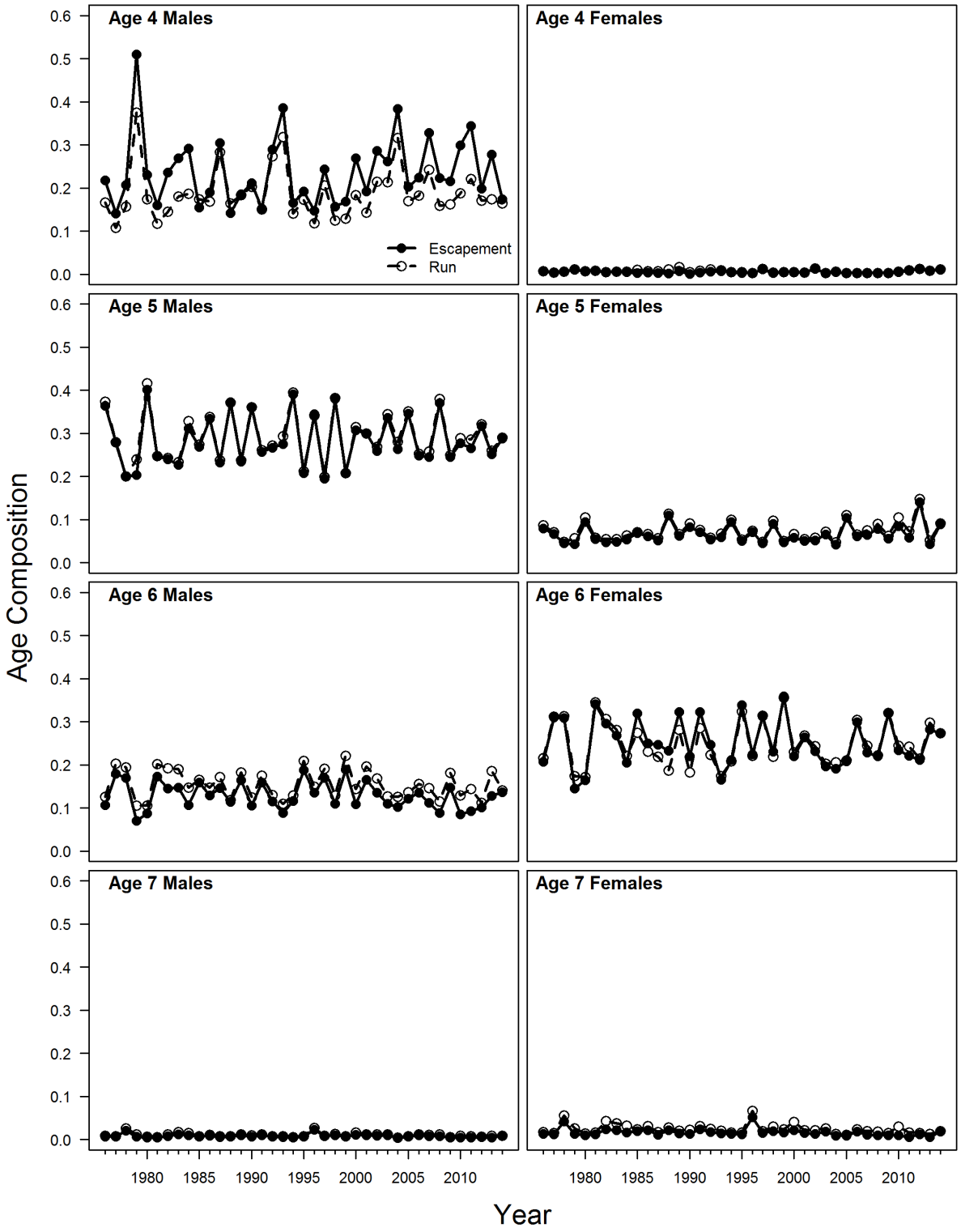

Figure 3.10 Spawner abundance that produces maximum sustained catch under unrestricted and restricted gill net mesh types. Estimates derived from an age/sex structured equilibrium model via numerical search for the harvest rate that maximizes catch with a penalty on the sex ratio that prevented all males from being harvested.

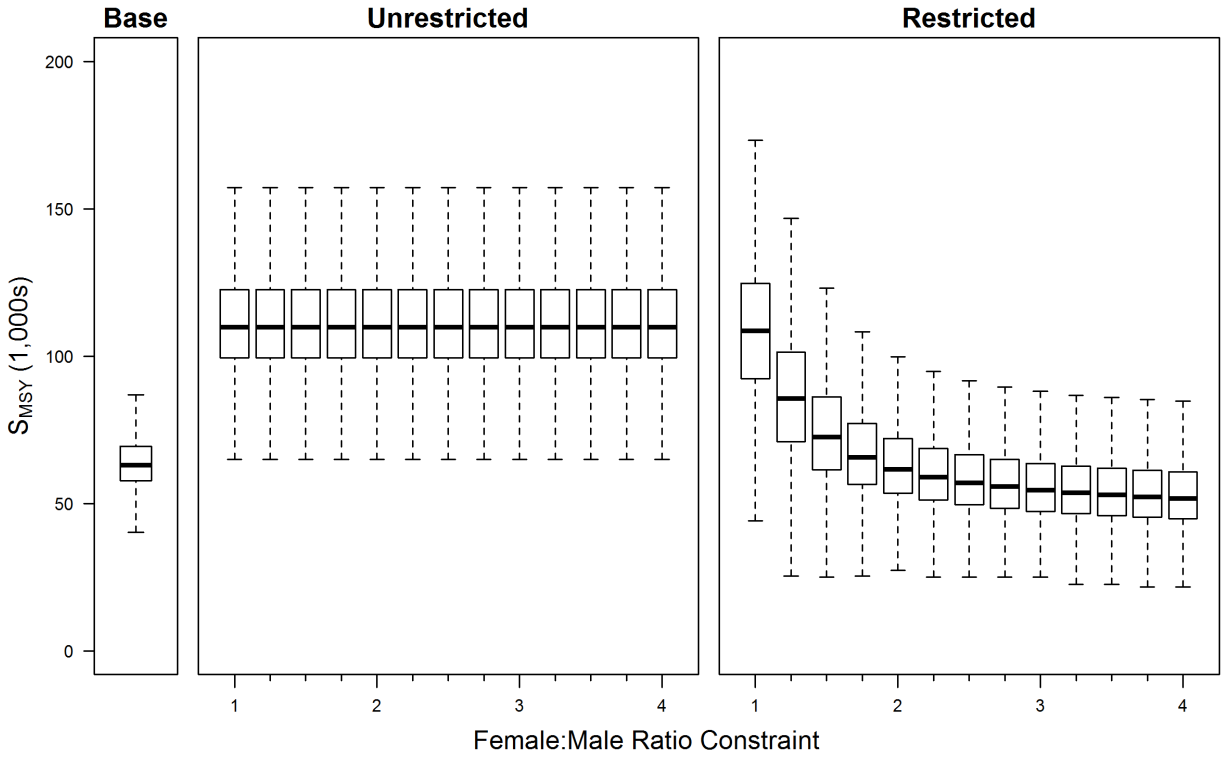

CHAPTER 3
TABLES

Table 3.01 Spawner-recruit and maturity parameters from the spawner quality model and a model that ignores spawner quality (Base; Chapter 2, this Thesis).

Parameter	Spawner Quality	Base Model
α	0.002 (0.0009-0.003)	6.33 (2.45-12.36)
β	2.98E-9 (1.81E-9-4.31E-9)	8.91E-6 (6.33E-6-1.17E-5)
σ_R	0.34 (0.23-0.48)	0.23 (0.15-0.34)
ϕ	0.62 (0.21-0.95)	0.81 (0.50-0.98)
D	129.12 (80.94-202.00)	75.28 (42.25-134.23)
π_4	0.20 (0.18-0.22)	0.19 (0.17-0.22)
$\pi_{4,M}$	0.19 (0.17-0.21)	—
$\pi_{4,F}$	0.007 (0.004-0.01)	—
π_5	0.36 (0.34-0.39)	0.39 (0.36-0.42)
$\pi_{5,M}$	0.29 (0.27-0.32)	—
$\pi_{5,F}$	0.07 (0.06-0.09)	—
π_6	0.40 (0.38-0.42)	0.39 (0.35-0.42)
$\pi_{6,M}$	0.15 (0.14-0.17)	—
$\pi_{6,F}$	0.25 (0.23-0.29)	—
π_7	0.03 (0.02-0.04)	0.03 (0.02-0.05)
$\pi_{7,M}$	0.01 (0.006-0.02)	—
$\pi_{7,F}$	0.02 (0.01-0.03)	—

APPENDIX II
SPAWNER QUALITY MODEL CODE

```
##############################################################################################
############################## ESCAPEMENT QUALITY MODEL CODE ##################################
##############################################################################################

model{
### Spawner-Recruit with Autocorrelated lag-1 residuals: for years with
spawner/recruit link
  lnalpha ~ dnorm(0,1.0E-2) %_% I(,6)
  beta ~ dunif(-10,10)
  for (y in (A+a.min):(Y+A-1)) {
    log.R[y] ~ dnorm(log.R.mean2.a[y],tau.white)
    R[y] <- exp(log.R[y])
    log.R.mean1.a[y] <- lnalpha + log(n.eggs.t[y-a.max]) - beta * n.eggs.t[y-a.max]
    log.resid.a[y] <- log(R[y]) - log.R.mean1.a[y]

    # RPS: Return per spawner
    RPS.a[y] <- R[y]/S.tot[y-a.max]
  }
  log.R.mean2.a[A+a.min] <- log.R.mean1.a[A+a.min] + phi * log.resid.0
  for (y in (A+a.min+1):(Y+A-1)) {
    log.R.mean2.a[y] <- log.R.mean1.a[y] + phi * log.resid.a[y-1]
  }

  ### monitoring quantities that don't start at y=1
  log.resid <- log.resid.a[(A+a.min):(Y+A-1)]
  RPS <- RPS.a[(A+a.min):(Y+A-1)]
  log.R.mean1 <- log.R.mean1.a[(A+a.min):(Y+A-1)]
  log.R.mean2 <- log.R.mean2.a[(A+a.min):(Y+A-1)]

  ### Priors for SR portion
  phi ~ dunif(-1,0.99) #dnorm(0,1.0E-4)%_%I(-1,1)
  tau.white ~ dgamma(0.01,0.01)
  log.resid.0 ~ dnorm(0,tau.red)#%_%T(-3,3)
  tau.red <- tau.white * (1-phi*phi)
  sigma.white <- 1 / sqrt(tau.white)
  sigma.red <- 1 / sqrt(tau.red)
  alpha <- exp(lnalpha)

  ### Brood year returns without SR link; drawn from a common lognormal dist
  mean.log.R0 ~ dnorm(0,1.0E-4)#%_%I(0,)
  tau.R0 ~ dgamma(0.1,0.1)
  R.0 <- exp(mean.log.R0)
  sigma.R0 <- 1 / sqrt(tau.R0)
  for (y in 1:a.max) {
    log.R[y] ~ dnorm(mean.log.R0,tau.R0)
    R[y] <- exp(log.R[y])
  }

  ### transform alpha(R/egg) into alphahat (R/spawner)
  for (a in 1:A) {
    # SPR0 = average maturity at age * mean eggs at age
    SPR0.a[a] <- pi[a + a.min] * tot.mean.eggs[a]
  }
  SPR0 <- sum(SPR0.a[])
  alpha.hat <- alpha * SPR0
  beta.hat <- beta * SPR0

  ### Generate Y+A-1=41 maturity schedules, one per brood year
  ### Proportion mature (returning to spawn) at age modeled as drawn from a dirichlet
distribution across brood years
  D.scale ~ dunif(0,1)
  D.sum <- 1 / (D.scale * D.scale)
  for (i in 1:7) { prob[i] ~ dbeta(1,1) }
```

```
  pi[1]<- prob[1]
  pi[2] <- prob[2] * (1 - pi[1])
  pi[3] <- prob[3] * (1 - pi[1] - pi[2])
  pi[4] <- prob[4] * (1 - pi[1] - pi[2] - pi[3])
  pi[5] <- prob[5] * (1 - pi[1] - pi[2] - pi[3] - pi[4])
  pi[6] <- prob[6] * (1 - pi[1] - pi[2] - pi[3] - pi[4] - pi[5])
  pi[7] <- prob[7] * (1 - pi[1] - pi[2] - pi[3] - pi[4] - pi[5] - pi[6])

  pi[8] <- 1 - pi[1] - pi[2] - pi[3] - pi[4] - pi[5] - pi[6] - pi[7]

  for (a in 1:A*2) {
    gamma[a] <- D.sum * pi[a]
    for(y in 1:(Y+A-1)){
      g[y,a] ~ dgamma(gamma[a],1.0)
      p[y,a] <- g[y,a]/sum(g[y,])
    }
  }

  ### male is [,,1], female is [,,2]
  for (y in 1:(Y+A-1)) {
    for (a in 1:A) {
      p.array[y,a,1] <- p[y,a]
      p.array[y,a,2] <- p[y,a+a.min]
    }
  }

  ### Calculate the numbers at age and sex array as brood year recruits at age *
proportion that matured that year
  for (s in 1:2) {
    for (t in 1:Y) {
      for (a in 1:A) {
        N.ta[t,a,s] <- R[t+A-a] * p.array[t+A-a,a,s]
      }
    }
  }

  ### SELECTIVE HARVEST PROCESS MODEL: APPLY SELECTIVE CATCHES BY RESTRICTED AND
UNRESTRICTED-MESH FISHERIES

  # Fix female age 4 and 7 as 1 in each gear
  select.unrestr[4,2] <- 1
  select.restrict[1,2] <- 1

  select.unrestr[4,1] ~ dbeta(1,1)
  select.restrict[1,1] ~ dbeta(1,1)

  for (s in 1:2) {
    select.unrestr[1,s] ~ dbeta(1,1)
    select.unrestr[2,s] ~ dbeta(1,1)
    select.unrestr[3,s] ~ dbeta(1,1)

    select.restrict[2,s] ~ dbeta(1,1)
    select.restrict[3,s] ~ dbeta(1,1)
    select.restrict[4,s] ~ dbeta(1,1)
  }

  ### APPLY UNRESTRICTED MESH TO ALL SUBSISTENCE HARVEST
  for (t in 1:Y) {
    U.max.sub[t] ~ dunif(0,0.99)
    U.max.com[t] ~ dunif(0,0.99)
  }

  for (s in 1:2) {
```

```
    for (t in 1:Y) {
      for (a in 1:A) {
        H.ta.sub[t,a,s] <- N.ta[t,a,s] * U.max.sub[t] * select.unrestr[a,s]

        # in-river at time and age..whats left after subsistence harvest is taken-at-
age
        IR.ta[t,a,s] <-  max(N.ta[t,a,s] - H.ta.sub[t,a,s], 1)
      }
    }
  }

  ### apply unrestricted years to commerical harvest
  for (s in 1:2) {
    for (t in 1:9) {
      for (a in 1:A) {
        H.ta.com[t,a,s] <- IR.ta[t,a,s] * U.max.com[t] * select.unrestr[a,s]
        S.ta[t,a,s] <- max(IR.ta[t,a,s] - H.ta.com[t,a,s], 1)
      }
    }
  }

  ### apply restricted years to commercial harvest
  for (s in 1:2) {
    for (t in 10:Y) {
      for (a in 1:A) {
        H.ta.com[t,a,s] <- IR.ta[t,a,s] * U.max.com[t] * select.restrict[a,s]
        S.ta[t,a,s] <- max(IR.ta[t,a,s] - H.ta.com[t,a,s], 1)
      }
    }
  }

  ### sum across ages to get calendar year N, H.com, H.sub, S, and mu
  for (s in 1:2) {
    for (t in 1:Y) {
      N[t,s] <- sum(N.ta[t,1:A,s])
      S[t,s] <- sum(S.ta[t,1:A,s])

      H.com[t,s] <- sum(H.ta.com[t,1:A,s])
      H.sub[t,s] <- sum(H.ta.sub[t,1:A,s])

      mu.sex[t,s] <- 1 - (S[t,s] / N[t,s])
      # break out total harvest rate by time and age
      for (a in 1:A) {
        mu.ta[t,a,s] <- 1 - (S.ta[t,a,s] / N.ta[t,a,s])
      }
    }
  }

  for (t in 1:Y) {
    N.tot[t] <- sum(N[t,])
    S.tot[t] <- sum(S[t,])
    H.sub.tot[t] <- sum(H.sub[t,])
    H.com.tot[t] <- sum(H.com[t,])
    mu[t] <- 1 - (S.tot[t] / N.tot[t])
    n.eggs.t[t] <- sum(n.eggs.ta[t,1:A])
    EPS[t] <- n.eggs.t[t]/S[t,2]
    for (a in 1:A) {
      n.eggs.ta[t,a] <- S.ta[t,a,2] * mean.eggs.ta[t,a]
    }
  }

  ### OBSERVE AGE COMPOSITION IN SUB AND COMM FISHERIES, ALSO ESCAPEMENT
  for (s in 1:2) {
```

```
  for (t in 1:Y) {
    for (a in 1:A) {
      # proportion harvest-at-age, escapement-at-age
      qs[t,a,s] <- H.ta.sub[t,a,s] / H.sub.tot[t]
      qc[t,a,s] <- H.ta.com[t,a,s] / H.com.tot[t]
      qe[t,a,s] <- S.ta[t,a,s] / S.tot[t]
    }
  }
}

for (t in 1:Y) {
  qs.vec[t,1:4] <- qs[t,1:A,1]
  qs.vec[t,5:8] <- qs[t,1:A,2]
  qc.vec[t,1:4] <- qc[t,1:A,1]
  qc.vec[t,5:8] <- qc[t,1:A,2]
  qe.vec[t,1:4] <- qe[t,1:A,1]
  qe.vec[t,5:8] <- qe[t,1:A,2]

  ### fit scale counts
  xs[t,] ~ dmulti(qs.vec[t,],ns[t])
  xc[t,] ~ dmulti(qc.vec[t,],nc[t])
  xe[t,] ~ dmulti(qe.vec[t,],ne[t])
}

### OBSERVE ESTIMATES OF SUBSISTENCE CATCH, COMMERCIAL CATCH
for (t in 1:Y) {
  ### fit subsistence catch to data
  sigma.H.sub[t] <- sqrt(log(pow(cv.H.sub[t], 2) + 1))
  tau.log.H.sub[t] <- 1/pow(sigma.H.sub[t], 2)
  log.H.sub[t] <- log(H.sub[t,1] + H.sub[t,2])
  Hhat.sub[t] ~ dlnorm(log.H.sub[t], tau.log.H.sub[t])

  ### fit commercial catch to data
  sigma.H.com[t] <- sqrt(log(pow(cv.H.com[t], 2) + 1))
  tau.log.H.com[t] <- 1/pow(sigma.H.com[t], 2)
  log.H.com[t] <- log(H.com[t,1] + H.com[t,2])
  Hhat.com[t] ~ dlnorm(log.H.com[t], tau.log.H.com[t])
}

### Escapement Indices
for (j in 1:20) {
  r[j] ~ dgamma(0.001, 0.001)
  k[j] ~ dnorm(10, 1E-8) %_% I(0,)
}

### Negative binomial likelihood fitting escapement indices
for (i in 1:num.index) {
  est.esc[i] <- S.tot[esc.year[i]]/k[trib[i]]
  p.esc[i] <- r[trib[i]]/(est.esc[i]+r[trib[i]])
  index[i] ~ dnegbin(p.esc[i], r[trib[i]])
}

### Weekly commericial CPUE
tau.cat ~ dgamma(0.001, 0.001)
for (q in 1:3) {
  ln.Q[q] ~ dnorm(0, 1E-10)
  Q[q] <- exp(ln.Q[q])
}
q.unr <- Q[1]
q.res <- Q[2]
q.mono <- Q[3]

### estimated commercial catch and fitting it to obs
```

```
  for (i in 1:num.com) {
    est.c.catch[i] <- log(pp[i] * N.tot[c.year[i]] * (1 - exp(-Q[gear[i]] *
effort[i])))
    catch[i] ~ dlnorm(est.c.catch[i], tau.cat)
  }

  #in river likelihood. using total estimated escapement (mark recap+lower river
expansion).  Keeps model internally consistent.
  for (i in 28:32) {
    log.S[i] <- log(S.tot[i])
    inr.s[i] ~ dlnorm(log.S[i], tau.inr.s[i])
  }
}

### END OF MODEL ###
```

CHAPTER 4

USE OF SEVERAL HIERARCHICAL MODEL SELECTION TECHNIQUES IN THE DEVELOPMENT OF A HABITAT MODELING APPROACH FOR ALASKAN CHINOOK SALMON

ABSTRACT

Management strategies for Alaska Chinook salmon rely on biological reference points (e.g., S_{MSY}) to set harvest targets which are traditionally derived using spawner-recruit analysis. However, not all stocks in Alaska are sampled intensively enough to allow for derivation of reference points through spawner-recruit analyses, yet their management must still be based on stock-specific reference points. Habitat-based methods have been developed to predict S_{MSY} for stocks without adequate spawner-recruit information based on a subset of stocks that do have this information. These models form a linear predictive relationship between S_{MSY} and certain habitat characteristics (e.g., drainage area) that can be used for more data-limited stocks. Here I build on this work by developing a hierarchical modeling approach for Alaskan Chinook salmon stocks that incorporates the uncertainty in stock-specific S_{MSY} and applying a suite of model selection techniques to select habitat variables that have predictive credibility. Findings showed that hierarchical inclusion of uncertainty in S_{MSY} did not remove the relationship between drainage area and S_{MSY}, showing that this relationship may still be used even when including this additional source of variation. Three of the four variable selection techniques consistently agreed on the best variables. The deviance information criterion performed poorly at distinguishing models and potential explanations are discussed. Drainage area as the sole predictor was unanimously chosen by the best model under the three remaining model selection approaches.

INTRODUCTION

Management strategies for Chinook salmon (*Oncorhynchus tshawytscha*) stocks rely on estimates of biological reference points (e.g. S_{MSY}) to set harvest targets. Ideally, these reference points are derived using spawner-recruit analysis on a time series of spawner and return counts which provides information regarding productivity, carrying capacity, and strength of compensation of the stock. However, many Chinook salmon stocks are not sampled intensively enough for reliable estimation of biological reference points via spawner-recruit analysis. In these more data-limited situations, habitat-based assessment approaches have been used. These methods use habitat variables that are related to salmon productivity and capacity to build models using estimates from stocks with adequate spawner-recruit data. The coefficient estimates from this model can then be used for prediction of reference points for stocks that have inadequate spawner-recruit data.

One habitat variable that has shown promise in these models is the area of the drainage for each stock. Parken et al. (2006) developed such a model using stocks from Oregon, Washington, British Columbia, and Alaska. However, a predictive model has not yet been developed for exclusively Alaskan stocks (i.e., those that spawn in rivers that originate in Alaska), which will be the focus of this chapter. Although several of the stocks used in the present analysis were also used by Parken et al (2006), the data for these stocks have since been updated with more current information and the individual spawner-recruit analyses for each stock used a more rigorous Bayesian state-space approach (Catalano 2012).

The methodology for the modeling approach presented here differs in two primary ways from that of Parken et al. (2006). First, Parken et al. (2006) treated the reference points (i.e., the response variable) as known quantities, when they are really derived from parameters estimated

from a spawner-recruit analysis. Spawner-recruit relationships are inherently noisy and as a result, their parameters and the derived reference points (equations 2.09-2.011, Chapter 2, this Thesis) contain substantial uncertainty. Treating the reference points as known quantities ignores this uncertainty and may lead to conclusions that would not be valid were this uncertainty included (Brooks and Debora 2015). For this reason, a hierarchical modeling approach is implemented here to allow for incorporation of the uncertainty in the reference points that the model is fit to. The model is cast in the Bayesian mode of inference which allows for an intuitive framework to include this additional source of uncertainty. Second, model uncertainty will be introduced into the habitat-based modeling approach by examining additional habitat variables. These additional variables are hypothesized to influence salmon productivity and capacity and are available via remote sensing techniques.

The Parken et al. (2006) model is not the only predictive habitat-based model for Chinook salmon. Liermann et al. (2010) developed an integrated hierarchical model that included an intrinsic link between watershed area and spawner-recruit parameters in the model fitting. Thus, the Liermann et al. (2010) model used not only the stock-specific spawner-recruit data but also habitat information to estimate the spawner-recruit relationships for stocks used in their model. This habitat relationship linkage between stocks was intended to improve predictive performance by reducing uncertainty in the predictive relationship. Although the analyses presented in this chapter do not share information between stocks when fitting the spawner-recruit relationships, as in the Liermann et al. (2010) analysis, the regression coefficients of the habitat model are estimated from all stocks.

Model selection is an area of active research in ecological modeling as a means to variable selection (Hooten and Hobbs 2015; Anderson et al. 2008). Of particular interest are

methods for model selection for analyses in the Bayesian mode of inference as no one unified approach performs well for all models (Hooten and Hobbs 2015). Much of this disagreement revolves around the requirement of the prior in Bayesian analyses because objective methods for choosing appropriate priors do not exist. This deficiency remains one of the most prevalent criticisms of the Bayesian framework, as two investigators can obtain different results based on prior beliefs. The prior makes information theoretic approaches to Bayesian model selection particularly troublesome, as there are no truly free parameters in the Bayesian context due to the information content in the prior, however uninformative it may be (Hooten and Hobbs 2015). Thus, four different approaches are applied here to selecting habitat variables based on their predictive abilities while accounting for uncertainty in the response variable: variable indicator selection, the deviance information criterion (DIC), the Akaike information criterion (AIC) using randomized posterior samples, and leave-one-out cross validation. So in addition to investigating the relationship between various habitat variables with S_{MSY}, this chapter also presents a comparison of various approaches to model selection. The objectives of the analyses presented in this chapter are to (1) develop a habitat-based predictive model for data-poor Alaskan Chinook salmon stocks that explicitly incorporates uncertainty in the estimates that it is fit to by (2) evaluating the agreement in the best predictor variables between a variety of model selection techniques.

METHODS

Study Area and Species

This study uses information from Chinook salmon stocks across the state of Alaska (Figure 4.01). Chinook salmon are an important species for commercial, subsistence, and recreational fisheries across the state. In the past decade, many Chinook salmon stocks across the

state have seen declines in productivity, making adequate treatment of uncertainty in management quantities of paramount importance (Schindler et al. 2013). Catalano (2012) conducted a meta-analysis of 15 Chinook salmon stocks across the state of Alaska by developing Bayesian state-space spawner-recruit models for each stock that gave marginal posterior distributions for stock-specific S_{MSY}. The summaries of these posterior distributions are used to fit the regression models in this chapter.

The stocks used in this analysis cover a wide range in terms of maximum productivity (2.08 – 8.95 recruits per spawner), stock abundance (8,800 – 244,000 average recruits), and drainage area (562 – 286,000 km^2). Geographically, these stocks are spread all throughout the state (Figure 4.01) including southeastern Alaska (Stikine, Taku, and Alsek), Kodiak Island (Karluk), western Alaska (Goodnews, Kuskokwim, and Unalakleet), and the interior (Chena+Salcha; two rivers, assessed as one stock).

Selected Habitat Variables

Habitat variables were selected based on a hypothesized effect on salmon productivity or stream carrying capacity. Both productivity and capacity impact the S_{MSY} reference point, so any habitat variable that may impact these two quantities should be included in the analysis. Three habitat variables were selected that each have biological justification for inclusion in the model, as outlined in the following sections. The value of these variables for each stock were accessed using the Riverscape Analysis Project (RAP) online database (Whited et al. 2012; http://rap.ntsg.umt.edu). Four of the 15 stocks were outside of the RAP study area, and thus were excluded from this analysis. All habitat variables were standardized (scaled and centered) such that no one data point fell too far from zero, as recommended by Kéry (2010).

The area (km^2) of the drainage (watershed) of a particular river was hypothesized to influence the value of S_{MSY} because a larger area results in more spawning and rearing grounds for salmon, which directly impacts the capacity of a system. Drainage area has been shown to have predictive power for S_{MSY} in both stream-type (Alaskan stocks) and ocean-type (more southern stocks) Chinook salmon (Parken et al. 2006). This variable was log-transformed to linearize the relationship with $\log(S_{MSY})$, following Parken et al. (2006).

Tributaries are the areas within the drainage in which adult salmon typically spawn and juvenile salmon spend much of their lives before migrating to sea. Therefore, it stands to reason that drainages that have more tributaries should produce more salmon. This variable was expressed as per km^2 to remove collinearity with area; larger drainages have more tributaries. Tributary node density was not log-transformed as the range was so small that a log-transformation had no effect in linearizing the relationship with $\log(S_{MSY})$.

The shifting habitat mosaic hypothesis predicts that productivity is maximized at high levels of stream complexity (Standford et al. 2005). Channel nodes are an indicator of this complexity as they represent the amount of braiding in the stream channel and floodplains and so was selected for analysis. This variable was standardized by area (km^2) for the same reason as tributary nodes. Channel node density was not log-transformed as the relationship with $\log(S_{MSY})$ appeared linear.

Model Structure

Consider the normal linear model where the response variable, y_i, is the natural logarithm of S_{MSY} for stock i and $\beta_{0:n}$are coefficients that describe the linear relationship between habitat variable $x_{1:n}$ and y_i for stock i. Residual variation in this relationship (variation in y not explained

by the habitat variables $x_{1:n}$) is assumed to be independently and identically normally distributed with a mean of zero and some standard deviation σ that is freely estimated.

To incorporate uncertainty in y_i (due to estimation and process error in the spawner-recruit relationship and measurement error in the data collection) an additional source of variation was required, which made the model hierarchical in nature (i.e., having multiple sources of statistical uncertainty). First, a model prediction was made based on the underlying linear process that was assumed to give rise to the mean log(S_{MSY}) for each stock:

$$\mu_i=\beta_0+\beta_1 x_{1,i}...\beta_n x_{n,i} \quad (3.01)$$

The quantity μ_i constitutes the linear predictor, but it is obvious that there is noise in the relationship due to factors other than the selected habitat variables. This additional source of variation is commonly referred to as process error. Thus, a stock-specific latent state log(S_{MSY}) was sampled from a normal distribution that represents the true log(S_{MSY}) after accounting for this process variation around the deterministic relationship:

$$\psi_i \sim N(\mu_i, \tau_\psi) \quad (3.04)$$

where ψ_i is the latent state for stock *i* as produced by the habitat relationship and unexplained noise and had some estimated precision (inverse of the variance) parameter τ_ψ that was common across all stocks. The response variable y_i was related to the latent ψ_i via another stochastic node:

$$y_i \sim N(\psi_i, \tau_i) \quad (3.05)$$

where y_i is the posterior mean log(S_{MSY}) and τ_i is the inverse of the posterior variance for stock *i*, as presented by Catalano (2012). τ_i can be interpreted as an assumed measurement error on the true state, and its inclusion allowed for the incorporation of uncertainty in the estimated S_{MSY} from the analysis presented by Catalano (2012). It is this additional source of uncertainty in the

response variable (measurement as well as process variation) that is not included in a typical multiple regression.

Habitat Variable Selection

Four different methods were used for selecting which variables should be included in the final predictive habitat-based model. A brief overview of each method is outlined below.

Indicator Variable Selection (*Parameter Inclusion Probability*)

This method used binary indicator parameters that included or excluded habitat variables in each Markov Chain Monte Carlo (MCMC) iteration to select variables that were justified in the model. The approach sampled an indicator parameter ω from an uninformative Bernoulli distribution for each slope coefficient in the process model:

$$\omega_{1:n} \sim Bernoulli(0.5) \tag{3.06}$$

These indicators were then included in the linear predictor in equation 3.03

$$\mu_i = \beta_0 + \omega_1 \beta_1 x_{1,i} \ldots \omega_n \beta_n x_{n,i} \tag{3.07}$$

For each MCMC iteration, each coefficient was included ($\omega = 1$) or excluded ($\omega = 0$). The posterior mean of ω_n can be interpreted as the probability that $\beta_n x_n$ should be included in the model. This is a technique for incorporating model uncertainty into the model fitting. The combination of coefficients being included or excluded in each MCMC iteration results in a total of eight different models. Thus, a model probability can be calculated by taking the proportion of MCMC iterations the respective coefficients were included in the same MCMC iteration.

If a variable is excluded from the linear predictor in an iteration ($\omega = 0$), its coefficient is still sampled on that iteration. As noted by Hooten and Hobbs (2015), independent diffuse priors in this setting can cause computational problems in the MCMC sampling. For example, if the

coefficient is excluded in one iteration, and the sampler draws a value of the corresponding coefficient with a highly diffuse prior, it is possible for the MCMC to get "lost". Essentially, the sampled value can be so far from the majority of the posterior density that the MCMC algorithm cannot return to that density by sampling a more likely value and the indicator parameter is never included again. This issue can be addressed in at least two ways: (1) through the use of informative priors that prevent the MCMC sampler from getting "lost" by making extreme values so unlikely that they are never sampled or (2) the use of reversible jump MCMC (RJMCMC), where if $\omega = 0$ for a given iteration, the corresponding coefficient is not sampled that iteration. Since a general RJMCMC algorithm has not yet been developed for use in JAGS (or OpenBUGS), informative priors were chosen to remedy this issue (Table 4.01).

Deviance Information Criterion (DIC)

Information theoretic approaches have gained substantial support in model selection techniques and ecological analysis (Anderson et al. 2008). However, as mentioned previously, the information contained in the prior makes information theoretic approaches to Bayesian model selection troublesome (Spiegelhalter et al. 2014). However, one proposed solution is the deviance information criterion (DIC; Spiegelhalter et al. 2002). DIC is the Bayesian analog to the Akaike information criterion (AIC) for models fit in the frequentist mode of inference, in that it uses a measure of statistical fit and penalizes it by the number of parameters in the model (Plummer 2008). DIC is calculated as:

$$DIC = \widehat{D} + p_{\mathrm{D}} \tag{3.08}$$

where $\widehat{D}$ is the posterior expectation for model deviance calculated at the posterior means of all unknown quantities (Hooten and Hobbs 2015). p_{D} is the effective number of parameters, calculated as $\overline{D}$ (mean posterior deviance) minus $\widehat{D}$.

Randomization with AIC Model Selection

Another way to incorporate posterior uncertainty in S_{MSY} into the model fitting and selection is to randomize and sample from these posterior samples, fit each model to each randomized sample, and conduct AIC model selection using each sample. The distribution of the model selections across all randomized samples can then serve as the basis for inference on justified variables. The posterior distributions of S_{MSY} for each stock contain approximately 10,000 samples each (less than 10,000 after removing the very rare negative S_{MSY}). These samples were randomized and all valid samples were used for this exercise. Models for this randomization component were fit using ordinary least-square methods with the normal linear model instead of Bayesian methods. Inference regarding which variables were most important was made using three criteria: (1) frequency of placement of each variable in the best model, (2) the distribution of the position of each model in the model selection across all samples, and (3) the distribution of model weight for each model across all samples. Although the term AIC is used to describe this method of model selection, the information theoretic calculation that was used was the version corrected for small sample sizes (AIC_C; Anderson et al. 2008).

Leave-One-Out Cross Validation

The fourth and final model selection technique used in this analysis is referred to as "*k*-fold cross-validation". The premise of this method is to test the capability of a model to predict datasets that are not included in the model fitting (i.e., the model is unaware of them). *K* datasets were sequentially left out of the model fitting, then compared to their corresponding model prediction to calculate the predictive loss of that model (Hooten and Hobbs 2015). In the case where *n* is small, like in the scenario presented in this chapter, one data point can be left out at a

time (hence, leave-one-out cross-validation). Hooten and Hobbs (2015) present a cross-validation score calculation for a single model:

$$\sum_{k=1}^{K} \log \frac{\sum_{t=1}^{T} P(y_k | y_{-k}, \theta_t)}{T} \tag{3.09}$$

where y_k is the measured value of the data point left out in the k^{th} run of the model out of K total runs, y_{-k} is the model prediction for that data point given by the parameters θ on the t^{th} MCMC iteration fit with y_k left out and T is the number of saved MCMC samples. Since the models assume a normal error structure, it is appropriate to use a sum-of-squared residual in place of the likelihood calculation in the numerator of equation 3.09. The altered cross-validation score used in this analysis is:

$$\sum_{k=1}^{K} \frac{\sum_{t=1}^{T} (y_k - y_{-k})^2}{T} \tag{3.10}$$

This process was then repeated for all subsets of the full model and the scores were compared across models, where the lowest score indicates the least predictive loss (i.e., accurately predicts data points not included in the model) and the best model for prediction.

Computation

All analyses were conducted using the R statistical environment (R Core Development Team; 2014). The indicator variable selection and cross validation methods were conducted using JAGS (Just Another Gibbs Sampler; Plummer 2013) using the R package "rjags" (Plummer 2014). JAGS is an implementation of the BUGS (Bayesian Inference Using Gibbs Sampling) language, which is a flexible and intuitive platform for specifying and fitting Bayesian hierarchical models. The DIC approach was conducted using the "dic.samples" function in the "rjags" package (Plummer 2014). Marginal posterior distributions were summarized as the mean and 95% credible intervals (i.e., 2.5 and 97.5 percentiles). Randomization procedures were conducted using original R code to randomly select individual posterior samples of S_{MSY} for each

stock as the response variable and the R package "MuMIn" (i.e., multi-model inference; Barton 2015) to conduct AIC model selection for all eight models for each randomized sample.

RESULTS

Convergence of all models fit with MCMC methods was confirmed by a Gelman-Rubin statistic for all estimated parameters of <1.1 (Gelman et al. 2004).

Indicator Variable Selection

In terms of which variables should be included in the model, drainage area received the most posterior support for inclusion in the model, followed by channel node density, and tributary node density received the least support (Table 4.02). Barberi and Berger (2004) suggested that variables with indicator parameter values of greater than 0.5 contain justifiable predictive information. Following this threshold, drainage area was the only habitat variable that can be reliably used for prediction.

There was little supporting evidence for the inclusion of more than one predictor variable (Table 4.03). The model that carried the most probability was the drainage area-only model, followed by the channel node density-only model. The intercept-only model carried more probability than any of the other five models, which suggested that the mean S_{MSY} across all stocks was a better predictor of stock-specific S_{MSY} than the combinations of the habitat variables in these five lower models. Tributary node density appeared in the worst four models, which indicated that it was a very poor predictor of S_{MSY} for the stocks included in this analysis. These findings were further supported by the estimated effect size for each parameter and whether its credible interval included zero (Table 4.04). These effects were calculated from the posterior distribution of each parameter when the parameter was included to prevent the coefficient samples that did not influence the likelihood from affecting the posterior mean. Drainage area

had the largest effect and it was the only parameter with a 95% credible interval that did not overlap zero.

Since informative priors were used to aid the MCMC sampler, the influence of prior information was investigated graphically (Figure 4.02). It is clear that the seemingly informative prior (Table 4.01) was indeed flat over the range of the posterior density for each coefficient. All posterior samples where $\omega = 0$ were removed for this plot to assess the influence of the prior on the posterior since these were the only samples where the data influenced the posterior draw.

Coefficients were combined using model averaging according to how often they were included in the model fitting and were used to make a predictive diagnostic plot (Figure 4.03). This is an "observed versus predicted" plot where points are pairs of model predictions (x-axis) and observed data points (y-axis). The dotted line is the 1:1 line where a model prediction is the exact same as the data. For stocks with low S_{MSY}, the model performed well at predicting their value, but the stock with observed S_{MSY} of approximately 80,000 was not predicted well by the model-averaged coefficients. This abnormal stock is the Kuskokwim River in western Alaska, and it seems that it requires more escaping fish to attain maximum sustainable yield than would be predicted by the habitat variables included in this model.

Deviance Information Criterion

The DIC analysis showed that each of the models had p_D within one parameter of one another (Table 4.03). In general, models with the same number of predictor variables had the same number of effective parameters (e.g., the area-only and the channel node density-only model had p_D of 9.62 and 9.63, respectively; Table 4.03). However, this was not always the case as the intercept-only model that contained no coefficients for habitat predictor variables and the full model that contained coefficients for all three habitat variables resulted in essentially the

same p_D (10.02 versus 10.03, respectively; Table 4.03). This showed that in some cases the sampler was able to adequately estimate the number of free parameters, but that in other cases the number of free parameters changed in an unpredictable manner.

Randomization with AIC Model Selection

Drainage area and channel node density were supported by this randomization analysis, whereas tributary node density showed very little support, as it was in all four of the worst models (Tables 4.02, 4.03; Figure 4.04). Drainage area and channel node density were present in the best model in 71% and 27% of the randomized samples, respectively (Table 4.02). Tributary node density was present in the best model in only 2% of the samples.

Leave-One-Out Cross Validation

In terms of predictive ability for data points left out of the model fitting, the drainage area-only model exhibited the lowest predictive loss and the additive area and channel node density had the next lowest loss (Table 4.03). The intercept-only model placed fifth in predictive loss, which indicated that there are combinations of variables that perform more poorly at out-of-sample prediction than simply the mean of the included stocks. This intercept-only model had approximately 50% more loss than the area-only model. The worst two models, the full model and the additive channel node density and tributary node density model, each had 78% more predictive loss than the best model.

DISCUSSION

Overall, the different model selection techniques agreed very well in regard to which variables have predictive credibility. All methods except DIC selected drainage area as the best predictor of S_{MSY}, followed by channel node density. Tributary node density gained very little support under three out of the four methods (DIC disagreed), perhaps due to the lack of

resolution in this variable (all stocks had approximately 0.1 tributaries/km^2). Additionally, the same three out of the four methods favored selecting only one predictor for the best model, and this single predictor was drainage area. This finding lends more credibility to the Parken et al. (2006) model that considered only drainage area. DIC showed little to no separation between models, making inference based its findings very difficult.

The model weight column of Table 4.03 (randomization method) is analogous in interpretation to the model probabilities shown in the first column (variable indicator method) because the AIC model weight is defined as the probability that the model is the best, among those selected for analysis. This definition is equivalent to the model probability presented in Table 4.03. Upon comparison of these two findings, it is clear that the two methods give very similar results. All models carried approximately the same weight under both approaches, with the primary difference being that the intercept-only model placed third best under the Bayesian indicator selection and fourth best in the randomization.

Based on this consistent agreement with the randomization approach, it seems that the Bayesian indicator variable approach is an adequate technique for model selection for this hierarchical model. However, the indicator variable technique only returned these results when the specific prior in Table 4.01 was used for the coefficients. When the prior was made more diffuse in preliminary runs of the analysis, the indicator variables tended to select the intercept-only model as the best, and with high certainty (approximately 0.8 probability). This was likely due to the MCMC sampler "getting lost" as previously mentioned. So while the Bayesian model selection technique did return very similar inference to the more frequentist method, its findings were contingent on the prior specification, which warrants some caution. As there is no objective way to decide how informative of a prior one should use to correct the "getting lost" problem, it

is possible that two investigators would come to very different conclusions using these same data. This discrepancy is potentially due to two linked mechanisms: (1) the small sample size and (2) the hierarchical incorporation of uncertainty in the response variable. Including the uncertainty in the response variable required more parameters and placed a high demand of the small number of stocks used. There were 11 stocks used to fit the variable indicator model, and each had a mean S_{MSY} and an inverse variance that were provided to the model as data, which lead to a total of 22 pieces of information used by the model (ignoring priors). If the effective number of parameters returned by the DIC analyses would be trusted, then the model had approximately 10 free parameters, which means that there were approximately two pieces of information for every free parameter. This information-to-parameter ratio puts this model on the fringes of over-parameterization. If it were possible to include more data points, it is possible that a more diffuse prior specification could be used on the coefficients.

The hierarchical inclusion of posterior uncertainty in $\log(S_{MSY})$ from the Catalano (2012) analysis was effective at increasing the uncertainty in the area-$\log(S_{MSY})$ relationship. When a Bayesian hierarchical model with unstandardized area only and uninformative priors on the coefficients (mean = 0, precision = 1E-8) was compared to a frequentist analysis that treated the $\log(S_{MSY})$ as known quantities, the estimates showed more uncertainty under the Bayesian analysis. The estimate of the area effect was 0.35 (0.08-0.61) under the Bayesian analysis and 0.35 (0.10-0.60) under the frequentist analysis. While these estimates and intervals are very similar, the residual standard error was greater under the Bayesian analysis (0.79) than under the frequentist analysis (0.72). This greater uncertainty in the area-$\log(S_{MSY})$ relationship is due to the inclusion of uncertainty in $\log(S_{MSY})$, however one could argue that the difference is not large enough to discredit treating $\log(S_{MSY})$ as known quantities under a frequentist analysis.

DIC proved ineffective at distinguishing between models, and thus inference based on its results should be done so carefully. The full model included three more coefficients than the intercept-only model, however the DIC model selection indicated that there was no difference in the effective number of parameters between these models. This was an unexpected finding, but one can speculate as to why this was the case. The model used a linear predictor to make the mean prediction for each stock based on habitat variables (μ_i), then sampled a latent state variable (ψ_i) from a distribution with the linear prediction (μ_i) as the mean and a common process error (τ_ψ). These latent states were then fit to the mean log(S_{MSY}) and their variances from Catalano (2012) in the likelihood. When there were predictor variables included in the model, there was information about the value of the latent state contained in the linear predictor. Conversely, when only the intercept was used as the linear predictor, the only information about the latent state was the mean log(S_{MSY}) across all stocks. In the latter case, the latent states were more "free" as they were less informed by habitat data and thus could have resulted in a similar p_D as the full model. Regardless of the cause the lack of model separation in the DIC analysis, its nature renders inference based on this method regarding the best predictor variables highly uncertain and essentially impossible.

Furthermore, Plummer (2008) noted that DIC is only useful for models in which the ratio of data points to parameters is large. If this is not the case, then more complex models will be underpenalized (Plummer 2008). Although Plummer (2008) never defined what "large" means for this ratio, certainly the ratio in the present analysis was small. There was a total of 11 stocks used in this analysis (Figure 4.01) and the model used latent variables for each stock, plus coefficients for the habitat predictors, and a common precision parameter for the latent variable

sampling distributions. This is another potential cause for the DIC model selection results lacking differentiation between models.

It is worth noting that while the results of these model selection exercises gave credence to Parken et al.'s (2006) choice of drainage area as the sole predictor of S_{MSY}, the coefficients from the present analysis are not directly comparable to this previous study. Parken et al. (2006) censored drainage area based on accessible habitat: that area of the drainage that feeds the stream below natural and man-made barriers. Drainage area used in the present study was not censored using this criterion. Thus, one unit of area in the Parken et al. (2006) approach can support more spawners than one unit of area in the present study. This statement agrees with the coefficient estimates from both studies: Parken et al. (2006) reported an effect size of $0.69/km^2$ whereas a model using only unstandardized drainage area under the present study estimated an effect size of $0.35/km^2$. It could be argued that not censoring area based on accessible habitat makes the model more straight-forward to implement for managers, but it also may introduce an additional source of variation into the model.

REFERENCES

Anderson, D.R., K.P. Burnham, W.L. Thompson. 2008. Null hypothesis testing: problems, prevalence, and an alternative. Journal of Wildlife Management. 64(4): 912-923.

Barberi, M.M, and J.O. Berger. 2004. Optimal predictive model selection. The Annals of Statistics. 32(3): 870-897.

Barton, K. 2015. MuMIn: Multi-Model Inference. R package version 1.13.4. http://CRAN.R-project.org/package=MuMIn.

Catalano, M. J. 2012. Comparative analysis of patterns in productivity for AYK and selected non-AYK Chinook salmon stocks. Workshop Background Paper (unpublished working paper) *In* AYK SSI Chinook salmon Synthesis Workshop, May 2-3, 2012. Arctic-Yukon-Kuskokwim Sustainable Salmon Initiative, Anchorage, AK.

Gelman, A., J.B. Carlin, H.S. Stern, and D.B. Rubin. 2004. Bayesian Data Analysis. Second ed. CRC/Chapman & Hall, Boca Raton, Florida.

Kery, M. 2010. Introduction to WinBUGS for ecologists. Academic Press, Burlington, Massachusetts.

R Development Core Team. 2014. R: A Language and Environment for Statistical Computing. R Foundation for Statistical Computing. Version 3.1.0. Vienna, Austria. http://www.R-project.org.

Plummer, M. 2014. rjags: Bayesian graphical models using MCMC. R package version 3-14. http://CRAN.R-project.org/package=rjags.

Plummer, M. 2013. JAGS Version 3.4.0 user manual.

Plummer, M. 2008. Penalized loss functions for Bayesian model comparison. Biostatistics. 9(3): 523-539.

Parken, C. K., R. E. McNicol, and J. R. Irvine. 2006. Habitat-based methods to estimate escapement goals for data limited Chinook salmon stocks in British Columbia, 2004. Department of Fisheries and Oceans, Canadian Scientific Advisory Secretariat Research Document 2006/083.

Schindler, D., C. Kreuger, P. Bisson, M. Bradford, B. Clark, J. Conitz, K. Howard, M. Jones, J. Murphy, K. Myers, M. Scheuerell, E. Volk, and J. Winton. 2013. Arctic-Yukon-Kuskokwim Chinook Salmon Research Action Plan: Evidence of Decline of Chinook Salmon Populations and Recommendations for Future Research. Prepared for the AYK Sustainable Salmon Initiative (Anchorage, AK), 79 pp.

Spiegelhalter, D.J., N.G. Best, B.P. Carlin, and A. van der Linde. 2002. Bayesian measures of model complexity and fit. Journal of the Royal Statistical Society: Series B. 64(4): 583-689.

Spiegelhalter, D.J., N.G. Best, B.P. Carlin, and A. van der Linde. 2014. The deviance information criterion: 12 years on. Journal of the Royal Statistical Society: Series B 76(3): 485-493.

Stanford, J.A., M.S. Lorang, and F.R. Hauer. 2005. The shifting habitat mosaic of river ecosystems. Proceedings of the International Society of Limnology. 29(1): 123-136.

Thomas, A., B. O'Hara, U. Ligges, and S. Sturtz. 2006. Making BUGS open. R News. 6(1): 12-17.

Whited, D.C., J.S. Kimball, J.A. Lucotch, N.K. Maumenee, H. Wu, S.D. Chilcote, and J.A. Stanford. 2012. A riverscape analysis tool developed to assist wild salmon conservation across the north Pacific Rim. Fisheries. 37(7): 305-314.

CHAPTER 4
FIGURES

Figure 4.01 Distribution of stocks included in this analysis.

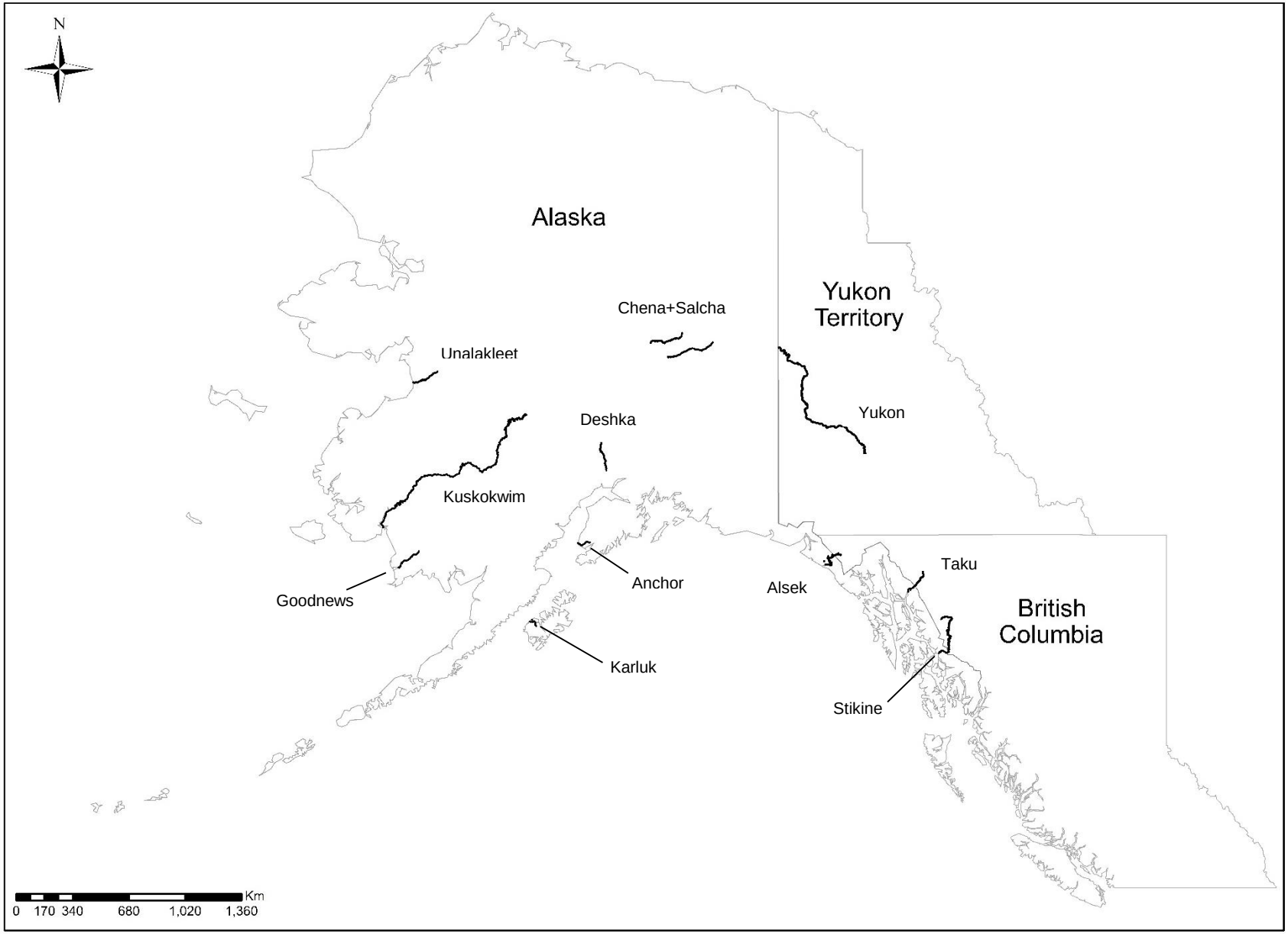

Figure 4.02 Posterior distribution for each slope coefficient after iterations where the corresponding indicator variable was turned off (solid line) were excluded and the prior shown in Table 4.01 (dashed line).

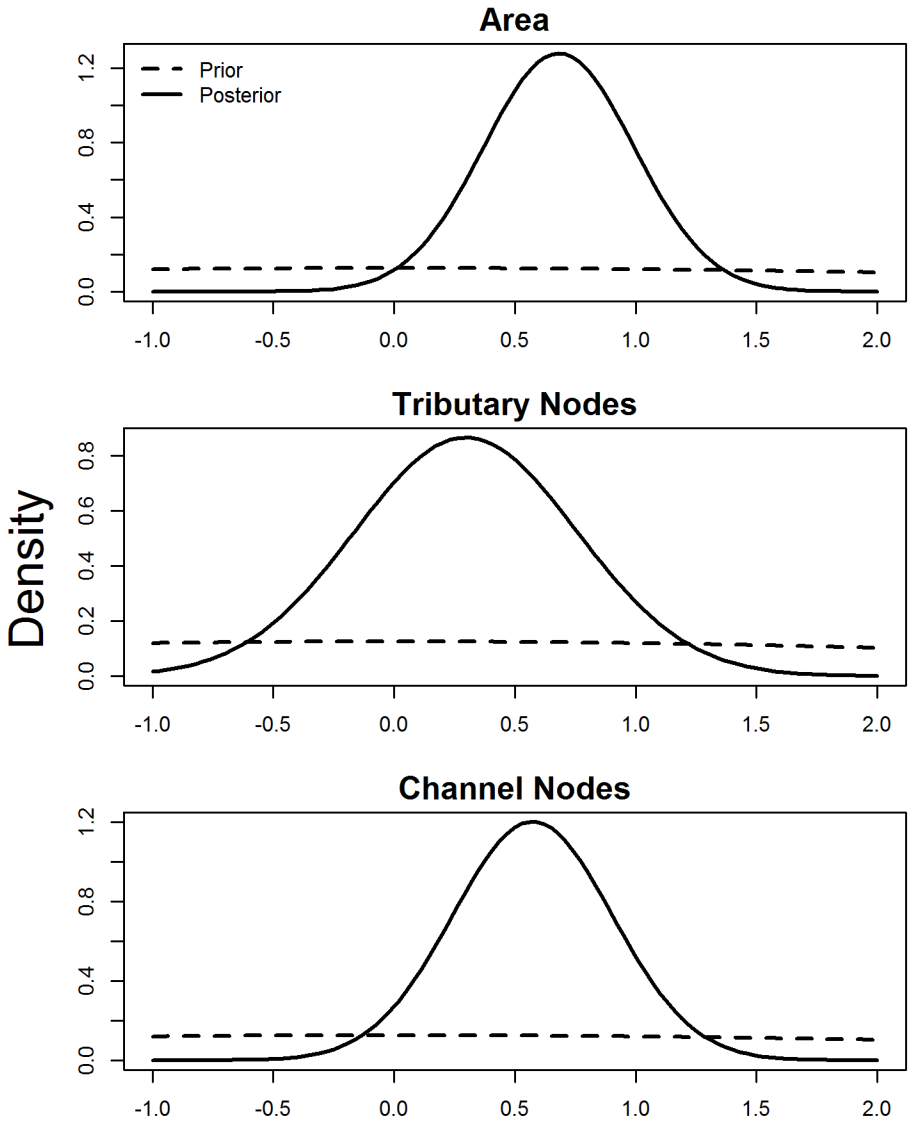

Figure 4.03 Observed vs. predicted plot for each of the 11 stocks included in the variable indicator selection method. Observed data points are the posterior means presented in Catalano (2012) and predictions were made using model-averaged coefficients from the variable indicator selection. Error bars in the vertical direction are 95% Bayesian credible intervals from the Catalano (2012) analysis and credible intervals for the model predicted S_{MSY} from the variable indicator model.

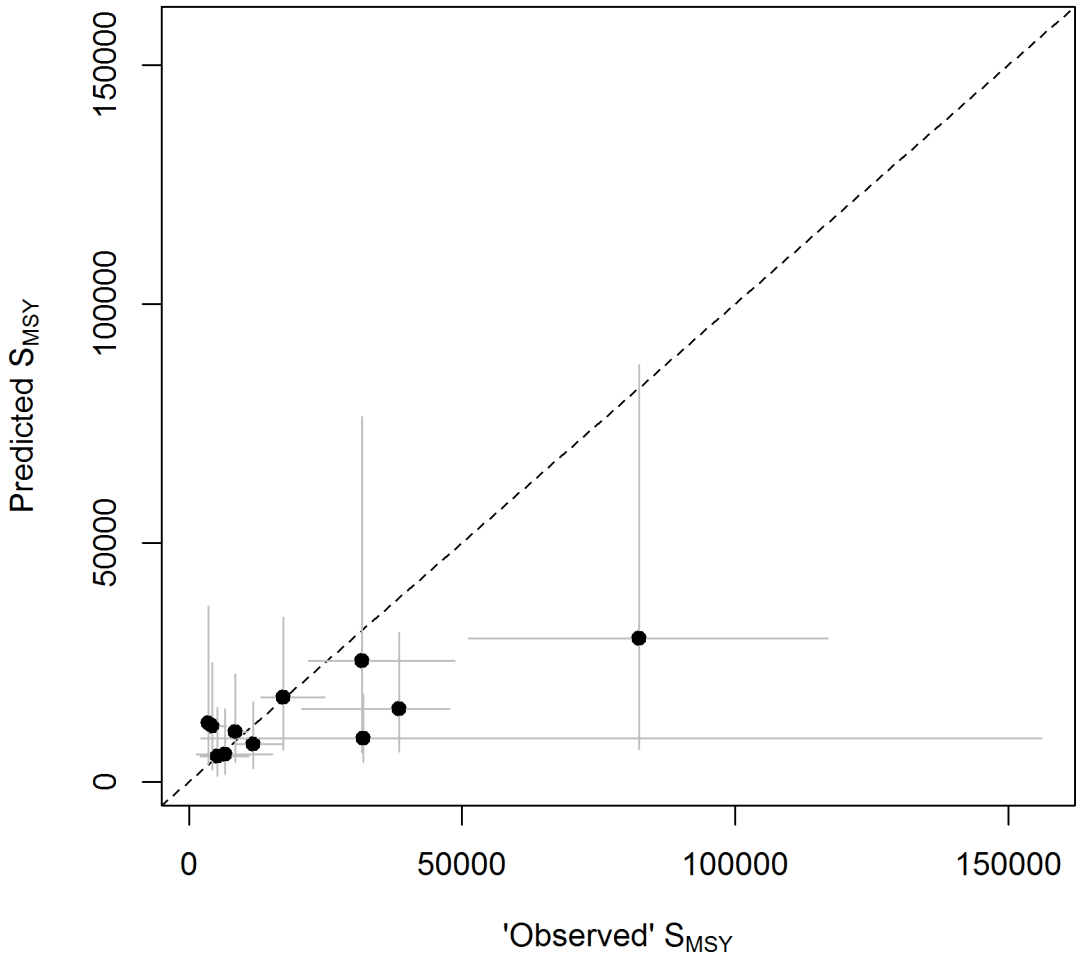

Figure 4.04 Distributions of model selection outcomes from the randomization procedures. Bar height represents the proportion of randomized posterior samples that each model showed up in each model placement. Divided into two panels for ease of presentation.

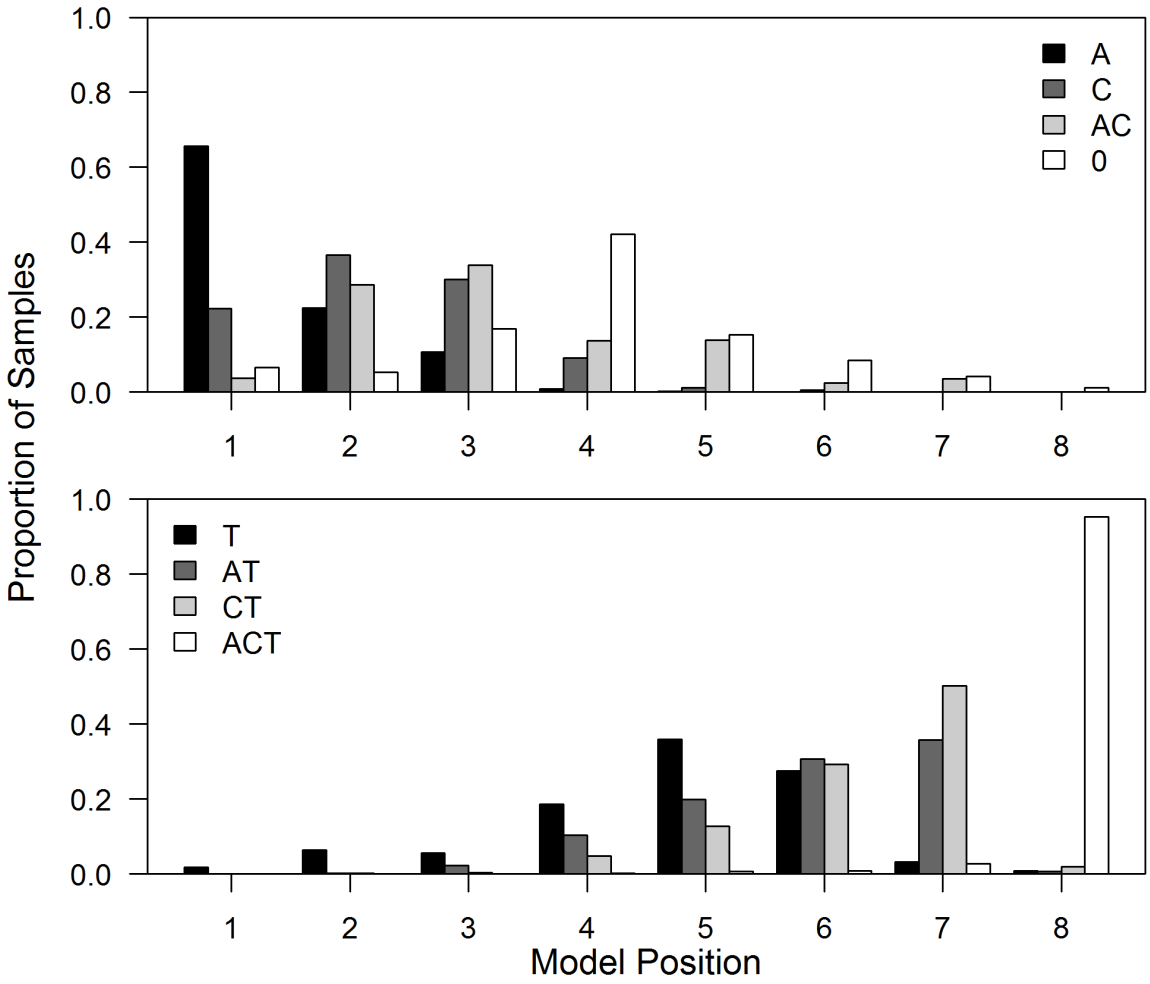

CHAPTER 4
TABLES

Table 4.01 Prior distributions for all unknown parameters in the Bayesian hierarchical regression models. $\omega_{1:3}$ were only included in the variable indicator selection method. Note that the dispersion parameter of the normal distribution is the precision (as opposed to variance) which is the inverse of variance.

Parameter	Prior Distribution
$\beta_{0:3}$	$N(0, 0.1)$
τ_{ψ}	$Gamma(0.01, 0.01)$
$\omega_{1:3}$	$Bernoulli(0.5)$

Table 4.02 Parameter inclusion probability from the indicator variable selection method (labeled Bayes) and the proportion of randomized samples that resulted in each variable being selected in the best model (labeled AIC). A = log(area), C = channel node density, T = tributary node density.

Variable	(Bayes) Inclusion Parameter (ω)	(AIC) Proportion In best model
A	0.56	0.71
C	0.36	0.27
T	0.15	0.02

Table 4.03 Results from the four model selection approaches. Models are ordered by the strength of support under the variable indicator selection method (first column). Bolded values are the selected best model under each approach. The values in the parentheses in the Randomize w/AIC column are the standard deviation of the placement and weight across all randomized posterior samples.

	Variable Ind.	DIC		Randomize w/AIC		Cross-Validation	
Model	Model Probability	pD	DIC	Model Position	Model Weight	Score	% Change from Best Model
A	**0.37**	9.62	11.77	**1.48 (0.78)**	**0.37 (0.14)**	**9.23**	**0%**
C	0.19	**9.63**	**11.52**	2.33 (1.02)	0.23 (0.12)	12.17	32%
0	0.16	10.01	12.61	4.03 (1.42)	0.11 (0.10)	13.75	49%
AC	0.13	9.59	11.64	3.27 (1.37)	0.16 (0.10)	12.01	30%
T	0.06	10.06	12.25	4.80 (1.33)	0.07 (0.07)	14.40	56%
AT	0.04	9.88	12.19	5.90 (1.11)	0.03 (0.01)	13.13	42%
CT	0.03	9.62	11.62	6.29 (0.96)	0.03 (0.02)	16.40	78%
ACT	0.02	10.03	12.31	7.91 (0.45)	0.01 (0.01)	16.39	78%

Table 4.04 Coefficient estimates from the variable indictor selection method after samples where $\omega = 0$. Values in parentheses indicate the 95% credible interval of these thinned posteriors.

Variable	Mean (95% CI)
A	0.69 (0.07, 1.27)
C	0.56 (-0.07, 1.19)
T	0.28 (-0.62, 1.11)

APPENDIX III: DATA

Table A-1: Habitat variables before standardizing.

Stock	A	T	C
Alsek	10.31497	0.012856	0.007819
Anchor	6.331502	0.010676	0.007117
Chena+Salcha	9.304283	0.013382	0.019663
Deshka	7.407328	0.012743	0.027306
Goodnews	7.882315	0.012453	0.053962
Karluk	6.43935	0.011182	0.015974
Kuskokwim	11.6786	0.013218	0.067099
Stikine	10.82146	0.013238	0.044405
Taku	9.777868	0.013039	0.049606
Unalakleet	8.574329	0.013034	0.022667
Yukon	12.56375	0.012629	0.034927

Table A-2: log(S_{MSY}) posterior summaries; used in DIC and indicator variable selection methods (note: SD was transformed to be an inverse variance for JAGS)

Stock	Mean	SD
Alsek	8.309908	0.277004
Anchor	8.411187	0.455808
Chena+Salcha	9.038798	0.107132
Deshka	9.351489	0.17418
Goodnews	8.168945	0.183109
Karluk	8.409064	0.617513
Kuskokwim	11.29503	0.257912
Stikine	9.743034	0.163446
Taku	10.23734	0.250491
Unalakleet	9.107516	1.104626
Yukon	10.33829	0.210793

APPENDIX IV
CODE FOR VARIABLE SELECTION TECHNIQUES

```
##############################################################################################
########### INDICATOR VARIABLE SELECTION (PARAMETER INCLUSION PROBABILITY) ###########
##############################################################################################

# PACKAGES
library(R2OpenBUGS)
library(rjags)
source("C:/Users/bas0041/Desktop/run_functions_source.R")
main.dir=getwd()

# RESPONSE VARIABLES: REFERENCE POINTS
col = c("mean", "sd", "median", "lower95", "upper95")
log.S.msy = read.csv(paste(main.dir, "log_Smsy.csv", sep="/"), row.names=1)
colnames(log.S.msy)=col

# PREDICTOR VARIABLES: HABITAT VARIABLES
habitat = read.csv(paste(main.dir, "habitat_vars.csv", sep="/"), row.names=1)

#pullout only stocks we can use
no.na = which((!is.na(habitat$WS_A_KM2) & !is.na(habitat$MCND_NUM))
tribs.nat = habitat$TND_NUM/habitat$WS_A_KM2
chans.nat = habitat$MCND_NUM/habitat$WS_A_KM2

# habitat variables
habitat.vars = data.frame(area = log(habitat$WS_A_KM2),tribs =  tribs.nat, chans =
chans.nat)
habitat.vars = habitat.vars[no.na,]
rownames(habitat.vars) = rownames(habitat)[no.na]

# reference points: use posterior means
log.S.msy.mean = log.S.msy[no.na, 1]
log.S.msy.tau = 1/(log.S.msy[no.na, 2])^2

dat = list(
  #dependent variables
  obs.mu = log.S.msy.mean,
  obs.tau = log.S.msy.tau,
  n.stocks = length(log.S.msy.mean),

  #independent variables
  area = as.numeric(scale(habitat.vars$area)),
  trib_nodes = as.numeric(scale(habitat.vars$tribs)),
  chan_nodes = as.numeric(scale(habitat.vars$chans)))

windows(record=T)
for(i in 4:6){
  plot(dat$obs.mu~dat[[i]], main=names(dat)[i])
}

### SPECIFY MODEL ###
mod=function(){
  #PRIORS
  for(i in 1:3){
    beta[i] ~ dnorm(0, 0.1)
    w[i] ~ dbern(0.5)
```

```
  }
  int ~ dnorm(0, 0.1)
  tau.proc ~ dgamma(0.01, 0.01)

  for(i in 1:n.stocks){
    obs.mu[i] ~ dnorm(ref.proc[i], obs.tau[i])
    ref.proc[i] ~ dnorm(pred.ref[i], tau.proc)

    pred.ref[i] <- int + w[1]*beta[1]*area[i] + w[2]*beta[2]*trib_nodes[i] +
w[3]*beta[3]*chan_nodes[i]

    #derived quantities
    resid.pred[i] <- obs.mu[i]-pred.ref[i]
    resid.proc[i] <- obs.mu[i]-ref.proc[i]
  }
  sigma.proc <- 1/sqrt(tau.proc)
}

# WRITE MODEL TO A TXT FILE
model.file = "param_inclus.txt"
write.model(mod,paste(main.dir, model.file, sep="/"))

### PARAMETERS TO MONITOR ###
parameters = c(
  #parameters
  "beta", "w", "tau.proc", "ref.proc", "int",
  #calculated quantities
  "sigma.proc", "pred.ref", "resid.pred", "resid.proc")

# RUN FREQUENTIST MODEL TO GET INITIAL VALUES FOR PARAMETERS
freq.mod = lm(obs.mu~area+trib_nodes+chan_nodes, data = dat)
full = summary(freq.mod)
freq.coef = coef(full)[,1]
freq.sigma = full$sigma

# COMPILE INITS
inits1 = list(int=freq.coef[1], beta=freq.coef[2:4], w=rep(1, 3),
tau.proc=1/freq.sigma^2)
inits2 =list(int=freq.coef[1]*runif(1), beta=freq.coef[2:4]*runif(1), w=rep(0, 3),
tau.proc=(1/freq.sigma^2)*runif(1))

inits = list(inits1, inits2)

# MCMC SPECIFICATIONS
nc = 2
ni = 100000
nb = 50000
nt = 20
ni/nt

### RUN JAGS ###

# INITITATE THE MODEL (ADAPTING PHASE)
jmod = jags.model(file=paste(main.dir, model.file, sep="/"), data=dat, n.chains=nc,
inits=inits, n.adapt=1000)
```

```
# BURNIN
update(jmod, n.iter=nb, by=1, progress.bar='text')

# SAMPLE THE POSTERIOR
post = coda.samples(jmod, parameters, n.iter=ni, thin=nt)

#### LOOK AT OUTPUT ####
gelman.diag(post, multivariate=F)

# COERCE TO MATRIX AND PULL OUT POSTERIORS OF INTEREST
mypost = as.matrix(post)
w = mypost[, c("w[1]", "w[2]", "w[3]")]
beta = mypost[,c("beta[1]", "beta[2]", "beta[3]")]

# remove w == 0 from betas
beta1 = beta[w[,1] == 1 ,1]
beta2 = beta[w[,2] == 1 ,2]
beta3 = beta[w[,3] == 1 ,3]

summ = function(x){c(mean = mean(x), quantile(x, c(0.025, 0.975)))}

eff = rbind(summ(beta1), summ(beta3), summ(beta2))
rownames(eff) = c("A", "C", "T")
#write.csv(eff, "effectsizes.csv")

### MODEL PROBABILITITES ###
models = as.matrix(table(paste(w[,1],w[,2], w[,3], sep="")))/dim(w)[[1]]
modprobs = as.matrix(as.matrix(models[order(models[,1],decreasing = T),]))
round(modprobs, 2)

# MODEL AVERAGED COEFFNS
parmas = beta*w
results = t(rbind(mean=colMeans(parmas),
                  sd=apply(parmas,2,sd),
                  apply(parmas,2,quantile,c(0.025,0.5, 0.975)),
                  inclusion_probs=colMeans(w)))


###### END PARAMETER INCLUSION PROBS ######
```

```
##############################################################################################
################## RANDOMIZATION OF POSTERIOR SAMPLES W/AIC SELECTION #################
##############################################################################################

# PACKAGES
library(MuMIn)
library(pbapply)

main.dir=getwd()

# READ IN THE POSTERIOR SAMPLES
post.samp=read.csv("log.S.msy.post.csv")

# PREDICTOR VARIABLES: HABITAT VARIABLES
habitat = read.csv(paste(main.dir, "habitat_vars.csv", sep="/"), row.names=1)

#pullout only stocks we can use
no.na = which((!is.na(habitat$WS_A_KM2) & !is.na(habitat$MCND_NUM)))# &
rownames(habitat)!="kuskokwim")

tribs.nat = habitat$TND_NUM/habitat$WS_A_KM2
chans.nat = habitat$MCND_NUM/habitat$WS_A_KM2

#habitat variables
habitat.vars = data.frame(area = log(habitat$WS_A_KM2),tribs =  tribs.nat, chans =
chans.nat)
habitat.vars = habitat.vars[no.na,]
rownames(habitat.vars) = rownames(habitat)[no.na]

use.stocks=rownames(habitat.vars)
use.stocks[length(use.stocks)]="yukon"

#pull out only those stocks' posteriors
post.samp=post.samp[,use.stocks]
colnames(post.samp)

# RANDOMIZE THE POSTERIORS FOR EACH STOCK
n.samp=nrow(post.samp)
post.samp=as.matrix(post.samp)
sub.samp=apply(post.samp, 2, function(x) sample(x, n.samp, replace=F))
models = c("null", "area", "chans", "area.chans", "tribs", "area.tribs",
"chans.tribs", "full")

n.pulls = n.samp
do.plot = F

# CONTAINERS FOR RANDOMIZED RESULTS
boot.results = list()
null.pos  = numeric(n.pulls)
null.wt  = numeric(n.pulls)
area.pos = numeric(n.pulls)
area.wt = numeric(n.pulls)
chans.pos = numeric(n.pulls)
chans.wt = numeric(n.pulls)
area.chans.pos = numeric(n.pulls)
```

```
area.chans.wt = numeric(n.pulls)
tribs.pos = numeric(n.pulls)
tribs.wt = numeric(n.pulls)
area.tribs.pos = numeric(n.pulls)
area.tribs.wt = numeric(n.pulls)
chans.tribs.pos = numeric(n.pulls)
chans.tribs.wt = numeric(n.pulls)
full.pos = numeric(n.pulls)
full.wt = numeric(n.pulls)

# INITIATE THE FITTING TO POSTERIOR SAMPLES
pb = startpb(0, n.pulls)
for(i in 1:n.pulls){
  Sys.sleep(0.1)

  # make a new data set
  dat = data.frame(area = as.numeric(scale(habitat.vars$area)),
                   tribs = as.numeric(scale(habitat.vars$tribs)),
                   chans = as.numeric(scale(habitat.vars$chans)), smsy = sub.samp[i,])

  if(i == 1 & do.plot == T) windows(record = T)
  if(do.plot == T) {
    par(mfrow = c(2,2), oma = c(0, 1, 2, 0), mar = c(2,2,2,2))
    plot(smsy ~ area, data = dat, main = "Area", xlab = "", ylab = "")
    plot(smsy ~ chans, data = dat, main = "Chans",  xlab = "", ylab = "")
    plot(smsy ~ tribs, data = dat, main = "Tribs",  xlab = "", ylab = "")
    mtext(side = 3, outer = 2, as.character(i), cex = 2, line = 0, font = 2)
    plot.new()
  }
  # fit all models
  fit = lm(smsy ~ area + chans + tribs, data = dat, na.action = na.fail)

  dd = dredge(fit)

  #combine important model selection
  boot.results[[i]] = data.frame(model = models[as.numeric(rownames(dd))], weight =
dd$weight)

  null.pos[i] = which(boot.results[[i]]$model == "null")
  null.wt[i] = boot.results[[i]]$weight[null.pos[i]]

  area.pos[i]= which(boot.results[[i]]$model == "area")
  area.wt[i] = boot.results[[i]]$weight[area.pos[i]]

  chans.pos[i]= which(boot.results[[i]]$model == "chans")
  chans.wt[i] = boot.results[[i]]$weight[chans.pos[i]]

  area.chans.pos[i]= which(boot.results[[i]]$model == "area.chans")
  area.chans.wt[i] = boot.results[[i]]$weight[area.chans.pos[i]]

  tribs.pos[i] = which(boot.results[[i]]$model == "tribs")
  tribs.wt[i] = boot.results[[i]]$weight[tribs.pos[i]]

  area.tribs.pos[i] = which(boot.results[[i]]$model == "area.tribs")
  area.tribs.wt[i] = boot.results[[i]]$weight[area.tribs.pos[i]]
```

```
  chans.tribs.pos[i] = which(boot.results[[i]]$model == "chans.tribs")
  chans.tribs.wt[i] = boot.results[[i]]$weight[chans.tribs.pos[i]]

  full.pos[i] = which(boot.results[[i]]$model == "full")
  full.wt[i] = boot.results[[i]]$weight[full.pos[i]]
  setpb(pb,i)
}

# close the progress bar
closepb(pb)

# COMBINE RAW OUTPUT
positions = data.frame(null = null.pos, area = area.pos, chans = chans.pos, area.chans
= area.chans.pos,
           tribs = tribs.pos, area.tribs = area.tribs.pos, chans.tribs =
chans.tribs.pos, full = full.pos)
weights = round(data.frame(null = null.wt, area = area.wt, chans = chans.wt,
area.chans = area.chans.wt,
                    tribs = tribs.wt, area.tribs = area.tribs.wt, chans.tribs =
chans.tribs.wt, full = full.wt),2)

# SUMMARIZE RAW OUTPUT
positions.mean = sort(apply(positions, 2, mean))
positions.sd = apply(positions, 2, sd)[names(positions.mean)]

weights.mean = sort(apply(weights, 2, mean), decreasing = T)
weights.sd = apply(weights, 2, sd)[names(weights.mean)]

short.models = c("0", "A", "C", "AC", "T", "AT", "CT", "ACT")

names(short.models) = models

# PLOT MEAN MODEL POSTION AND WEIGHT
windows()
par(mfrow = c(2,1), mar = c(3, 3, 2, 2))
mp.1 = barplot(positions.mean, names.arg = short.models[names(positions.mean)], main =
"Mean Model Position", col = "white",
               ylim = c(0, max(positions.mean + positions.sd) + 1), las = 1)
arrows(mp.1, positions.mean - positions.sd, mp.1, positions.mean + positions.sd, code
= 3, length = 0.05, angle = 90)
axis(side = 1, at = mp.1, labels = rep("", length(models)))
box()

mp.2 = barplot(weights.mean, names.arg = short.models[names(weights.mean)], main =
"Mean Model Weight", col = "white",
               ylim = c(0, max(weights.mean + weights.sd) + 0.1), las = 1)
axis(side = 1, at = mp.2, labels = rep("", length(models)))
arrows(mp.2, weights.mean - weights.sd, mp.2, weights.mean + weights.sd, code = 3,
length = 0.05, angle = 90)
box()

# PULL OUT DISTRIBUTION OF MODEL PLACEMENT
pos.count = apply(positions, 2, function(x) table(x))
count.mat = matrix(NA, nrow = 8, ncol = 8)
```

```
colnames(count.mat) = as.character(1:8)
rownames(count.mat) = models

for(i in 1:length(models)){
  count.mat[models[i], as.character(names(pos.count[[i]]))] = pos.count[[i]]
}

count.mat[is.na(count.mat)] = 0
prop.mat = count.mat/n.samp
best = prop.mat[c("area", "chans", "area.chans", "null"),]
worst = prop.mat[c("tribs", "area.tribs", "chans.tribs", "full"),]

# PLOT DISTRIBUTIONS OF MODEL PLACEMENT
windows()
par(mfrow = c(2,1), mar = c(2,2,3,2), oma = c(3,3,0,0))
barplot(best, beside = T, col = c("black", "grey40", "grey80", "white"),cex.lab = 1.5,
cex.main = 2, ylim = c(0, 1),las = 1, main = "4 Best Models", xlab = "", ylab =
"Frequency")
axis(side = 1, at = seq(3, 40, by = 5), labels = rep("", 8))
legend("topright", legend = short.models[rownames(best)], fill = c("black", "grey40",
"grey80", "white"), bty = "n")

barplot(worst, beside = T, col = c("black", "grey40", "grey80", "white"), cex.lab =
1.5, cex.main = 2, ylim = c(0, 1), las = 1,main = "4 Worst Models", xlab = "", ylab =
"")
axis(side = 1, at = seq(3, 40, by = 5), labels = rep("", 8))
legend("topleft", legend = short.models[rownames(worst)], fill = c("black", "grey40",
"grey80", "white"), bty = "n")

mtext(side = 1, outer = T, "Model Position", cex = 1.5, line = 0.6)
mtext(side = 2, outer = T, "Proportion of Samples", cex = 1.5, line = 1)

# NUMBER OF TIMES EACH VARIABLE SHOWED UP IN THE BEST MODEL
area = sum(count.mat[c("area", "area.chans", "area.tribs", "full"), 1])
chans = sum(count.mat[c("chans", "area.chans", "chans.tribs", "full"), 1])
tribs = sum(count.mat[c("tribs", "area.tribs", "chans.tribs", "full"), 1])
null = sum(count.mat["null",1])
tot = sum(area, chans, tribs)
param.inclus = round(t(data.frame(area = area/tot, chans = chans/tot, tribs =
tribs/tot)),2)

##### END RANDOMIZATION CODE #####
```

```
##############################################################################################
############################## LEAVE-ONE-OUT CROSS VALIDATION ################################
##############################################################################################

##### LOAD PACKAGES AND MY FUNCTIONS #####
library(R2OpenBUGS)
library(rjags)
source("C:/Users/bas0041/Desktop/run_functions_source.R")

main.dir=getwd()

##### GET RAW DATA READ IN AND FORMATED #####

# RESPONSE VARIABLES: REFERENCE POINTS
col = c("mean", "sd", "median", "lower95", "upper95")

# log of ref. posteriors with the negatives removed
log.S.msy = read.csv(paste(main.dir, "log_Smsy.csv", sep="/"), row.names=1);
colnames(log.S.msy)=col

# PREDICTOR VARIABLES: HABITAT VARIABLES
habitat = read.csv(paste(main.dir, "habitat_vars.csv", sep="/"), row.names=1)

#pullout only stocks we can use
no.na = which((!is.na(habitat$WS_A_KM2) & !is.na(habitat$MCND_NUM)))# &
rownames(habitat)!="kuskokwim")

tribs.nat = habitat$TND_NUM/habitat$WS_A_KM2
chans.nat = habitat$MCND_NUM/habitat$WS_A_KM2

#habitat variables
habitat.vars = data.frame(area = log(habitat$WS_A_KM2),tribs =  tribs.nat, chans =
chans.nat)
habitat.vars = habitat.vars[no.na,]
rownames(habitat.vars) = rownames(habitat)[no.na]

#reference points: use posterior means
log.S.msy.mean = log.S.msy[no.na, 1]
log.S.msy.tau = 1/(log.S.msy[no.na, 2])^2

area = as.numeric(scale(habitat.vars$area))
trib = as.numeric(scale(habitat.vars$tribs))
chan = as.numeric(scale(habitat.vars$chans))

##### SPECIFY MODEL #####
mod=function(){
  #PRIORS
  for(i in 1:nvars){
    beta[i] ~ dnorm(0, 0.1)
  }
  #int ~ dnorm(0, 0.1)
  tau.proc ~ dgamma(0.01, 0.01)

  for(i in 1:n.stocks){
    obs.mu[i] ~ dnorm(ref.proc[i], obs.tau[i])
```

```
    ref.proc[i] ~ dnorm(pred.ref[i], tau.proc)

    pred.ref[i] <- sum(beta * X[i,])

    #derived quantities
    resid.pred[i] <- obs.mu[i] - pred.ref[i]
    resid.proc[i] <- obs.mu[i] - ref.proc[i]
  }
  sigma.proc <- 1/sqrt(tau.proc)
}

model.file = "model.txt"
write.model(mod,paste(main.dir, model.file, sep="/"))

##### PARAMETERS TO MONITOR ######
parameters = c(
  #parameters
  "beta", "tau.proc", "ref.proc",
  #calculated quantities
  "sigma.proc", "pred.ref", "resid.pred", "resid.proc")

##### MCMC SPECIFICATIONS #####
nc = 2
ni = 100000
nb = 50000
nt = 20
ni/nt
n.saved = (ni * nc)/nt

##### MAKING DATA FOR EACH MODEL AND FOR EACH LEAVE ONE OUT RUN #####
# habitat data
K = 11
n.stocks = 10
int = rep(1,n.stocks)
hab = list()
for(k in 1:K){
  hab[[k]] = list(mod1 = cbind(int, area[-k]), mod2 = cbind(int, trib[-k]), mod3 =
cbind(int, chan[-k]),
                  mod4 = cbind(int, area[-k], trib[-k]), mod5 = cbind(int, area[-k],
chan[-k]),
                  mod6 = cbind(int, trib[-k], chan[-k]), mod7 = cbind(int, area[-k],
trib[-k], chan[-k]),
                  mod8 = cbind(int))
}

# reference points
ref = list()
for(k in 1:K){
  ref[[k]] = list(obs.mu = log.S.msy.mean[-k], obs.tau = log.S.msy.tau[-k])
}

# number of predictors for each model
n.vars = c(2,2,2,3,3,3,4,1)

##### RUN ALL 8 MODELS OVER ALL 11 COMBINATIONS OF THE LEAVE-ONE-OUT #####
```

```
n.models = 8
beta = list()
tau.proc = list()
starttime = Sys.time()
# i models
# k datasets
for(i in 1:n.models){
  beta[[i]] = list()
  tau.proc[[i]] = list()
  for(k in 1:K){
    ### SET UP DATA ###
    dat = list(
      obs.mu = ref[[k]]$obs.mu,
      obs.tau = ref[[k]]$obs.tau,
      n.stocks = n.stocks,
      nvars = n.vars[i],

      X = matrix(unlist(hab[[k]][i]), nrow = 10, ncol = n.vars[i])
      )

    ### RUN JAGS ###
    print(paste("Model", as.character(i), "running with stock", as.character(k),
"removed"))
    jmod = jags.model(file=paste(main.dir, model.file, sep="/"), data=dat,
n.chains=nc, inits=NULL, n.adapt=1000, quiet = T)
    update(jmod, n.iter=nb, by=1, progress.bar='text')
    post = coda.samples(jmod, parameters, n.iter=ni, thin=nt)

    ### PULL OUT OUTPUT ###
    if(i == 8) beta.name = "beta" else beta.name = "beta["
    beta[[i]][[k]] = get.post(post, beta.name, do.post = T)$posterior
    tau.proc[[i]][[k]] = get.post(post, "tau.proc", do.post = T)$posterior
  }
}
Sys.time() - starttime

##### CALCULATE THE SCORE FROM HOOTEN AND HOBBS (2015) #####
# get the habitat variables with all data
n.stocks.full = 11
int.full = rep(1,n.stocks.full)
hab.full = list(mod1 = cbind(int.full, area), mod2 = cbind(int.full, trib), mod3 =
cbind(int.full, chan),
                mod4 = cbind(int.full, area, trib), mod5 = cbind(int.full, area,
chan),
                mod6 = cbind(int.full, trib, chan), mod7 = cbind(int.full, area,
trib, chan),
                mod8 = cbind(int.full))

# get the reference points with all data
ref.full = log.S.msy.mean


# calculate model predicted S.msy for the left out stock under each model
y.minus.k = list()
for(i in 1:n.models){
```

```
  y.minus.k[[i]] = list()
  for(k in 1:K){
    y.minus.k[[i]][[k]] = numeric(n.saved)
    for(t in 1:n.saved){
      if(any(i == 1:7)){
        y.minus.k[[i]][[k]][t] = sum(beta[[i]][[k]][t,] * hab.full[[i]][k,])
      }
      if(i == 8){
        y.minus.k[[i]][[k]][t] = sum(beta[[i]][[k]][t] * hab.full[[i]][k,])
      }
    }
  }
}

# use sum of squared residual as the measure of statistical "closeness"
score.i.k = list()
for(i in 1:n.models){
  score.i.k[[i]] = numeric(11)
  for(k in 1:K){
    score.i.k[[i]][k] = sum((ref.full[k] - y.minus.k[[i]][[k]])^2)/n.saved
  }
}

##### INFERENCE #####
scores = unlist(lapply(score.i.k, sum))
model.names = c("A", "T", "C", "AT", "AC", "CT", "ACT", "0")
names(scores) = model.names

sorted = round(sort(scores),2)
best = min(sorted)

pct.chng = round((sorted - best)/best,2)

##### END LEAVE-ONE-OUT CROSS VALIDATION CODE #####
```